DEVELOPMENT OF GLYCOSYLATION BASED CANCER THERAPIES USING METABOLIC OLIGOSACCHARIDE ENGINEERING

by

Mohit Philip Mathew

A dissertation submitted to Johns Hopkins University in conformity with the requirements for the degree of Doctor of Philosophy

Baltimore, Maryland

March, 2016

ABSTRACT

Abnormal glycosylation is a universal feature of cancer; however**,** in the past these changes have been viewed as passive by products of abnormal metabolism with efforts largely being directed at using these characteristic abnormalities as biomarkers for cancer detection. More recently glycosylation has been shown to play a number of crucial roles in the activity and localization of proteins and in the overall behavior of cells. While cancer related glycosylation abnormalities may have a metabolic origin, they likely play a much larger role in the maturation of the disease phenotype and in its eventual progression. In order to study changes in glycosylation, alterations in the glycan patterns need to be made this can either be done by genetic manipulation of the glycosylation machinery or by altering fluxes through the pathway via metabolic oligosaccharide engineering. One of the major advantages of using a flux based approach is that it can make use of pharmacologically relevant small molecules that are easier to use than genetic means. However a significant roadblock to use to metabolic oligosaccharide engineering is the low uptake efficiency of sugar molecules, this is overcome by the use of short chain acid (SCFA) linked sugar molecules. The addition of these SCFA groups converts these molecules into a unique form of prodrug in that they need to resist esterase processing outside the cell and require intracellular esterase processing to release the core sugar. The first part of this thesis characterizes the esterase processing of these sugar analog prodrugs. The analogs were found to be fairly resistant to extracellular inactivation surviving for between 2 and 4 h in 100% fetal bovine serum. In comparison intracellular processing was shown to be much faster, interestingly there appeared to be an activation of the intracellular esterases by analog treatments. Investigation of this

crosstalk revealed that increased sialylation of carboxyl esterases led to a stabilization of more active trimeric and hexameric forms of this enzyme. The next portion of the study used metabolic oligosaccharide engineering as a tool to alter glycosylation and the epidermal growth factor receptor's sialylation is observed to increase. The effect of increased sialylation on the epidermal growth factor receptor (EGFR) is investigated and shown to lead to an inhibition of EGFR signaling. This understanding of the functional significance of altered glycosylation is then translated towards clinical end points with 1,3,4-*O*-Bu_3ManNAc shown to have remarkable synergy when used in conjunction with EGFR targeting drugs Erlotinib and Gefitinib. Finally, the underlying molecular mechanism by which this analog induced change in glycosylation affects receptor signaling is characterized. Increased sialylation caused by analog treatment was found to disrupt the galectin lattice which led to an increase in non clathrin mediated endocytosis wherein the resulting endosomes are fated primarily for degradation, this leads to a decrease in EGFR surface localization and increased signal attenuation.

THESIS COMMITTEE

Kevin J. Yarema (primary advisor, reader)

Associate Professor, Department of Biomedical Engineering

Johns Hopkins University School of Medicine

Jordan J. Green (reader)

Associate Professor, Department of Biomedical Engineering

Johns Hopkins University School of Medicine

Michael J. Betenbaugh

Professor, Department of Chemical and Biomolecular Engineering

Johns Hopkins University

ACKNOWLEDGEMENTS

This work would not be possible without the guidance and support of a number of people. I would like to start by thanking my thesis advisor Dr. Kevin Yarema whose door was always open for advice and questions regardless of how large, small, important or mundane the problem. I truly appreciate how open to new ideas and supportive of varied projects he was. I also am thankful for the collaborative atmosphere he nurtured in the laboratory and how I was given the opportunity to be a part of a number of different, diverse projects.

I would also like to thank my thesis committee members Dr. Jordan Green, and Dr. Michael Betenbaugh for their help and guidance throughout my time at Hopkins.

Further, a portion of the results described here was done in collaboration with Dr. Green and his lab. It has been a pleasure working with him and various other members in his lab in particular Randall Meyer, and David Wilson. In fact, a lot of the work described here has been done in collaboration with other labs, a testament both to Dr. Yarema's ability and willingness to form such collaborations and to the collaborative atmosphere here at Hopkins. This includes working closely with Dr. Hui Zhang's lab, experts in mass spectrometry, as well as working on projects with Dr. Hafiz Ahmed's group.

While I've been fortunate to work on interesting projects, I've been equally lucky to work with amazing labmates. In particular Elaine Tan, Christopher Sauei, Dr. Rahul Bhattacharya and Dr. Jian Du regardless of how my projects were going it was always

reassuring to have them around to help trouble shoot experiments and bounce ideas around with.

Finally, I want to thank my family, my parents Kandathil Nainan Mathew and Talitha Elizabeth Cherian Mathew who have supported me at every stage of my education and who molded me into the person I am today, my brother Rohan Cherian Mathew who was a wonderful companion growing up and whose wit and humor has often helped keep me grounded. I'd like to thank my wife, Deepthi George Varghese who has stoically put up with the various degrees of penny pinching associated with grad school, put her own career on hold to support me while I started mine and with whom I have the most beautiful baby girl, Finally, I'd like to thank my daughter (and grumpy cat impersonator) Ruth Elizabeth Mathew for allowing me to sleep on occasion and whose smile brightens my life.

TABLE OF CONTENTS

LIST OF TABLES

LIST OF FIGURES

CHAPTER 1

INTRODUCTION TO THE THESIS

1.1 OUTLINE OF THE THESIS

Chapter 2 will familiarize the reader with some of the important concepts and ideas related to the research presented in later chapters. The chapter is divided into three main sections. The first gives a brief introduction to the field of metabolic engineering. The second section provides some background information on the field of metabolic oligosaccharide engineering. The third section looks at the process and importance of N-glycosylation.

The thesis is split up into three specific aims. In Aim 1, a MOE based small molecule approach to alter glycosylation is developed and characterized, the extracellular and intracellular processing in particular were assayed and characterized.

Aim 2 then applies this approach to alter glycosylation in SW1990 pancreatic cancer cells and specific proteins whose glycosylation profiles are being affected are identified, this aim then explores the functional effect of alterations of glycosylation on the behavior of the epidermal growth factor receptor (identified in Aim1) and then focuses on developing novel therapeutic approaches for pancreatic cancer using complementary EGFR targeting drugs in combination. Finally non-natural sugar analogs that open further therapeutic opportunities are also screened for similar effects.

In Aim 3, the molecular mechanism by which analog induced changes in glycosylation affect EGFR signaling is explored and characterized using computational and experimental approaches.

1.2 SPECIFIC AIMS OF THE THESIS

Specific Aim 1: Was to develop and evaluate metabolic flux-based tools to manipulate glycosylation focusing on the extracellular and intracellular processing of these sugar analog prodrugs.

Aim 1 is divided into two specific sub aims:

a. Characterization of the extracellular processing and inactivation of short chain fatty acid (SCFA) linked sugar analogs.
b. Elucidation of the intracellular processing of the SCFA-linked sugar analogs by esterases and their effect on the availability of the core sugar within the cell for metabolic flux modulation.

This aim focuses on the characterization of both extracellular and intracellular processing of short chain fatty acid linked sugar analogs in order to determine their viability as small molecule glycosylation effectors. This aim further explores the intriguing crosstalk between SCFA linked sugar analogs and the intracellular esterases that process them.

In order to effectively use MOE sugar analogs as 'pseudo pro drugs' a thorough understanding of the extracellular processing and inactivation of these compounds by

serum esterases is needed. The results for Specific aim 1.a. are given in **Chapter 3** wherein SW1990 cells are used as a reporter cell line and short chain fatty acid linked sugar inactivation is characterized in 10%, 25% and 100% fetal bovine serum.

After entry into a cell these sugar analog pro drugs need to be processed by intracellular esterases to yield the core sugar that can then intercept the glycosylation machinery and cause alterations in the glycosylation profile of the cell. **Chapter 4** is focused on specific aim 1.b. and elucidates the intracellular processing of these sugar analogs, the chapter further explores the intriguing crosstalk and feed forward activation of these intracellular esterases observed on analog treatment.

Specific Aim 2: Applied these flux based tools to identify surface receptors susceptible to changes in glycosylation in cancer cells, determine the effect of altered glycosylation on receptor function and apply this toward new therapeutic strategies for pancreatic cancer

Aim 2 consists of four specific sub aims:

a. Glycoproteomics analysis of proteins from cancer cells subject to metabolic oligosaccharide engineering

b. Surface receptors altered by MOE were functionally characterized using western blotting to (i) probe alterations in response/phosphorylation to the receptor's ligand and activation of downstream components at various stages of the signaling pathway.

c. Interactions between the sugar analogs and orthogonal therapeutic strategies such as drugs that target the same receptor but act by an alternative mode of action were characterized and chemically modified sugar analogs were screened for similar effects.

This aim will test the hypothesis that metabolic flux through glycosylation pathways plays an important role in determining the glycosylation profile of a cell and that glycosyltransferases are not the only determinant of observed patterns of glycosylation. It will also test the hypothesis that certain surface receptors are more susceptible to alterations in glycosylation profile and will be selectively affected when using sugar analogs to alter flux through glycosylation pathways. This aim will then test the hypothesis that changes in a cell surface receptor's glycosylation profile correspond to changes in its signaling. This aim will further test the hypothesis that MOE based therapies can be used to augment existing orthogonal therapeutic strategies and that non-natural functionalized sugar analogs can elicit similar effects as their natural counterparts

Specific aim 2 is addressed in **Chapter 5** which describes the use of glycoproteomic mass spectrometry in SW1990 pancreatic cancer cells to identify proteins whose glycosylation profiles are changed in response to treatment with 1,3,4-*O*-Bu_3ManNAc. characterization of the functional effect of increased sialylation of the epidermal growth factor receptor (identified in Aim 1.c as having increased sialylation on 1,3,4-*O*-Bu_3ManNAc treatment) and the development of a combinatorial approach wherein the sugar analog is shown to have synergy when co-administered with EGFR targeting drugs

(Erlotinib and Gefitinib). The azido derivative of this sugar analog (1,3,4-*O*-Bu_3ManNAz) is also shown to exhibit this synergistic interaction with Erlotinib.

Specific Aim 3: To characterize the molecular mechanisms by which changes in glycosylation leads to altered receptor signaling, using EGFR as a model system:

Aim 3 can be divided into two specific sub aims:

a) A computational model of EGFR trafficking and recycling was implemented and used to predict possible molecular mechanisms for experimental observations from specific aim 2 b.

b) Model predictions that internalization and recycling were key factors in the mechanism by which analog induced increases in EGFR sialylation affect its signaling were experimentally verified.

c) Further characterization of internalization patterns showed a shift from clathrin coated endocytosis toward non clathrin coated endotcytosis consistent with modelling results

This aim will attempt to identify the specific molecular mechanism by which analog induced changes in glycosylation affect receptor function.

Specific Aim 3 is the focus of **Chapter 6**. Here a mathematical model is implemented and used to predict potential mechanisms by which increased sialylation could suppress EGFR signaling, based on the model's predictions that recycling and internalization were

critical factors experiments were performed that showed that the effect of the sugar analog was likely via a shift from clathrin coated endocytosis toward non clathrin coated endocytosis mediated by a disruption in the galectin lattice caused by increased sialylation masking the galectin's binding epitope (terminal galactose residues).

CHAPTER 2

THE ROLE OF GLYCOSYLATION AND EMERGING METABOLIC OLIGOSACCHARIDE ENGINEERING IN CANCER PROGRESSION AND THERAPIES

ABSTRACT

This introductory chapter covers three topics that are fundamental to the subsequent work described in this thesis. First, in Section 2.1, an overview of an often underappreciated driving force behind cancer progression – which is the role of glycosylation – is covered. Then, in Section 2.2, N-glycans – which is a subset of glycosylation that virtually all cell surface and secreted glycans are subject to – are discussed. Finally, in Section 2.3 "metabolic oligosaccharide engineering" is covered; this emerging technology is the basis of the cancer therapies described in the remainder of this thesis including (1) the metabolic processing of prodrug sugar analogs (in Specific Aim 1/Chapters 3 and 4), (2) the understanding of the functional role analog induced changes in glycosylation play in EGFR signaling (in Specific Aim 2/Chapter 5); and the underlying molecular mechanism by which increased sialylation acts (in Specific Aim 3/Chapter 6).

2.1 GLYCOSYLATION IN THE CONTEXT OF CANCER

2.1.1 The Importance of Glycosylation

The post translational modifications of proteins is crucial in developing the complex functions involved in human health and disease, of these modifications glycosylation is one of the most complex and ubiquitous (1, 2). Numerous enzymes and transporters work in concert to attach a plethora of oligosaccharide structures to proteins and lipids. Glycosylation has been shown to play a number of important roles in the functioning of proteins and lipids. The 'Yin-Yang' relationship between O-GlcNAcylation phosphorylation of cytoplasmic and nuclear proteins plays a role in dynamic signaling processes (3, 4). The proper folding and thus effective functioning of nascent proteins has been shown to be dependent on the attachment of N-linked oligosaccharides (5). The surface of a cell is decorated with a vast variety of glycans that help modulate numerous essential cell recognition and binding events (1, 6). Glycans on the cell surface not only determine how a cell is perceived and how it perceives its environment but also makes up a storage system for a wealth of information (7). This 'carbohydrate code' plays an important role in human health and disease whereby alterations in the glycan display can help to direct and mediate the immune system (6, 8, 9). Considering the vast repertoire of functions glycosylation is associated with it is not surprising that abnormalities and anomalies are correlated to diseases such as cancer (10), congenital diseases (11) and immune dysfunction (12).

Despite the importance and prevalence of glycosylation attempts to decipher the molecular mechanisms behind their functions has lagged behind studies on protein and nucleic acids (13). This is partially due to the difficulty in genetically manipulating

glycan structures but also due to the innate heterogeneity caused by the non template driven nature of the glycosylation biosynthetic process (1). While homogenous glycans can be produced by chemical (14) or enzymatic (15) methods cellular studies necessitate a means to modulate these glycans in their natural environment. It is from this need that the field of metabolic oligosaccharide engineering (MOE) was born (1).

2.1.2 Abnormal Glycosylation is a Hallmark of Cancer (16, 17, 90, 91).

Glycosyltransferases such as MGAT5 have been implicated as key factors in generating the characteristic alterations in glycosylation observed in cancer (17, 91). However, glycosylation is a non-template driven process and as a result, apart from the availability of the necessary enzymes the flux of substrate through the pathways could also influence the types of structures being produced. In fact, the Warburg effect (which has recently been recognized as 'next generation' hallmark of cancer (18, 92)) wherein cells take up large amounts of glucose to allow the cell to use glycolysis as a primary mode of energy production could lead to significant changes in metabolic flux through the glycosylation machinery as a small fraction of glucose taken up is shunted into the hexose biosynthetic pathway. Hence, it too could play a role in generating the characteristic glycosylation patterns observed in cancer. While a number of studies target the glycosyltransferases as a means of studying changes in glycosylation (19, 93), MOE provides an alternative means of modulating glycosylation patterns and since it starts out using the cells existing glycosylation machinery it could prove a useful tool for identifying proteins that are susceptible to alteration in glycosylation as well as what changes in glycosylation patterns cancer cells are predisposed towards.

2.1.3 Understanding the Functional Role of Abnormal Glycosylation in Cancer Progression

For the most part the changes in glycosylation pattern have been viewed as passive by products of abnormal metabolism with efforts largely being directed at using these characteristic abnormalities as biomarkers for cancer detection (20, 21, 94, 95). More recently glycosylation has been shown to play a number of crucial roles in the activity and localization of proteins and in the overall behavior of cells (19, 22-26, 93, 96-100). For example α2-6 sialylation has been shown to modulate carcinoma diffentiation in vivo (19, 93) and the N-linked glycosylation of IL-13 Rα2 has been shown to be essential of IL-13 activity (26, 100). While cancer related glycosylation abnormalities may have a metabolic origin they likely play a much larger role in the maturation of the disease phenotype and in its eventual progression. With cell surface receptor known to be universally glycosylated, understanding the effect of alterations in the glycans attached to them on their behavior is essential for a more complete understanding of the disease. Altered glycosylation could play a role in altering the sensitivity of cancer cells to environmental cues and may color how cancer cells perceive their environment. In addition, many surface receptors are linked to numerous phosphorylation cascades and altered behavior of these proteins could be amplified downstream and could lead to alteration in gene expression in their own right which could play a role in the progression of the disease. In addition to this glycosylation forms a large portion of the external interface by which cells interact with their environment, as a result alterations in glycosylation affect not only how a cell perceives its environment but also how it is viewed by the environment/immune system etc. Determining the molecular mechanism

by which altered glycosylation can affect receptor function will not only improve our understanding of the role glycosylation play in the progress of cancer but could also suggest possible orthogonal therapeutics that could synergistically be combined with glycosylation based therapy.

2.1.4 Applying Glycosylation Based Therapies Towards Pancreatic Cancer.

Pancreatic cancer which has one of the worst prognoses of any type of cancer with 5 year survival rates of as low as 4% (27, 101). As a result there is a pressing need for new therapeutic strategies. One approach that is being explored is to target EGFR, as the overexpression of EGFR in pancreatic cancer has been linked to poor prognosis (28-30, 102-104). Gefitinib and erlotinib are two such EGFR antagonists that block ATP binding to EGFR tyrosine kinase and thus reduce signaling down the EGFR signaling cascade and hence inhibiting cancer cell proliferation and survival (31-33, 105-107). Since altered glycosylation induced by analog treatment likely acts by an orthogonal mechanism there is a possibility that they will have synergistic interactions with these drugs. Metabolic Oligosaccharide Engineering has been shown to be an effective method of installing novel functional groups on the surface of cells (34, 35, 108, 109). In addition since increased sialylation is one of the alterations commonly observed in cancer, with cancer cells often possessing elevated levels of sialyltransferases (19, 36, 37, 93, 110, 111). As a result increased sialylation has been used as a means of identifying tumors by MRI (38, 112) and Ac_4ManNAz has been shown to preferentially label tumor tissue over healthy tissue (39, 113). Hence, the development of an effective therapeutic delivery system aimed at a synthetic functional group in conjunction with MOE could prove to be an

means of better directing therapeutics towards cancer cells and help avoid some of the side effects of chemotherapy caused by non-specific activity of the drugs used.

This study aims to improve our understanding of some of the functional roles glycosylation plays and to translate this information towards clinical end points. It will also provide a procedural template by which the effect of altered glycosylation on protein and cell behavior can be effectively studied in the context of different types of cancer as well as in other diseases.

2.2 N-LINKED GLYCOSYLATION

2.2.1 A General Introduction to N-linked Glycosylation

N-linked glycosylation is the covalent linking of a carbohydrate to a protein via an asparagine residue in the consensus sequence Asn-X-Ser/Thr where X can be any amino acid except proline (40-42). Glycan size, complexity, composition and structure varies between glycans at different glycosites on a protein, between glycoproteins and between cell types, tissues and species (43, 44). N-Linked glycans are typically large, hydrophilic structures with molecular weights that range from around 1800 to 2800 KDa (45). The size and complexity of glycans sets them apart from other common post translational modifications which tend to be limited to involve a few molecules at most, whereas the size of glycans by volume can rival the size of the protein itself. As a result the addition of the sugar structures could dramatically alter the activity and function of a given protein (46).

2.2.2 N-Linked Glycan Synthesis and Processing

Although the final glycan structure displayed on a protein has been shown to be highly heterogeneous the initial 'core glycan' that is attached to nascent polypeptides inside the endoplasmic reticulum (ER) is quite homogenous ($GlcNAc_2Man_9Glc_3$) as depicted in **figure 2.1** (5, 46).

The first step in N-glycosylation is the attachment of this core glycan to membrane bound dolichylpyrophosphate precursor molecule on the cytoplasmic side of the ER (40, 44, 47). The enzyme flippase then 'flips' the glycan onto the inside of the ER. Enzymes within the ER then transfer the glycan from the dolichylpyrophosphate molecule onto the asparagine residue in the consensus sequence in the growing polypeptide (48-50). The 'sugar tree' is then 'trimmed' within the ERby mannosidases and glucosidases (44, 51). Finally the glycoproteins are transferred to the Golgi apparatus where further removal of mannose residues occurs. Often new sugar residues are also added within the golgi apparatas to produce complex glycan structures (5). A rough schematic representation of this process is shown in **figure 2.2.** While the biosynthetic processes in the ER are subject to significant quality control, the Golgi complexes do not have the same mechanisms in place and as a result mutations to glycosyltransferases and glucosidases can lead to abnormal glycans being attached to glycoproteins within the Golgi (52, 53). The absence of enzymes at the ER stage of the pathway leads to proteins that lack the oligosaccharide entirely, whereas absent enzymes in the Golgi can lead to alterations branching patterns and abnormal fucosylation. Numerous congenital disorders of glycosylation have been identified and shown to be due to the lack of certain enzymes or defective enzymes along this pathway (11, 54).

2.2.3 The Roles of N-Glycosylation

One of the most important and well characterized roles played by N-linked glycosylation is in the regulation of folding of newly synthesized polypeptides (43, 55). The necessity for glycan attachment can vary from protein to protein and also be glycosite dependent within the same protein with glycans presenting both 'global' and 'local' effects (5). The effects on folding can be direct or indirect. Direct effects on folding include: interacting with nearby residues and helping organize them into secondary structures (56, 57), large polar oligosaccharides can serve to orient sections of the peptide toward the solvent facing surface of the protein (46, 58), these glycans can also play a role in the refolding of proteins in a role similar to the one played by molecular chaperones (59). Although these glycans are not typically essential in maintaining the conformation of these proteins after the protein has been properly folded they have been shown to continue to have minor stabilizing effects (46, 55, 56).

A good example of the indirect effects of N-glycosylation is observed in the ER with the calnexin-calreticulin cycle which is a unique chaperone system (60-62). Calnexin (membrane bound) and calreticulin are lectins (proteins that bind to glycans). These proteins bind to the newly formed glycan which serves as a means of entry into the cycle, the two lectins bind transiently to the glycan whilst a co-chaperone ERp57 ensures the synthesis of necessary disulphide bridges in the protein. The cycle serves to make folding process of the protein more deliberate and accurate (63-67).

ER associated degradation (ERAD) is also modulated by N-glycosylation (68, 69), here the trimming of the nascent glycan by mannosidase aids the sorting process and ensures that proteins that don't attain the required conformation are ubiquitinated and fated for

degradation (68, 70, 71). The slow activity of the mannosidases is also believed to play an essential role in a timing mechanism wherein the lifetime of a protein is determined (55, 72, 73).

Lectins like ERGIC-53 and VIP36 which are specific to mannose are thought to serve as cargo capture and transport receptors for transport of glycoproteins from ER-to-Golgi. ERGIC-53 helps to speed up in a glycan dependent manner Cathepsin Z transport from the ER to the Golgi (74).

Lectins also work to sequester lysosomal hydrolases from the trans-golgi network. Lysosomal hydrolases in the cis-golgi compartment are specifically modified with the addition of a GlcNAc phosphate onto terminal or sub terminal mannose residues by enzymes localized to that compartment. The removal of these GlcNAc residues results in the presentation Mannose-6-Phosphate (M-6-P) groups. M-6-P is recognized by a series of receptors, this interaction plays a key role in transport of these hydrolases via clathrin coated vesicles to endosomes and lysosomes (75).

2.3 METABOLIC OLIGOSACCHARIDE ENGINEERING

2.3.1 Metabolic Engineering

Metabolic engineering aims to alter cellular properties by modifying specific cellular pathways or introducing new ones. Typically metabolic engineering focuses on the importance of using metabolic fluxes as determinants of cellular physiology and as a means of control of metabolism. The idea of looking at pathways in their entirety rather

than at individual components or reactions in isolation is a key concept of metabolic engineering. It aspires to shift focus away from individual enzymatic reactions and towards a more comprehensive integrated metabolic network (76).

In order to quantitatively characterize and understand metabolic networks the concepts of metabolic fluxes were developed as a means by which reaction stoichiometry can be used to organize a mathematical framework upon which metabolic flux distributions can be structured (77).

The first attempts to manipulate metabolic pathways were to improve productivity of microorganisms and started with the use of chemical mutagenesis and selective techniques. The field took a significant step forward with advent of molecular biology techniques that facilitated DNA recombination. The ability to make specific targeted changes to enzymes within a metabolic network led to the development of a number of metabolic engineering applications (78, 79). Metabolic engineering was used in microbes to improve their productivity and yield of native products (80-83). It enabled the expansion of substrate ranges in certain organisms and facilitated the production of metabolites that were either new to the host cell (84-86) or entirely novel (87, 88). Cellular properties were also engineered with cells imbued with the ability to tolerate hypoxic fermentation conditions (89), prevent overflow metabolism (90), etc. Finally another broad application of metabolic engineering has been in the study of entire organs or tissues and in the identification of targets for disease control (91).

In order to explore and expand the landscape of protein structure and function, some studies looked at the incorporation of non-natural into proteins. While a handful of

analogs were tolerated and incorporated by the existing natural t-RNA synthetases (e.g. azidohomoalanine (92)) most required a corresponding mutation to its t-RNA synthetase (93-96). In contrast, incorporation of non-natural sugar analogs by metabolic oligosaccharide engineering was far easier and could be performed in almost any mammalian cell line without the need to tweak the biosynthetic machinery. Sialic acid engineering was especially attractive due to the observed permissivity of the sialic acid biosynthetic pathway (97-100).

2.3.2 A Brief History of Metabolic Oligosaccharide Engineering

Observation that changes in sialic acid metabolism promoted carcinogenesis in the early 1980s led to attempts to inhibit sialic acid production (101). N-Acetyl-D-mannosamine (ManNAc) is the primary feedstock in the sialic acid pathway. The first passes at MOE focused on the use of fluoro analogs of ManNAc to inhibit the biosynthesis of sialic acid (102, 103). Numerous groups also attempted to develop mono and disaccharide analogs to inhibit glycosylation pathways as well as specific glycan motifs leading to the successful inhibition of sialyl lewis X (104, 105) and poly sialic acid structure production (106, 107). Like the discovery of penicillin, a series of unusual observations led to a ground breaking finding. These ManNAc analogs that had been designed to inhibit the sialic acid pathway were instead being converted into the corresponding non-natural forms of sialic acid and being installed into sialosides that were presented on the surface of the cell (102, 103). Reutter's group expanded on these findings to show that ManNAc analogs with extended N-acyl groups could be used to deliberately engineer the cell surface (108, 109). This permissivity of the sialic acid biosynthetic pathway allowed a number of ManNAc analogs bearing functional groups such as hydroxyls (100), thiols

(97), azides (99) and ketones (98) to be incorporated onto the cell surface via the non-natural forms of sialic acid. **Figure 2.3** presents a summary of various MOE approaches.

2.3.3 Developing and Characterizing SCFA-Linked Sugar Analogs as Tools for Metabolic Oligosaccharide Engineering (MOE).

The uptake of naked sugar analogs is very inefficient and often requires millimolar concentration ranges for adequate uptake. To address this issue short chain fatty acid (SCFA) groups like the acetate group were attached to the analogs to make them more hydrophobic and hence facilitate their diffusion into the cell. These acetylated analogs were metabolized almost 900 fold more efficiently leading to more robust cellular responses in micro molar concentration ranges (104, 110). Attempts to further improve cellular uptake by increasing hydrophobicity using longer chain SCFAs like propionate and butyrate groups led to 1800 fold and 2100 fold higher flux through the sialic acid pathway respectively when compared to regular ManNAc (111).

The SCFA-linked sugar analog acts somewhat like a prodrug in that it needs to be processed by esterases to yield the core sugar that can then influence the flux through glycosylation pathways. However, extracellular esterases present in serum could also process the analogs leading to inactivation of the analog. Therefore the extracellular processing of SCFA-linked sugar analogs needs to be properly characterized. Secondly, once inside the cell the SCFA groups must be removed by intracellular esterases in order to release the core sugar. Thus the intracellular processing of esterases must also be studied, in addition to this intracellular esterases exist in the golgi apparatus and hence can be glycosylated and possibly affected by the change in flux through glycosylation

pathways and hence possible crosstalk between the sugar analogs and the esterases that are responsible for their processing must also be accounted for.

2.3.4 New Layers of Complexity and Whole Molecule Effects

For the most part it was assumed that these hybrid molecules were completely hydolysed and that resulting activity was because of the liberated core sugar or SCFA. One SCFA that was studied was n-butyrate. n-Butyrate is a known histone deacetylase inhibitor (HDACi) and therfore can inhibit the growth of cancer cells by up-regulating the production of cell cycle checkpoint p21 proteins. Similar to ManNAc, n-butyrate had poor pharmacological properties. However, when the two were combined the resulting compound had much better pharmacological properties than either on its own the two acted as 'mutual prodrugs' (112).

Bu_4ManNAc depicted in **figure 2.4** exhibited higher toxicity in cancer cells than a Bu_5Mannose compound that had previously been evaluated as a means of delivery of n-butyrate to cancer cells (111-113). Surprisingly, the two tributanoylated forms of ManNAc -1,3,4-*O*-Bu_3ManNAc and 3,4,6-*O*-Bu_3ManNAc showed markedly different behavior. The 1,3,4-*O*-Bu_3ManNAc showed a high flux through the sialic acid pathway with low toxicity whereas the 3,4,6-*O*-Bu_3ManNAc showed very high toxicity (higher even than the Bu_4ManNAc) (113). This indicated that apart from their direct effect, the two individual components also displayed some whole molecule effects that were unique to each compound. Both Bu_4ManNAc and 3,4,6-*O*-Bu_3ManNAc were shown to result in cell apoptosis and downregulating the NF-κB pathway.

The discovery of whole molecule effects gave the understanding of extracellular and intracellular esterases that are involved in the processing of these sugar analogs a much greater importance. Apart from the complete hydrolysis of the compound that would render the SCFA-linked sugar analog unable to enter the cell at the much lower concentrations they are used at, the removal of a specific side group could fundamentally alter the activity of the analog (both qualitatively by selectively favoring certain patterns of SCFAs or quantitatively by changing the kinetics of butyrate removal). As a result the initial goal of this thesis was to characterize the extracellular esterase processing of these butyrated sugar analogs.

Initial studies on intracellular esterases led to some unusual findings. An esterase activity assay designed to titrate a fluorescent esterase substrate against the SCFA analogs showed an increase in activity rather than a decrease without a corresponding change in transcription levels of various esterases measured by RT-PCR data. These results further implicate the importance of characterizing the crosstalk between esterases which are responsible for analog processing but are also N-glycosylated and hence could in turn be affected by changes in glycosylation patterns caused by the release of the core sugar.

2.4 FIGURES

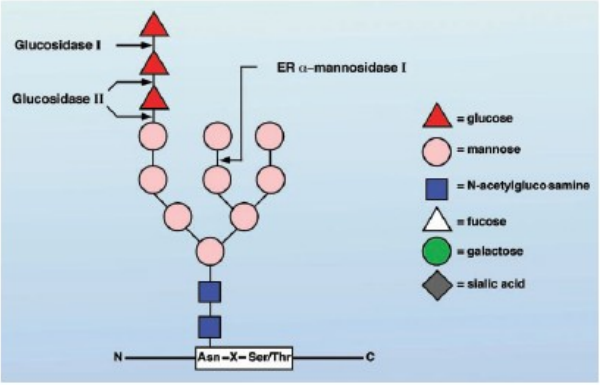

Figure 2.1 *the general core glycan structure of an N-linked glycan* (5).

Figure 2.2: Outline of N-linked glycoprotein biosynthesis showing topography and major biosynthetic events*. Production of the Dol-PP-14-mer begins on the cytosolic side of the ER and is flipped to the luminal side after the assembly of two GlcNAc and five Man residues* ***(A)****. An additional four Man and three Glc residues are added to create the* $GlcNAc_2Man_9Glc_3$ *14-mer that is transferred en bloc by an oligosaccharyltransferase (OST) to a newly synthesized, yet unfolded peptide* ***(B)****. Trimming of the Glc residues controls protein folding in the calnexin / calreticulin cycle in the ER* ***(C)****. This is followed by transfer to the cis-Golgi lumen* ***(D)*** *where removal of four Man residues produces the* $GlcNAc_2Man_5$ *'core' structure that is subsequently elaborated into a diverse array of high mannose, complex, and hybrid N-glycans. Enzyme abbreviations are shown (where known), and updated information on enzymatic activity (indicated by the E.C. number) can be found in online data bases such as Kyoto Encyclopedia of Genes and Genomes (KEGG) Glycan Pathway resources (http://www.genome.jp/kegg/glycan/ or http://www.genome.jp/kegg/pathway.html)* (114).

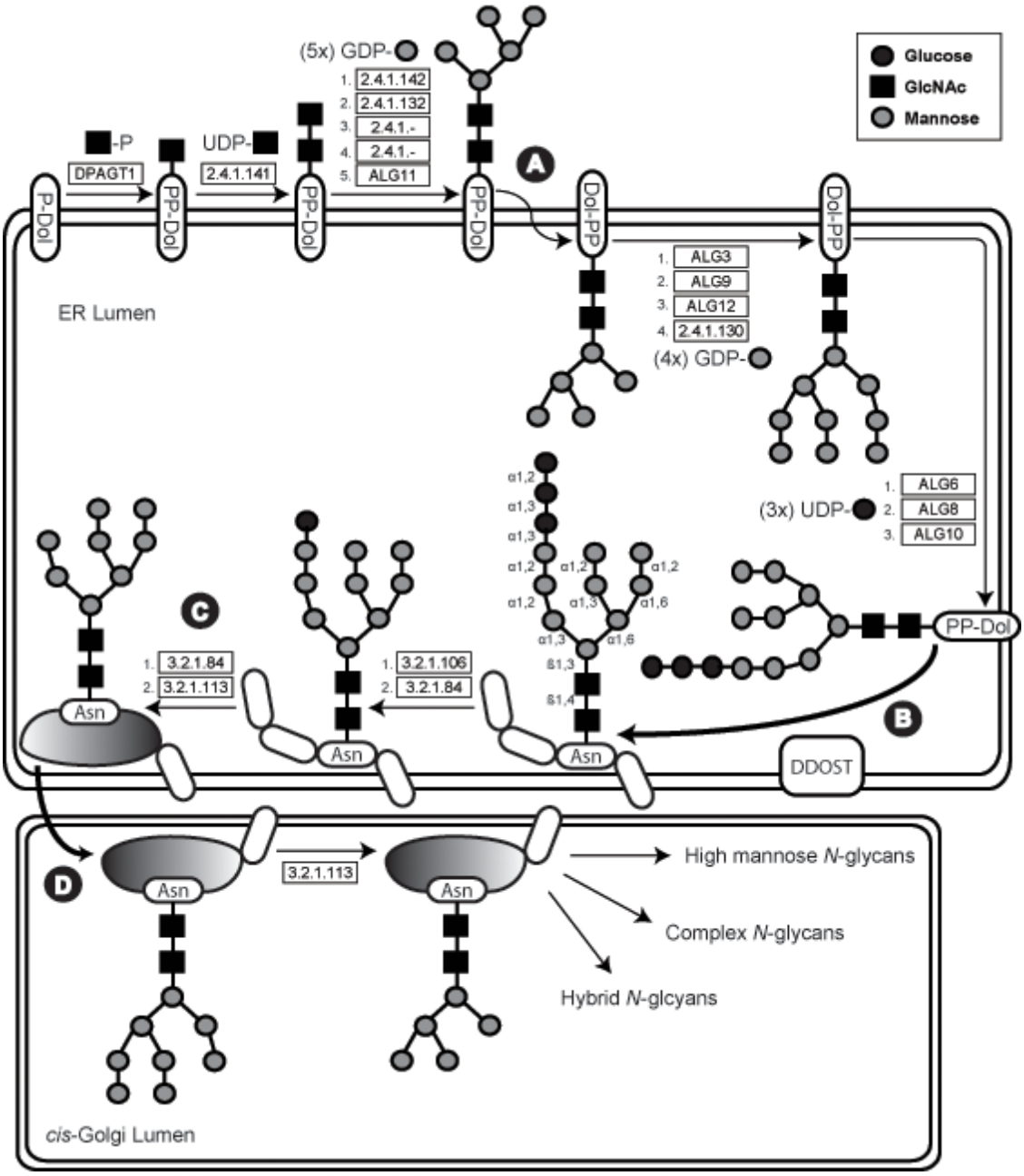
Glucose
GlcNAc
Mannose
(5x) GDP-
1. 2.4.1.142
2. 2.4.1.132
3. 2.4.1.-
4. 2.4.1.-
5. ALG11
-P
DPAGT1
UDP-
2.4.1.141
P-Dol
PP-Dol
A
Dol-PP
ER Lumen
1. ALG3
2. ALG9
3. ALG12
4. 2.4.1.130
(4x) GDP-
(3x) UDP-
1. ALG6
2. ALG8
3. ALG10
α1,2
α1,3
α1,6
PP-Dol
B
C
1. 3.2.1.84
2. 3.2.1.113
1. 3.2.1.106
2. 3.2.1.84
Asn
DDOST
D
3.2.1.113
High mannose N-glycans
Complex N-glycans
Hybrid N-glcyans
cis-Golgi Lumen

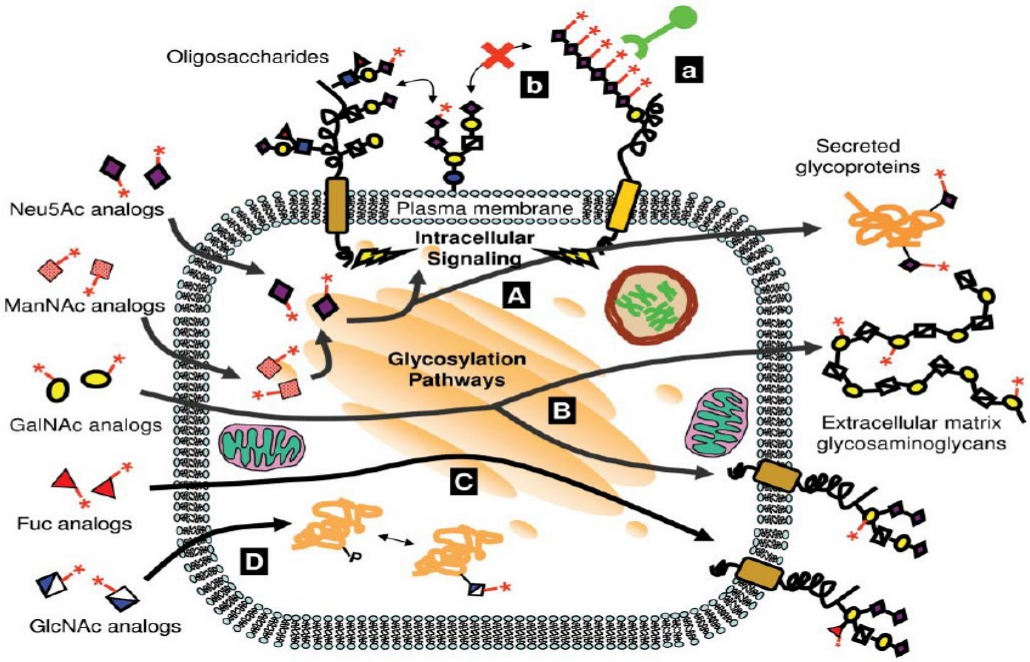

Figure 2.3 *Strategies for MOE involve the use of ManNAc, GalNAc, GlcNAc, Neu5Ac and fucose analogs. (A) Sialic acid engineering uses ManNAc or Neu_5Ac analogs, these analogs allow the incorporation of functional groups (*) into cell surface or secreted glycol proteins. Functional groups on surface proteins can serve as (a) chemical handles for binding of labels or (b) modifying the interactions between cell surface moieties such as integrins. (B) GalNAc analogs can be incorporated into O-linked glycans as well as ECM polysaccharides. (C) fuc analogs can be used to study modification to fucosylated glycans which include blood group antigens. (D) GlcNAc anaolgs can be used to label O-GlcNAcylated proteins* (4)

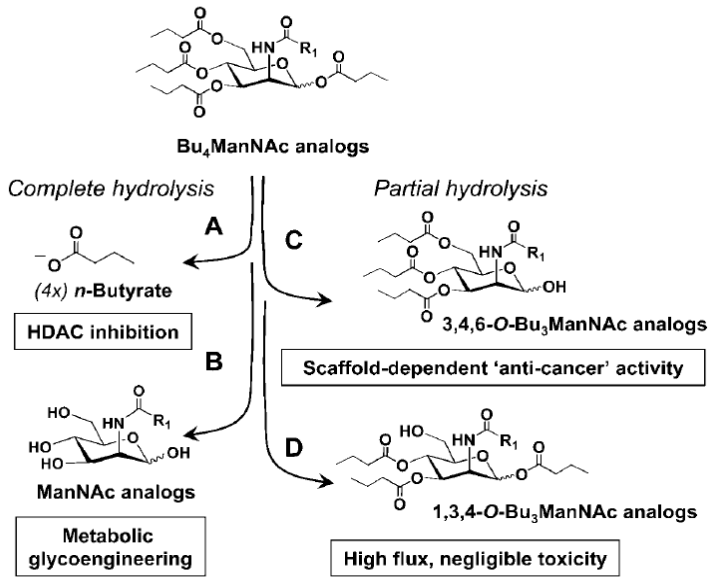

Figure 2.4 *The SCFA ManNAc analogs have 3 main modes of activity. The complete hydrolysis of the compound results in n-butyrate groups (A) and the carbohydrate (the R1 modified ManNAc). Partial hydrolysis can result in the formation of a butanoylated analog lacking a butyrate group at either the C1-OH or the C6-OH position. 3,4,6-O-Bu$_3$ManNAc (C) has been shown to have high scaffold dependent anti-cancer activity whereas 1,3,4-O-Bu$_3$ManNAc (D) is shown to have a high flux through the sialic acid pathway and negligible toxicity. In general, the absence of a SCFA at the C6-OH position results in 'inactive' analogs that have negligible toxicity, do not suppress oncogene activity and have a high flux through the sialic acid pathway* (115).

2.4 REFERENCES

1. Dube, D.H., and Bertozzi, C.R. (2003) Metabolic oligosaccharide engineering as a tool for glycobiology. *Curr.Opin.Chem.Biol.* **7,** 616-625

2. Venter, J.C., Adams, M.D., Myers, E.W., Li, P.W., Mural, R.J., Sutton, G.G., Smith, H.O., Yandell, M., Evans, C.A., and Holt, R.A. (2001) The sequence of the human genome. *Science.* **291,** 1304-1351

3. Zachara, N.E., and Hart, G.W. (2002) The emerging significance of O-GlcNAc in cellular regulation. *Chem.Rev.* **102,** 431-438

4. Campbell, C.T., Sampathkumar, S.G., and Yarema, K.J. (2007) Metabolic oligosaccharide engineering: perspectives, applications, and future directions. *Mol.BioSyst.* **3,** 187-194

5. Helenius, A. (2001) Intracellular functions of N-linked glycans. *Science.* **291,** 2364-2369

6. Rudd, P.M., Elliott, T., Cresswell, P., Wilson, I.A., and Dwek, R.A. (2001) Glycosylation and the immune system. *Science.* **291,** 2370-2376

7. Gabius, H.J., Siebert, H.C., André, S., Jiménez-Barbero, J., and Rüdiger, H. (2004) Chemical biology of the sugar code. *ChemBioChem.* **5,** 740-764

8. Daniels, M.A., Hogquist, K.A., and Jameson, S.C. (2002) Sweetn'sour: the impact of differential glycosylation on T cell responses. *Nat.Immunol.* **3,** 903-910

9. Kannagi, R. (2002) Regulatory roles of carbohydrate ligands for selectins in the homing of lymphocytes. *Curr.Opin.Struct.Biol.* **12,** 599-608

10. Fuster, M.M., and Esko, J.D. (2005) The sweet and sour of cancer: glycans as novel therapeutic targets. *Nat Rev Cancer.* **5,** 526-542

11. Freeze, H.H., and Aebi, M. (2005) Altered glycan structures: the molecular basis of congenital disorders of glycosylation. *Curr.Opin.Struct.Biol.* **15,** 490-498

12. Dube, D.H., and Bertozzi, C.R. (2005) Glycans in cancer and inflammation—potential for therapeutics and diagnostics. *Nat Rev Drug Discov.* **4,** 477-488

13. Bertozzi, C.R. (2001) Chemical glycobiology. *Science.* **291,** 2357-2364

14. Seeberger, P.H., and Haase, W.C. (2000) Solid-phase oligosaccharide synthesis and combinatorial carbohydrate libraries. *Chem.Rev.* **100,** 4349-4394

15. Sears, P., and Wong, C.H. (2001) Toward automated synthesis of oligosaccharides and glycoproteins. *Science.* **291,** 2344-2350

16. Kim, Y.J., and Varki, A. (1997) Perspectives on the significance of altered glycosylation of glycoproteins in cancer. *Glycoconj.J.* **14,** 569-576

17. Varki A, Kannagi R, Toole BP. Glycosylation changes in cancer. In: Varki A, Cummings RD, Esko JD, et al., editors. Essentials of Glycobiology. 2nd edition. Cold Spring Harbor (NY): Cold Spring Harbor Laboratory Press; 2009. Chapter 44. Available from: http://www.ncbi.nlm.nih.gov/books/NBK1963/

18. Hanahan, D., and Weinberg, R.A. (2011) Hallmarks of cancer: the next generation. *Cell.* **144,** 646-674

19. Hedlund, M., Ng, E., Varki, A., and Varki, N.M. (2008) α2-6–Linked sialic acids on N-glycans modulate carcinoma differentiation in vivo. *Cancer Res.* **68,** 388-394

20. Kuzmanov, U., Kosanam, H., and Diamandis, E.P. (2013) The sweet and sour of serological glycoprotein tumor biomarker quantification. *BMC Med.* **11,** 31-7015-11-31

21. Nie, S., Lo, A., Wu, J., Zhu, J., Tan, Z., Simeone, D.M., Anderson, M.A., Shedden, K.A., Ruffin, M.T., and Lubman, D.M. (2014) Glycoprotein biomarker panel for pancreatic cancer discovered by quantitative proteomics analysis. *J.Prot.Res.* **13,** 1873-1884

22. Tsuda, T., Ikeda, Y., and Taniguchi, N. (2000) The Asn-420-linked sugar chain in human epidermal growth factor receptor suppresses ligand-independent spontaneous oligomerization: Possible role of a specific sugar chain in controllable receptor activation. *J.Biol.Chem.* **275,** 21988-21994

23. Liu, Y., Yen, H., Chen, C., Chen, C., Cheng, P., Juan, Y., Chen, C., Khoo, K., Yu, C., and Yang, P. (2011) Sialylation and fucosylation of epidermal growth factor receptor suppress its dimerization and activation in lung cancer cells. *Proc.Natl.Acad.Sci.* **108,** 11332-11337

24. Ling, Y., Li, T., Perez-Soler, R., and Haigentz Jr, M. (2009) Activation of ER stress and inhibition of EGFR N-glycosylation by tunicamycin enhances susceptibility of

human non-small cell lung cancer cells to erlotinib. *Cancer Chemother.Pharmacol.* **64,** 539-548

25. Lajoie, P., Partridge, E.A., Guay, G., Goetz, J.G., Pawling, J., Lagana, A., Joshi, B., Dennis, J.W., and Nabi, I.R. (2007) Plasma membrane domain organization regulates EGFR signaling in tumor cells. *J.Cell Biol.* **179,** 341-356

26. Kioi, M., Seetharam, S., and Puri, R.K. (2006) N-linked glycosylation of IL-13Rα2 is essential for optimal IL-13 inhibitory activity. *The FASEB journal.* **20,** 2378-2380

27. Brenner, H. (2002) Long-term survival rates of cancer patients achieved by the end of the 20th century: a period analysis. *The Lancet.* **360,** 1131-1135

28. Yamanaka, Y., Friess, H., Kobrin, M.S., Buchler, M., Beger, H.G., and Korc, M. (1993) Coexpression of epidermal growth factor receptor and ligands in human pancreatic cancer is associated with enhanced tumor aggressiveness. *Anticancer Res.* **13,** 565-569

29. Tobita, K., Kijima, H., Dowaki, S., Kashiwagi, H., Ohtani, Y., Oida, Y., Yamazaki, H., Nakamura, M., Ueyama, Y., and Tanaka, M. (2003) Epidermal growth factor receptor expression in human pancreatic cancer: Significance for liver metastasis. *Int.J.Mol.Med.* **11,** 305-309

30. Korc, M. (1998) Role of growth factors in pancreatic cancer. *Surg.Oncol.Clin.N.Am.* **7,** 25-41

31. Durkin, A.J., Osborne, D.A., Yeatman, T.J., Rosemurgy, A.S., Armstrong, C., and Zervos, E.E. (2006) EGF receptor antagonism improves survival in a murine model of pancreatic adenocarcinoma. *J.Surg.Res.* **135,** 195-201

32. Frolov, A., Schuller, K., Tzeng, C., Cannon, E.E., Ku, B.C., Howard, J.H., Vickers, S.M., Heslin, M.J., Buchsbaum, D.J., and Arnoletti, J.P. (2007) ErbB3 expression and dimerization with EGFR influence pancreatic cancer cell sensitivity to erlotinib. *Cancer.Biol.Ther.* **6,** 548-554

33. Solorzano, C.C., Baker, C.H., Tsan, R., Traxler, P., Cohen, P., Buchdunger, E., Killion, J.J., and Fidler, I.J. (2001) Optimization for the blockade of epidermal growth factor receptor signaling for therapy of human pancreatic carcinoma. *Clin.Cancer Res.* **7,** 2563-2572

34. Chang, P.V., Chen, X., Smyrniotis, C., Xenakis, A., Hu, T., Bertozzi, C.R., and Wu, P. (2009) Metabolic labeling of sialic acids in living animals with alkynyl sugars. *Angew. Chem. Int. Ed. Engl.* **48,** 4030-4033

35. Laughlin, S.T., Agard, N.J., Baskin, J.M., Carrico, I.S., Chang, P.V., Ganguli, A.S., Hangauer, M.J., Lo, A., Prescher, J.A., and Bertozzi, C.R. (2006) Metabolic labeling of glycans with azido sugars for visualization and glycoproteomics. *Meth.Enzymol.* **415,** 230-250

36. Schneider, F., Kemmner, W., Haensch, W., Franke, G., Gretschel, S., Karsten, U., and Schlag, P.M. (2001) Overexpression of sialyltransferase CMP-sialic

acid:Galbeta1,3GalNAc-R alpha6-Sialyltransferase is related to poor patient survival in human colorectal carcinomas. *Cancer Res.* **61,** 4605-4611

37. Bos, P.D., Zhang, X.H., Nadal, C., Shu, W., Gomis, R.R., Nguyen, D.X., Minn, A.J., van de Vijver, Marc J, Gerald, W.L., and Foekens, J.A. (2009) Genes that mediate breast cancer metastasis to the brain. *Nature.* **459,** 1005-1009

38. Lemieux, G.A., Yarema, K.J., Jacobs, C.L., and Bertozzi, C.R. (1999) Exploiting differences in sialoside expression for selective targeting of MRI contrast reagents. *J.Am.Chem.Soc.* **121,** 4278-4279

39. Neves, A.A., Stockmann, H., Harmston, R.R., Pryor, H.J., Alam, I.S., Ireland-Zecchini, H., Lewis, D.Y., Lyons, S.K., Leeper, F.J., and Brindle, K.M. (2011) Imaging sialylated tumor cell glycans in vivo. *FASEB J.* **25,** 2528-2537

40. Burda, P., and Aebi, M. (1999) The dolichol pathway of N-linked glycosylation. *BBA-Gen Subjects.* **1426,** 239-257

41. Imperiali, B. (1997) Protein glycosylation: the clash of the Titans. *Acc.Chem.Res.* **30,** 452-459

42. Silberstein, S., and Gilmore, R. (1996) Biochemistry, molecular biology, and genetics of the oligosaccharyltransferase. *FASEB J.* **10,** 849-858

43. Paulson, J.C. (1989) Glycoproteins: what are the sugar chains for?. *Trends Biochem.Sci.* **14,** 272-276

44. Kornfeld, R., and Kornfeld, S. (1985) Assembly of asparagine-linked oligosaccharides. *Annu.Rev.Biochem.* **54,** 631-664

45. Meldal, M., and St Hilaire, P.M. (1997) Synthetic methods of glycopeptide assembly, and biological analysis of glycopeptide products. *Curr.Opin.Chem.Biol.* **1,** 552-563

46. Imperiali, B., and O'Connor, S.E. (1999) Effect of N-linked glycosylation on glycopeptide and glycoprotein structure. *Curr.Opin.Chem.Biol.* **3,** 643-649

47. Gahmberg, C.G., and Tolvanen, M. (1996) Why mammalian cell surface proteins are glycoproteins. *Trends Biochem.Sci.* **21,** 308-311

48. Von Heijne, G., and Manoil, C. (1990) Membrane proteins: from sequence to structure. *Protein Eng.* **4,** 109-112

49. Bause, E. (1983) Structural requirements of N-glycosylation of proteins. Studies with proline peptides as conformational probes. *Biochem.J.* **209,** 331-336

50. Imperiali, B., and Rickert, K.W. (1995) Conformational implications of asparagine-linked glycosylation. *Proc.Natl.Acad.Sci.* **92,** 97-101

51. Moremen, K., Trimble, R.B., and Herscovics, A. (1994) Glycosidases of the asparagine-linked oligosaccharide processing pathway. *Glycobiology.* **4,** 113-125

52. Palade, G. (1975) Ultrastructural aspects of the process of protein secretion. *Science.* **189,** 347-358

53. Stanley, P. (1984) Glycosylation mutants of animal cells. *Annu.Rev.Genet.* **18,** 525-552

54. Imbach, T., Schenk, B., Schollen, E., Burda, P., Stutz, A., Grunewald, S., Bailie, N.M., King, M.D., Jaeken, J., and Matthijs, G. (2000) Deficiency of dolichol-phosphate-mannose synthase-1 causes congenital disorder of glycosylation type Ie. *J.Clin.Invest.* **105,** 233-239

55. Helenius, A. (1994) How N-linked oligosaccharides affect glycoprotein folding in the endoplasmic reticulum. *Mol.Biol.Cell.* **5,** 253

56. Wormald, M.R., and Dwek, R.A. (1999) Glycoproteins: glycan presentation and protein-fold stability. *Structure.* **7,** R155-R160

57. O'Connor, S.E., and Imperiali, B. (1996) Modulation of protein structure and function by asparagine-linked glycosylation. *Chem.Biol.* **3,** 803-812

58. Kern, G., Kern, D., Jaenicke, R., and Seckler, R. (1993) Kinetics of folding and association of differently glycosylated variants of invertase from Saccharomyces cerevisiae. *Protein Sci.* **2,** 1862-1868

59. Jaenicke, R. (1991) Protein folding: local structures, domains, subunits, and assemblies. *Biochemistry (N.Y.).* **30,** 3147-3161

60. Parodi, A.J. (2000) Role of N-oligosaccharide endoplasmic reticulum processing reactions in glycoprotein folding and degradation. *Biochem.J.* **348,** 1-13

61. Helenius, A., Trombetta, E.S., Hebert, D.N., and Simons, J.F. (1997) Calnexin, calreticulin and the folding of glycoproteins. *Trends.Cell.Biol.* **7,** 193-200

62. Zapun, A., Jakob, C.A., Thomas, D.Y., and Bergeron, J.J.M. (1999) Protein folding in a specialized compartment: the endoplasmic reticulum. *Structure.* **7,** R173-R182

63. Hammond, C., Braakman, I., and Helenius, A. (1994) Role of N-linked oligosaccharide recognition, glucose trimming, and calnexin in glycoprotein folding and quality control. *P Natl Acad Sci.* **91,** 913-917

64. Molinari, M., and Helenius, A. (1999) Glycoproteins form mixed disulphides with oxidoreductases during folding in living cells. *Nature.* **402,** 90-93

65. Ou, W.J., Cameron, P.H., Thomas, D.Y., and Bergeron, J.J. (1993) Association of folding intermediates of glycoproteins with calnexin during protein maturation. *Nature.* **364,** 771-776

66. Oliver, J.D., van der Wal, F.J., Bulleid, N.J., and High, S. (1997) Interaction of the thiol-dependent reductase ERp57 with nascent glycoproteins. *Science.* **275,** 86-88

67. Huppa, J.B., and Ploegh, H.L. (1998) The eS-Sence of-SH in the ER. *Cell.* **92,** 145-148

68. Plemper, R.K., and Wolf, D.H. (1999) Retrograde protein translocation: ERADication of secretory proteins in health and disease. *Trends.Biochem.Sci.* **24,** 266-270

69. Klausner, R.D., and Sitia, R. (1990) Protein degradation in the endoplasmic reticulum. *Cell.* **62,** 611-614

70. Kopito, R.R. (1997) ER quality control: the cytoplasmic connection. *Cell.* **88,** 427-430

71. Bonifacino, J.S., and Weissman, A.M. (1998) Ubiquitin and the control of protein fate in the secretory and endocytic pathways 1. *Annu.Rev.Cell Dev.Biol.* **14,** 19-57

72. Liu, Y., Choudhury, P., Cabral, C.M., and Sifers, R.N. (1997) Intracellular disposal of incompletely folded human α1-antitrypsin involves release from calnexin and post-translational trimming of asparagine-linked oligosaccharides. *J.Biol.Chem.* **272,** 7946

73. Jakob, C.A., Burda, P., Roth, J., and Aebi, M. (1998) Degradation of misfolded endoplasmic reticulum glycoproteins in Saccharomyces cerevisiae is determined by a specific oligosaccharide structure. *J.Cell Biol.* **142,** 1223-1233

74. Hauri, H.P., Appenzeller, C., Kuhn, F., and Nufer, O. (2000) Lectins and traffic in the secretory pathway. *FEBS Lett.* **476,** 32-37

75. Kornfeld, S. (1990) Lysosomal enzyme targeting. *Biochem.Soc.Trans.* **18,** 367-374

76. Stephanopoulos, G. (1999) Metabolic fluxes and metabolic engineering. *Metab.Eng.* **1,** 1-11

77. Varma, A., and Palsson, B.O. (1994) Metabolic Flux Balancing: Basic Concepts, Scientific and Practical Use. *Bio-technol.* **12,**

78. Cameron, D.C., and Tong, I.T. (1993) Cellular and metabolic engineering. *Appl.Biochem.Biotechnol.* **38,** 105-140

79. Stephanopoulos, G., Aristidou, A.A., Nielsen, J.H., and Nielsen, J. (1998) Metabolic engineering: principles and methodologies*, Academic Pr*

80. Ikeda, M., and Katsumata, R. (1992) Metabolic engineering to produce tyrosine or phenylalanine in a tryptophan-producing Corynebacterium glutamicum strain. *Appl.Environ.Microbiol.* **58,** 781-785

81. Eikmanns, B.J., Kleinertz, E., Liebl, W., and Sahm, H. (1991) A family of Corynebacterium glutamicum/Escherichia coli shuttle vectors for cloning, controlled gene expression, and promoter probing. *Gene.* **102,** 93-98

82. Colon, G., Nguyen, T., Jetten, M.S.M., Sinskey, A., and Stephanopoulos, G. (1995) Production of isoleucine by overexpression of ilvA in a Corynebacterium lactofermentum threonine producer. *Appl.Microbiol.Biotechnol.* **43,** 482-488

83. Tong, I.T., Liao, H.H., and Cameron, D. (1991) 1, 3-Propanediol production by Escherichia coli expressing genes from the Klebsiella pneumoniae dha regulon. *Appl.Environ.Microbiol.* **57,** 3541-3546

84. Zhang, M., Eddy, C., Deanda, K., Finkelstein, M., and Picataggio, S. (1995) Metabolic engineering of a pentose metabolism pathway in ethanologenic Zymomonas mobilis. *Science.* **267,** 240-243

85. Kumar, V., Ramakrishnan, S., Teeri, T.T., Knowles, J.K.C., and Hartley, B.S. (1992) Saccharomyces cerevisiae cells secreting an Aspergillus niger β-galactosidase grow on whey permeate. *Nat.Biotechnol.* **10,** 82-85

86. Brabetz, W., Liebl, W., and Schleifer, K.H. (1991) Studies on the utilization of lactose by Corynebacterium glutamicum, bearing the lactose operon of Escherichia coli. *Arch.Microbiol.* **155,** 607-612

87. Slater, S.C., Voige, W., and Dennis, D. (1988) Cloning and expression in Escherichia coli of the Alcaligenes eutrophus H16 poly-beta-hydroxybutyrate biosynthetic pathway. *J.Bacteriol.* **170,** 4431-4436

88. Schubert, P., Steinbuchel, A., and Schlegel, H.G. (1988) Cloning of the Alcaligenes eutrophus genes for synthesis of poly-beta-hydroxybutyric acid (PHB) and synthesis of PHB in Escherichia coli. *J.Bacteriol.* **170,** 58375847

89. Khosla, C., and Bailey, J.E. (1988) Heterologous expression of a bacterial haemoglobin improves the growth properties of recombinant Escherichia coli. *Nature.* 633-635

90. Aristidou, A.A., San, K.Y., and Bennett, G.N. (1994) Modification of central metabolic pathway in Escherichia coli to reduce acetate accumulation by heterologous expression of the Bacillus subtilis acetolactate synthase gene. *Biotechnol.Bioeng.* **44,** 944-951

91. Yarmush, M.L., and Berthiaume, F. (1997) Metabolic engineering and human disease. *Nat.Biotechnol.* **15,** 525-528

92. Kiick, K.L., and Tirrell, D.A. (2000) Protein engineering by in vivo incorporation of non-natural amino acids: control of incorporation of methionine analogues by methionyl-tRNA synthetase. *Tetrahedron.* **56,** 9487-9493

93. Hohsaka, T., and Sisido, M. (2002) Incorporation of non-natural amino acids into proteins. *Curr.Opin.Chem.Biol.* **6,** 809-815

94. Chin, J.W., Martin, A.B., King, D.S., Wang, L., and Schultz, P.G. (2002) Addition of a photocrosslinking amino acid to the genetic code of Escherichia coli. *Proc.Natl.Acad.Sci.* **99,** 11020-11024

95. Chin, J.W., Santoro, S.W., Martin, A.B., King, D.S., Wang, L., and Schultz, P.G. (2002) Addition of p-Azido-l-phenylalanine to the Genetic Code of Escherichia c oli. *J.Am.Chem.Soc.* **124,** 9026-9027

96. Wang, L., Xie, J., and Schultz, P.G. (2006) Expanding the genetic code. *Annu.Rev.Biophys.Biomol.Struct.* **35,** 225-249

97. Sampathkumar, S.G., Li, A.V., Jones, M.B., Sun, Z., and Yarema, K.J. (2006) Metabolic installation of thiols into sialic acid modulates adhesion and stem cell biology. *Nat.Chem.Biol.* **2,** 149-152

98. Mahal, L.K., Yarema, K.J., and Bertozzi, C.R. (1997) Engineering chemical reactivity on cell surfaces through oligosaccharide biosynthesis. *Science.* **276,** 1125-1128

99. Saxon, E., and Bertozzi, C.R. (2000) Cell surface engineering by a modified Staudinger reaction. *Science.* **287,** 2007-2010

100. Collins, B.E., Fralich, T.J., Itonori, S., Ichikawa, Y., and Schnaar, R.L. (2000) Conversion of cellular sialic acid expression from N-acetyl-to N-glycolylneuraminic acid using a synthetic precursor, N-glycolylmannosamine pentaacetate: inhibition of myelin-associated glycoprotein binding to neural cells. *Glycobiology.* **10,** 11-20

101. Roth, J. (1993) Cellular sialoglycoconjugates: a histochemical perspective. *Histochem.J.* **25,** 687-710

102. Hadfield, A.F., Mella, S.L., and Sartorelli, A.C. (1983) N-acetyl-D-mannosamine analogues as potential inhibitors of sialic acid biosynthesis. *J.Pharm.Sci.* **72,** 748-751

103. Schwartz, E.L., Hadfield, A.F., Brown, A.E., and Sartorelli, A.C. (1983) Modification of sialic acid metabolism of murine erythroleukemia cells by analogs of N-acetylmannosamine. *BBA- Mol Cell Res.* **762,** 489-497

104. Sarkar, A.K., Fritz, T.A., Taylor, W.H., and Esko, J.D. (1995) Disaccharide uptake and priming in animal cells: inhibition of sialyl Lewis X by acetylated Gal beta 1--> 4GlcNAc beta-O-naphthalenemethanol. *Proc.Natl.Acad.Sci.* **92,** 3323-3327

105. Fuster, M.M., Brown, J.R., Wang, L., and Esko, J.D. (2003) A disaccharide precursor of sialyl Lewis X inhibits metastatic potential of tumor cells. *Cancer Res.* **63,** 2775-2781

106. Mahal, L.K., Charter, N.W., Angata, K., Fukuda, M., Koshland, D.E., and Bertozzi, C.R. (2001) A small-molecule modulator of poly-α2, 8-sialic acid expression on cultured neurons and tumor cells. *Science.* **294,** 380-381

107. Horstkorte, R., Mühlenhoff, M., Reutter, W., Nöhring, S., Zimmermann-Kordmann, M., and Gerardy-Schahn, R. (2004) Selective inhibition of polysialyltransferase ST8SiaII by unnatural sialic acids. *Exp.Cell Res.* **298,** 268-274

108. Kayser, H., Geilen, C.C., Paul, C., Zeitler, R., and Reutter, W. (1992) Incorporation of N-acyl-2-amino-2-deoxy-hexoses into glycosphingolipids of the pheochromocytoma cell line PC 12. *FEBS Lett.* **301,** 137-140

109. Kayser, H., Zeitler, R., Kannicht, C., Grunow, D., Nuck, R., and Reutter, W. (1992) Biosynthesis of a nonphysiological sialic acid in different rat organs, using N-propanoyl-D-hexosamines as precursors. *J.Biol.Chem.* **267,** 16934-16938

110. Jones, M.B., Teng, H., Rhee, J.K., Lahar, N., Baskaran, G., and Yarema, K.J. (2004) Characterization of the cellular uptake and metabolic conversion of acetylated N-acetylmannosamine (ManNAc) analogues to sialic acids. *Biotechnol.Bioeng.* **85,** 394-405

111. Kim, E.J., Sampathkumar, S.G., Jones, M.B., Rhee, J.K., Baskaran, G., Goon, S., and Yarema, K.J. (2004) Characterization of the metabolic flux and apoptotic effects of O-hydroxyl-and N-acyl-modified N-acetylmannosamine analogs in Jurkat cells. *J.Biol.Chem.* **279,** 18342-18352

112. Sampathkumar, S.G., Campbell, C.T., Weier, C., and Yarema, K.J. (2006) Short-chain fatty acid-hexosamine cancer prodrugs: The sugar matters. *Drug Future.* **31,** 1099-1116

113. Aich, U., Campbell, C.T., Elmouelhi, N., Weier, C.A., Sampathkumar, S.G., Choi, S.S., and Yarema, K.J. (2008) Regioisomeric SCFA attachment to hexosamines separates metabolic flux from cytotoxicity and MUC1 suppression. *ACS Chem Biol.* **3,** 230-240

114. Meledeo, M.A., Yarema, K.J., and Begley, T.P. (2007) Glycan Biosynthesis in Mammals. *Wiley Encyclopedia of Chemical Biology*.

115. Campbell, C.T., Aich, U., Weier, C.A., Wang, J.J., Choi, S.S., Wen, M.M., Maisel, K., Sampathkumar, S.G., and Yarema, K.J. (2008) Targeting pro-invasive oncogenes with short chain fatty acid-hexosamine analogues inhibits the mobility of metastatic MDA-MB-231 breast cancer cells. *J.Med.Chem.* **51,** 8135-8147

CHAPTER 3

EXTRACELLULAR AND INTRACELLULAR PROCESSING OF SCFA-HEXOSAMINE ANALOGS; IMPLICATIONS FOR METABOLIC GLYCOENGINEERING AND DRUG DELIVERY

ABSTRACT

This chapter provides a synopsis of the esterase processing of short chain fatty acid (SCFA)-derivatized hexosamine analogs used in metabolic glycoengineering by demonstrating that that extracellular hydrolysis of these compounds is comparatively slow (e.g., with a $t_{1/2}$ of ~ four hours to several days) in normal cell culture as well as in high serum concentrations intended to mimic *in vivo* conditions. Structure activity relationship (SAR) analysis of common sugar analogs revealed that *O*-acetylated and *N*-azido ManNAc derivatives were more refractory against extracellular inactivation by FBS than their butanoylated counterparts consistent with *in silico* docking simulations of Ac_4ManNAc and Bu_4ManNAc to human carboxylesterase 1 (hCE1). By contrast, all analogs tested rapidly (i.e., within two hours) supported increased sialic acid production intracellularly thereby establishing that esterase processing once the analogs are taken up by cells not rate limiting.

This chapter was originally published as **Mathew, M. P., Tan, E., Shah, S., Bhattacharya, R., Meledeo, M. A., Huang, J., ... & Yarema, K. J. (2012). Extracellular and Intracellular Esterase Processing of SCFA–Hexosamine Analogs: Implications for Metabolic Glycoengineering and Drug Delivery. *Bioorganic & Medicinal Chemistry letters*, *22*(22), 6929-6933.**

3.1 INTRODUCTION

Ester-containing small molecules are common in nature, exemplified by acetylsalicylic acid (aspirin), and they also proliferate as numerous prodrugs and profluorophores used medicinally, diagnostically, and for research purposes (1). The biological activity or therapeutic effects of these compounds depend intricately on the stability or lability of the ester group as well was the organ, tissue, or subcellular site of hydrolysis. A group of these compounds with emerging significance, hexosamine analogs with ester-linked short chain fatty acid (SCFA) groups used in metabolic glycoengineering (illustrated by Ac_4ManNAc and Bu_4ManNAc, or their "R"-modified analogs), face a conflicting set of challenges to be used successfully in both *in vitro* and animal experiments as outlined in **Figure 3.1.**. Metabolic glycoengineering originated in efforts to exploit *N*-acyl modified monosaccharides – epitomized by using *N*-acetylmannosamine (ManNAc analogs) to target the sialic acid pathway – to redecorate the cell surface with non-natural sugar epitopes (2, 3). The versatility of metabolic glycoengineering was expanded considerably when the Bertozzi group used monosaccharide analogs to install bioorthogonal chemical functional groups into the glycocalyx of living cells in the form of ketone (4) and azide groups (5). Finally, the chemical options available through this technique have continued to expand with the recent metabolic incorporation of thiols (6), aryl azides (7), alkynes (8), and diazarines (9) into cell surface displayed glycans.

There are many potential biomedical applications for metabolic glycoengineering ranging from imaging, diagnosis, to the treatment of diseases ranging from cancer (10, 11) to viral infections (12) with additional uses reviewed elsewhere (13, 14).

Unfortunately the *in vivo* use of non-natural monosaccharide analogs has been slowed by low efficiency by which cells take up and metabolize these compounds; typically concentrations in the tens of millimolar are required in cell culture, which translates to unacceptably high doses for large animal studies. This pitfall has been rectified in part by the introduction of short chain fatty acid (SCFA) protecting groups, most commonly acetate, into analog design to increase cellular uptake by 600 to 900-fold (15, 16); we have found that metabolic efficiency can be increased further, by ~1,800 and 2,100 fold for propionate- and butanoyl-modified hexosamines, respectively (17). This protecting group strategy that renders the core sugar more lipophilic and plasma membrane permeable is contingent the hope that the SCFA moieties will be ignored by extracellular esterases and lipases and reach the targeted cell unscathed.

The extracellular stability of a SCFA-protected monosaccharide prodrug is important for two reasons. First, when the primary intention is for the compound to enter a cell to intercept a glycosylation pathway, the SCFA moieties that enhance membrane permeability must remain attached to the core sugar until the analog reaches the membrane of the target cell. Alternately, if the intention is to elicit "whole molecule" therapeutic effects exhibited by some analogs (e.g., by Bu_4ManNAc or 3,4,6-*O*-Bu_3ManNAc (**Fig. 3.1.B**) as described in more detail below and in other publications (18-20)), the exact pattern of regioisomeric SCFA derivatization must remain intact until the analog has time to interact with a target cell. To illustrate this concept with a specific example, if the C6-substitutent of Bu_4ManNAc were hydrolyzed extracellularly, certain of the resulting molecules (e.g., 1,3,4-*O*-Bu_3ManNAc, **Fig. 3.1.C**) would not be able to elicit the anti-oncogenic properties held by the parent molecule (21). Instead, this analog

is a facile intermediate for further debutanoylation and incorporation into the sialic acid pathway and thus actually increases the oncogenic propensities of late stage cancer cells by increasing the sialylation of adhesion molecules implicated in metastasis (22).

Once a sugar analog used in metabolic glycoengineering is taken into a target cell, the SCFA protecting groups must be fully removed for the core sugar to intercept the targeted glycosylation pathway (which can also, in addition to sialic acid pathway targeted by ManNAc analogs in the current study), include the biosynthetic routes for fucose, GalNAc, or O-GlcNAcylation (14)). Thus, unlike in the extracellular milieu where the analog will ideally be refractory to hydrolysis of the SCFA groups, rapid deprotection inside the cell is necessary for facile metabolic glycoengineering of cellular glycans. This paper addresses these issues by providing experimental evidence that esterase/lipase inactivation of SCFA-derivatized ManNAc analogs is relatively slow outside of a cell (**Fig. 3.1.A**) allowing these compounds to be used for routine *in vitro* cell culture and, most likely *in vivo* applications, without undue concern for rapid degradation. By contrast, once taken up by a cell, esterase processing of analogs is relatively fast; or, to put it another way, cells have ample esterase activity to ensure that analog processing IS NOT the rate limiting step for the incorporation of SCFA-derivatized ManNAc analogs into the sialic acid pathway.

3.2 MATERIALS AND METHODS

3.2.1. Cell Culture and Seeding

3.2.1.1. Human Pancreatic Adenocarcinoma (SW1990) Cells

Human pancreatic cancer cells (SW1990; CRL-2172; ATCC; Gaithersburg, MD) were cultured in Dulbecco's modified Eagle's Medium (DMEM; Cellgro, Mediatech, Inc) supplemented with 10% FBS and 1% of a 100x penicillin/streptomycin stock solution. Cells were typically incubated in T-75 or alternatively in T-175 and T-25 flasks in a 5% CO_2, humidified environment at 37 ˚C. These adherent cells were always kept at a density below 1 x 10^5 cells/cm^2 to prevent them from reaching a confluent and quiescent growth stage. The cells were passaged every 2 days by aspirating the spent media, washing cells with 10 ml of phosphate buffer saline (PBS; pH=7.4), adding 2-3 ml of trypsin (TrypLe™ Express, Invitrogen), incubating in a 5% CO_2, humidified environment at 37 ˚C for 5-10 min, adding 10 ml of DMEM, transferring the cells to a 15 ml conical tube, centrifuging for 5 min at 1000g, aspirating the media, and resuspending in desired volume of DMEM. The SW1990 cells were then plated at a density of 2.5 x 10^4 cells/cm^2 and incubated in a flask at 5% CO_2, humidified environment at 37 ˚C.

3.2.1.2. Analog Treatment

Stock solutions of Bu_4ManNAc (100 mM), Ac_4ManNAc (100 mM) and 1,3,4-*O*-Bu_3ManNAc (100 mM), were prepared in filtered ethanol and stored at 4 ˚C. Appropriate volumes of stock solutions were added to each condition for the desired final concentration.

3.2.2. Measuring the Number of Cells Using the Z2™ Coulter Counter

After incubation, the spent media was aspirated, and the cells were washed with PBS. Trypsin was added and the plate was incubated in a 5% CO_2, humidified environment at 37 ˚C for 7 min. Then, DMEM media was added and the cells were then immediately counted using a Z2™ Coulter Counter (Beckman-Coulter, Brea, CA) with a 100 µm aperture, dilution factor of 1:101, and boundaries set between 7 and 25 µm.

3.2.3. Periodate Resorcinol Assay Used to Determine Sialic Acid Flux

A modified version of the periodate-resorcinol assay, originally described by Jourdian and co-workers, was used to determine sialic acid flux (16-18, 23). Treated cells were harvested with trypsin, washed twice with PBS, counted with the Z2 particle counter, and normalized such that equal amounts of cells (at least 1,000,000) were in each sample. Samples were freeze-thawed three times to lyse the cell membrane. The lysates were then oxidized with 0.4 M periodic acid and cooled on ice for 10 min. A resorcinol mixture containing 10% 0.5 M resorcinol, 10% 2.5 mM $CuSO_4$, 44% concentrated HCl, and 36% de-ionized H_2O was prepared. After oxidation, 500 µl of the resorcinol mixture was added to each sample and samples were heated at 100 °C for 10 min. After quickly cooling the heat block on ice, 500 µl of tert-butyl was added to each sample. The samples were then centrifuged for 2 min at 13000g and the absorbance was measured at a wavelength of 630 nm using a spectrophotometer. The sialic acid concentration was determined in each sample using a simultaneously developed standard curve that contained absorbance values at 630 nm of known concentrations (generally ranging from 0 to 200 µM) of sialic acid.

3.2.4. Inactivation Time Course for Analogs in Different Concentrations of Fetal Bovine Serum

3.2.4.1. Materials Preparation

FBS free DMEM media was prepared. This FBS free media was then supplemented with FBS to give 10% and 25% FBS solutions. For pretreatment the volume of the 100% FBS/10% FBS/25% FBS solution was chosen such that when it was added to the FBS free media and made up to 2 ml the final media's FBS content was 10% FBS which is the standard media composition for SW1990 cells. The amount of analog added was so as to make the concentration of the final 2 ml solution up to the desired concentration.

3.2.4.2. Pretreatment of Analogs With Fetal Bovine Serum

The Bu_4ManNAc, Ac_4ManNAc and 1,3,4-*O*-Bu_3ManNAc analogs were incubated in Fetal Bovine Serum (FBS) for different time periods (1 h, 2 h, 4 h, 24 h and 48 h) at 5% CO_2, humidified environment at 37 ˚C. The incubations were initiated such that all the pretreatments end at the same time. The SW1990 cells were used as an indicator cell line; these cells were seeded in six well plates at a seeding density of 10^6 cells per well as described in section 2.3.1.1., and allowed to grow on the plate for 24 h at 5% CO_2, humidified environment at 37 ˚C. This seeding was done such that the 24 h incubation coincides with the end of the analog pretreatment.

3.2.4.3. Exposing Cells to Pretreated Analogs

The media was aspirated for each of the wells after which the required amount of FBS free DMEM was added to each well. The analog in FBS solutions were then added such

that the final volume was 2 ml with the analog at the desired concentration. The cells were then incubated for 48 h at 5% CO_2, humidified environment at 37 ˚C.

3.2.4.4. Quantification of Amount of Sialic Acid Produced by Periodate-Resorcinol Assay

The cells are harvested and analyzed using the modified periodate-resorcinol assay outlined in section 2.3.3. The amount of sialic acid per cell is determined and the different time points are compared to the control (untreated) and the 0 h (un-pretreated) conditions.

3.2.5. Statistical Analysis

Experimental values are presented as means ± standard deviations or standard error mean. Each experiment above was repeated at least three times with a minimum of three technical replicates. In normalized data, all data points are normalized to the mean of the controls after which a one way ANOVA with a dunnett's post-test was performed using GraphPad Prism v5 (La Jolla, CA). A p-value of less than 0.05 was considered statistically significant.

3.3 RESULTS AND DISCUSSION

In the first set of experiments a functional assay was used to monitor the effects of analog incubation in fetal bovine serum. This assay, which has been described in detail previously in a study of Ac_4ManNAc uptake from tissue culture medium and incorporation into the sialic acid biosynthetic pathway (16) monitors the removal of

SCFA groups, which reduces cellular uptake of the core sugar and subsequently results in a measurable decrease in sialic acid biosynthesis compared to control cells incubated with non-esterase or serum-treated analog. Ac_4ManNAc was refractory to serum inactivation over a 48 h time period (**Fig. 3.2.A**), thereby providing evidence that peracetylated monosaccharides widely used in metabolic glycoengineering are sufficiently resistant to serum esterases for a wide range of *in vivo* applications. For example, in some applications such as treatment of hereditary inclusion body myopapthy (HIBM) with exogenously delivery ManNAc, sialic acid production peaked as soon as four hours after administration of Ac_4ManNAc (24) while in other cases the administration of SCFA-derivatized ManNAc analogs, e.g., Ac_4ManNProp, required repeated daily administration over several weeks to achieve maximal *in vivo* replacement of natural sialic acids with the non-natural, metabolically engineered counterparts (25).

Despite the serum stability of acetylated ManNAc analogs, butanoylated analogs have the advantage of 3- to 4-fold more efficient metabolic incorporation (17, 26) and importantly, offer added bioactivity of potential therapeutic value. For example, hydrolyzed *n*-butyrate can provide therapeutic benefit by functioning as a histone deacetylase inhibitor (27, 28). In addition, "whole molecule" activity – where biological responses emanate from the intact compound before esterase processing occurs – exemplify an emerging concept that sugar-based templates offer an attractive platform for drug development (29); the whole molecule effects of butanoylated hexosamines include suppression of NF-κB and metastatic oncogenes (21) and are described in more detail elsewhere (18-20). In the current work I found that fully *n*-butanoylated ManNAc (Bu_4ManNAc) was more rapidly inactivated by serum esterases than Ac_4ManNAc, with

the butanoylated analog showing a measurable reduction in sialic acid production in indicator cells after exposure to FBS for less than four hours while the acetylated sugar was stable for 48 h, the maximal time interval tested (**Fig. 3.2.A**). The reduction in sialic acid production observed for Bu_4ManNAc required the removal of at least 2 of the 4 butyrate groups during the pre-incubation period, which renders the dibutanoylated analog membrane impermeable.[18] By contrast, lower concentrations of FBS (e.g., 10% or 25%) did not result in a statistically significant reversion of Bu_4ManNAc-enhanced sialic acid production in the indicator cells (**Fig. 3.2.B**). These results have two implications: one is that under typical *in vitro* cell culture conditions, extracellular degradation of butanoylated analogs is not a substantial concern. Conversely, extrapolating the 100% serum treatment condition to the *in vivo* milieu (because, disregarding the cells present, blood can be regarded as 100% serum), the degradation of butanoylated analog after only a few hours shows that the *in vivo* stability of these compounds is a potential concern when translating metabolic glycoengineering to animal studies. However, pending detailed pharmacokinetic evaluation (which is beyond the scope of the present report), the half life of butanoylated analogs is "in the ballpark" for at least some *in vivo* applications (e.g., the ~ four hour kinetics for maximal sialic acid production observed in the Ac_4ManNAc-treated HIBM mouse model (24)).

The finding that Bu_4ManNAc likely has only marginally sufficient serum stability for effectively eliciting "whole molecule" effects *in vivo* raised the concern that tributanoylated analogs with otherwise favorable properties (for example, 3,4,6-*O*-Bu_3ManNAc has stronger "whole molecule" responses than Bu_4ManNAc (19, 20) and 1,3,4-*O*-Bu_3ManNAc has "high flux" properties with negligible side effects such as

cytotoxicity (18, 26)) might be even more rapidly inactivated by extracellular esterases. To evaluate this possibility, I compared 1,3,4-*O*-Bu_3ManNAc and 3,4,6-*O*-Bu_3ManNAc against the parent compound Bu_4ManNAc in relevant assays. First the high flux analog 1,3,4-*O*-Bu_3ManNAc did not lose its ability to supplement sialic acid production noticeably faster than Bu_4ManNAc, showing only a relatively minor reduction in analog-enhanced sialic acid production after four hours of serum treatment (**Fig. 3.2.C**), which was similar to the kinetics observed for the perbutanoylated analog (as shown in **Fig. 3.2.B**). Similarly when growth inhibition, a "whole molecule" property of 3,4,6-*O*-Bu_3ManNAc (18), was tested by monitoring the number of cells present after various time intervals of serum pretreatment, comparable kinetics were observed where loss of analog-enhanced cell growth inhibition began to be manifest between 2 and 4 hours, with a complete reversal after 24 hours (**Fig. 3.2.C**).

As a final test of extracellular esterase processing of ManNAc analogs, I evaluated azido-modified analogs pioneered by the Bertozzi group who first exploited them in modified Staudinger bio-orthogonal reactions (5); these compounds are now increasingly being used for metabolic glycoengineering because of their ability to be exploited in click reactions after installation into cellular glycoconjugates. By testing surface expression of azido-modified sialic acids in indicator cells, both Ac_4ManNAz and Bu_4ManNAz were refractory to a loss of signal over the first four hours of FBS treatment but did experience a reduction, but not complete reversal, of surface expression after 24 hours of pre-treatment (**Fig. 3.2.D**). This assay suggested that the butanoylated analog Bu_4ManNAz was more refractory to serum deactivation than Bu_4ManNAc, possibly because the presence of the *N*-azido group interfered with binding of the butanoylated analog to the

esterase(s). Despite this ambiguity, this result established that azido-modified analogs are not rapidly (e.g., within minutes) deactivated by serum enzymes but instead should again have sufficient longevity for *in vivo* applications using once a day (or less frequent) dosing regimens.

The requirement that intracellular esterase activity – in contrast to extracellular esterase activity as outlined above – occurs rapidly and thus is not a rate limiting step for sialic acid production was confirmed experimentally by monitoring production of this monosaccharide in cells treated with butanoylated ManNAc analogs over early time points. This issue is relevant because in organisms such as *Escherichia coli* strains that lack robust non-specific esterase activity, the strategy of providing esterified precursors for metabolic engineering is not viable (30). In my experiments in human cells, the perbutanoylated analog Bu_4ManNAc, the "high flux" analog 1,3,4-*O*-Bu_3ManNAc, and the 3,4,6-*O*-Bu_3ManNAc analog with enhanced "whole molecule" effects all gave rise to statistically identical levels of increased sialic acid production over the first 12 hours (Fig. 3A). These data diverge from previous results that showed that each compound supported different levels of sialic acid production when measured after 2 to 3 days of exposure to analog; for example, 1,3,4-*O*-Bu_3ManNAc was dubbed the "high flux" analog because of the very high sialic acid levels found in cells after 48 to 72 hours or exposure (18, 26). The current results indicate that this analog does not necessarily support a higher rate of metabolic flux *per se*, but instead the high levels of sialic acid observed in analog-treated cells after extended exposure are likely a consequence of the lack of cytotoxicity of this analog. For context, analogs that inhibit the robust growth of cells reduce ManNAc analog-mediated sialic acid production (16, 17, 31) and the lower

amounts of sialic acid observed after 2 or 3 days of exposure to Bu_4ManNAc or 3,4,6-*O*-Bu_3ManNAc likely result from the cytotoxicity of these analogs and not because esterase processing is a rate limiting step for incorporation into the sialic acid pathway. Instead, in mammalian cells downstream enzymes such as sialic acid synthase likely comprise a bottleneck for ManNAc-supported flux through the sialic acid biosynthetic pathway (32, 33).

To address a final loose end, I was curious about the apparent disparity (albeit a fortunate one) where esterase cleavage of SCFA groups was much slower extracellularly (e.g., at least four hours was generally needed to remove one or two SCFA groups, Fig. 2) than intracellularly (where, as shown in **Figure 3.3.A**, sialic acid production was observed within two hours for butanoylated ManNAc analogs. We have previously reported similar kinetics for intracellular sialic acid production from Ac_4ManNAc (34), which is only possible upon complete removal of SCFA groups from the core sugar. One explanation for these results is that the enzymes implicated in detoxification and most likely analog processing, such as human carboxylesterase 1 (hCE1), are intracellular while extracellular enzymes (e.g., butylcholinesterases) are not capable of facile hydrolysis of SCFA from monosaccharides. A second non-exclusive explanation is based on *in silico* docking simulations performed with AutoDock (following previously described procedures(19)) to evaluate the interaction of Ac_4ManNAc (-2.9 kcal/mol and K_d = 7.2 mM) and Bu_4ManNAc (-4.1 kcal/mol and K_d = 0.9 mM) with hCE1. While relatively weak, these binding values fall within the range of other carbohydrate ligands docked to proteins (35), making these results plausible and thereby providing an

attractive mechanism to explain why SCFA-ManNAc analogs are hydrolyzed slowly outside of a cell when in solution but rapidly inside a cell.

To explain in more detail, analog concentrations are sketched in **Figure 3.3.B**, showing that the nominal concentration in solution in culture medium is below the K_d for binding to hCE1 (e.g., 0.9 mM for Bu_4ManNAc) at concentrations typically used in metabolic glycoengineering experiments (e.g., <200 μM). As a result, the extracellular processing of the analog is slow and inefficient. Considering, however, that cellular membranes act as sinks for peracetylated ManNAc analogs (16) and this effect is exacerbated for the more lipophilic butanoylated analogs, we were able to extrapolate membrane concentrations for these compounds based on log P values calculated by ChemDraw. Specifically, tributanoylated analog concentration is expected to be enriched at least 12-fold in membranes compared to aqueous solution with an additional ~20 fold gain (to ~239 fold in total) for perbutanoylated analogs. Because hCE1 is a membrane associated enzyme, it is reasonable that the local concentration of analog near membranes thereby becomes sufficiently high to meet or exceed the *in silico* predicted K_d for this enzyme for concentrations of butanoylated analogs added to culture media in the 25 to 200 μM range typically used. Overall, although speculative at present, this mechanism satisfactorily explains the slow extracellular processing of analog (because, even if appropriate esterases are present in serum, analog concentrations in solution are considerably below the K_d, resulting in slow processing) as well as the facile intracellular processing (as just explained by the membrane sink effect).

In summary, this report provides experimental evidence based on an *in vitro* model system that two potential pitfalls for the *in vivo* use of metabolic glycoengineering

substrates – the potential rapid extracellular or the too slow intracellular esterase-mediated removal of the SCFA groups – are not a major concern. Consequently, this work provides a foundation for the continued development of metabolic glycoengineering by establishing a rationale for expanded translation from the "chemical glycobiology" origins of this methodology into more disease oriented animal model systems and biomedical applications.

3.4. ACKNOWLEDGEMENTS

Funding for the work described in this chapter was provided by the National Institutes of Health, grants R01CA112314 and R01AR054005.

3.5 FIGURES

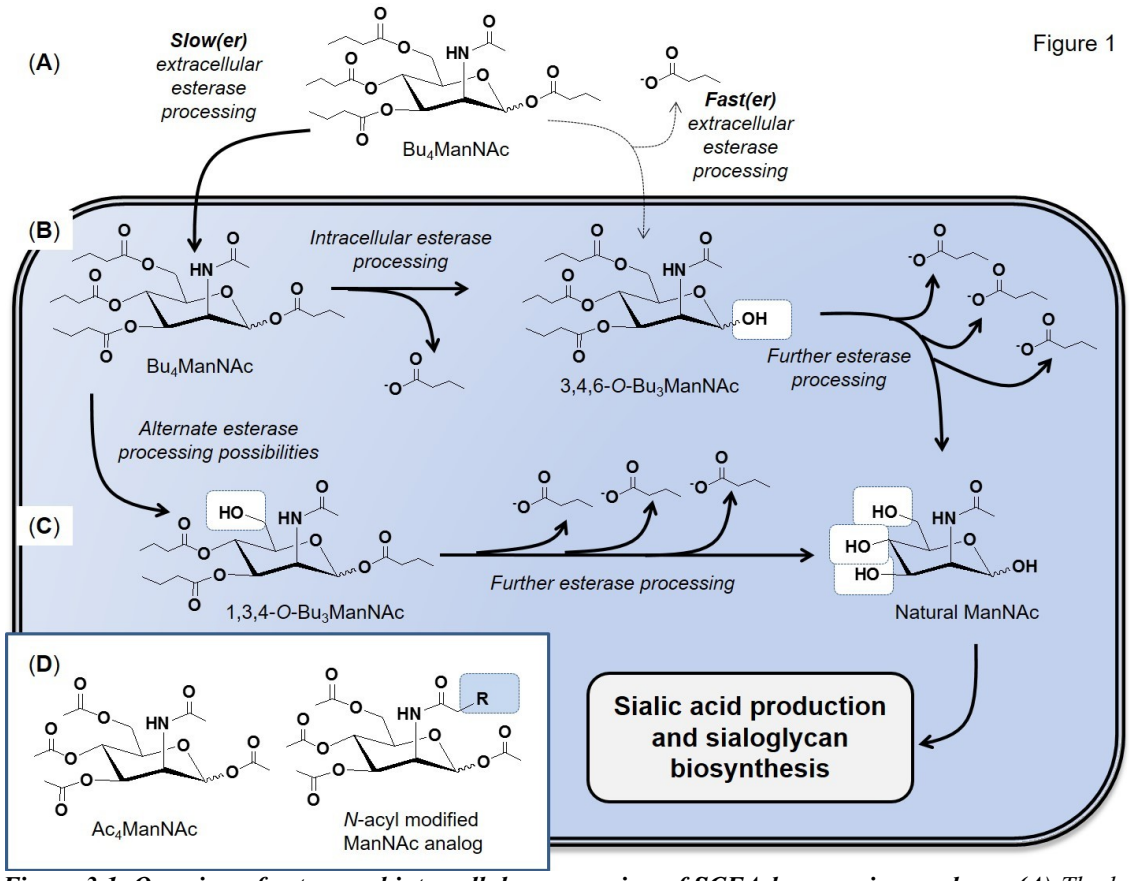

Figure 3.1. Overview of extra- and intracellular processing of SCFA-hexosamine analogs. ***(A)*** *The lead compound Bu_4ManNAc is used for illustrative purposives; outside of a cell if extracellular esterase/lipase degradation is relatively slow (left) then the intact molecule will enter the cell, otherwise if extracellular ester hydrolysis if relatively fast (right) a partially degraded metabolite such as 3,4,6-O-Bu_3ManNAc will enter a cell.* ***(B)*** *In either case the butanoylated analog is subject to further esterase processing to ultimately produce fully deprotected ManNAc: alternately 1,3,4-O-Bu_3ManNAc (or other partially deprotected intermediates, not shown) can be produced and similarly be deprotected to produce natural ManNAc (**C**), which is used by the sialic acid biosynthetic pathway (outlined in detail elsewhere [14,35]) to produced sialic acid and sialylated glycans.* ***(D)*** *Although illustrated with butanoylated ManNAc, similar considerations apply to peracetylated ManNAc (illustrated) and its hydrolysis products as well as N-acyl, R-modified analogs (such as the azido analogs shown in **Fig. 2D**).*

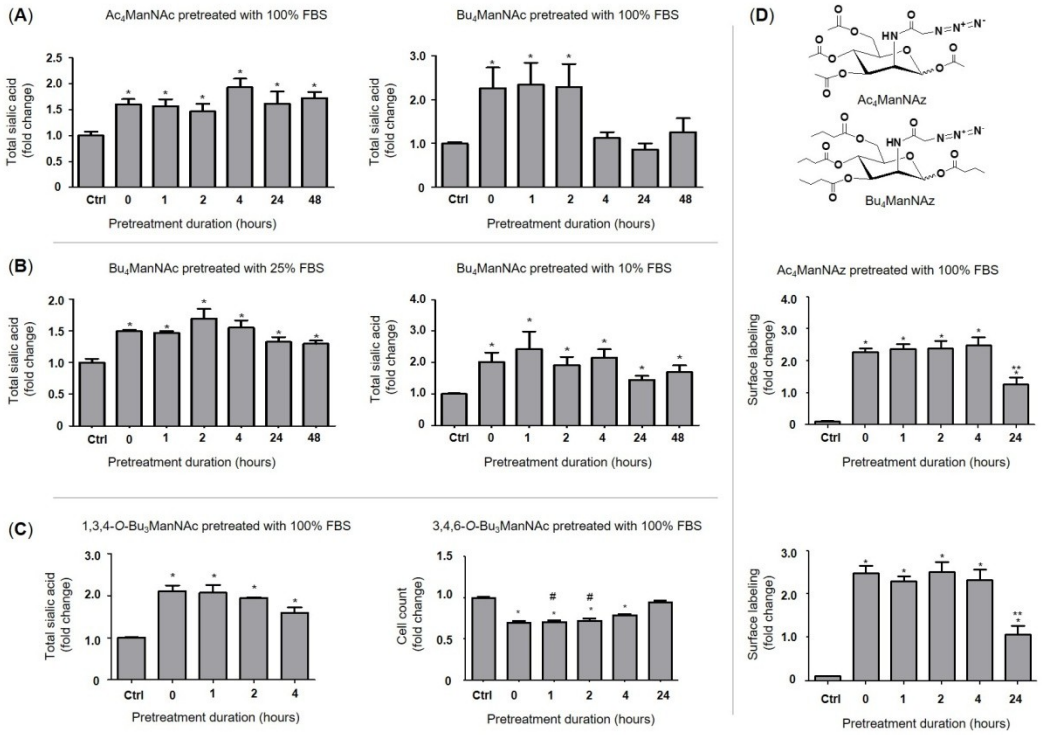

Figure 3.2. "Extracellular" esterase processing time course comparing various SCFA-derivatized ManNAc analogs. *Several lines of evidence establish that SCFA-ManNAc analogs are relatively refractory against extracellular esterase/lipase hydrolysis: (**A**) Enhanced sialic acid production emanating from FBS-treated Ac_4ManNAc continued for much longer (e.g., ≥ 48 h) compared to Bu_4ManNAc (e.g., for ~ 2 to 4 h); (**B**) Under conditions encountered in typical cell culture, e.g., with 10% (or even 25%) FBS, butanoylated ManNAc was resistant to esterases/lipase degration. (**C**) Tributanoylated ManNAc analogs showed moderate resistance to FBS degradation with the "1,3,4" analog evaluated in the sialic acid flux assay used in panels A and B while the "3.4,6" analog was tested by evaluating enhanced cytotoxity of analogs, measured by cell counts, with this particular SAR. (**D**) Azido-derivatived ManNAc analogs are shown (note that the structures of analogs used in panels A-C are given in Figure 1) along with surface labeling of Ac_4ManNAz and Bu_4ManNAz that had been pretreated with FBS. Analogs were synthesized and characterized as previously described: Ac_4ManNAc and Bu_4ManNAc;[17] 1,3,4-O-Bu_3ManNAc and 3,4,6-O-Bu_3ManNAc;[18] and Ac_4ManNAz and Bu_4ManNAc.[25] All data shown represents a minimum of n = 3 replicates; the "*" symbol indicates $p < 0.05$ compared to the control and the double "**" symbols in panel D indicate a statistical difference ($p < 0.05$) at 24 h $p < 0.05$ compared to both the control and earlier time points.*

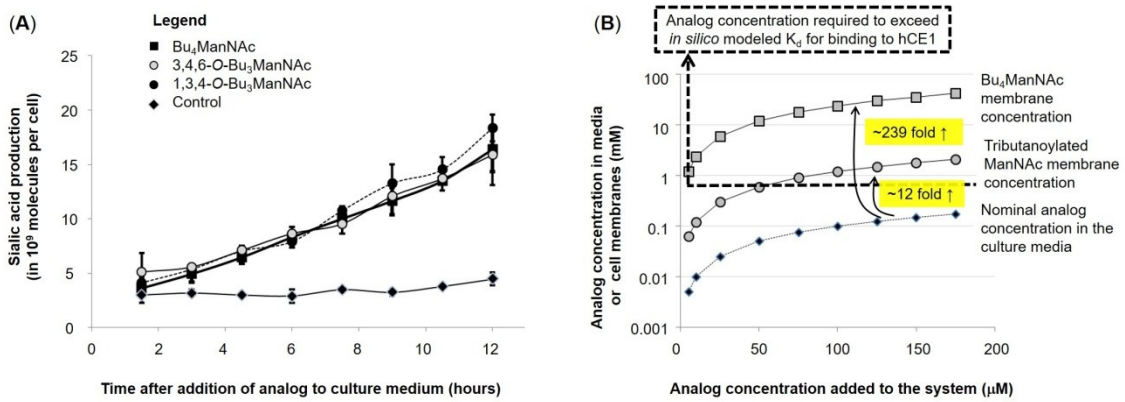

Figure 3.3. Intracellular esterase processing and an explanation for slow extracellular and fast intracellular analog hydrolysis. (A) *Sialic acid production in LS174T "indicator cells" incubated with different forms of butanoylated ManNAc analogs shows statistical no difference over the first several hours.* ***(B)*** *Theoretical explanation for the slow extracellular and rapid intracellular processing of SCFA-ManNAc analogs: tributanoylated and Bu_4ManNAc concentrations are estimated in solution and in (or near) membranes based on logP values calculated with ChemDraw. The K_d for association with hCE1 (a plausible model esterase) indicated with the dashed line, showing that the nominal concentration for analog in solution in media is typically below this threshold resulting in slow extracellular hydrolysis of SCFA groups while membrane-associated analog is typically at concentrations higher than this threshold, thus explaining the rapid intracellular hydrolysis of SCFA groups.*

3.6 REFERENCES

1. Lavis, L.D. (2008) Ester bonds in prodrugs. *ACS Chem. Biol.* **3,** 203-206

2. Kayser, H., Zeitler, R., Kannicht, C., Grunow, D., Nuck, R., and Reutter, W. (1992) Biosynthesis of a nonphysiological sialic acid in different rat organs, using N-propanoyl-D-hexosamines as precursors. *J.Biol.Chem.* **267,** 16934

3. Yarema, K.J., Mahal, L.K., Bruehl, R.E., Rodriguez, E.C., and Bertozzi, C.R. (1998) Metabolic delivery of ketone groups to sialic acid residues; Application to cell surface glycoform engineering.. *J.Biol.Chem.* **273,** 31168-31179

4. Mahal, L.K., Yarema, K.J., and Bertozzi, C.R. (1997) Engineering chemical reactivity on cell surfaces through oligosaccharide biosynthesis. *Science.* **276,** 1125

5. Saxon, E., and Bertozzi, C.R. (2000) Cell surface engineering by a modified Staudinger reaction. *Science.* **287,** 2007

6. Sampathkumar, S.G., Li, A.V., Jones, M.B., Sun, Z., and Yarema, K.J. (2006) Metabolic installation of thiols into sialic acid modulates adhesion and stem cell biology. *Nat. Chem. Biol.* **2,** 149-152

7. Han, S., Collins, B.E., Bengtson, P., and Paulson, J.C. (2005) Homomultimeric complexes of CD22 in B cells revealed by protein-glycan cross-linking. *Nat. Chem. Biol.* **1,** 93-97

8. Sawa, M., Hsu, T.L., Itoh, T., Sugiyama, M., Hanson, S.R., Vogt, P.K., and Wong, C.H. (2006) Glycoproteomic probes for fluorescent imaging of fucosylated glycans in vivo. *Proc.Natl.Acad.Sci.U.S.A.* **103,** 12371-12376

9. Tanaka, Y., and Kohler, J.J. (2008) Photoactivatable crosslinking sugars for capturing glycoprotein interactions. *J.Am.Chem.Soc.* **130,** 3278-3279

10. Mahal, L. K.; Yarema, K. J.; Lemieux, G. A.; Bertozzi, C. R. (1999) Chemical approaches to glycobiology: Engineering cell surface sialic acids for tumor targeting, in *Sialobiology and other novel forms of glycosylation*, Inoue, Y.; Lee, Y. C.; Troy, F. A., III, eds. Gakushin Publishing Company: Osaka, pp. 237-280.

11. Chefalo, P., Pan, Y., Nagy, N., Guo, Z., and Harding, C.V. (2006) Efficient metabolic engineering of GM3 on tumor cells by N-phenylacetyl-D-mannosamine. *Biochemistry (N.Y.).* **45,** 3733-3739

12. Keppler, O.T., Horstkorte, R., Pawlita, M., Schmidt, C., and Reutter, W. (2001) Biochemical engineering of the N-acyl side chain of sialic acid: biological implications. *Glycobiology.* **11,** 11R-18R

13. Campbell, C.T., Sampathkumar, S.G., and Yarema, K.J. (2007) Metabolic oligosaccharide engineering: perspectives, applications, and future directions. *Mol.BioSyst.* **3,** 187-194

14. Du, J., Meledeo, M.A., Wang, Z., Khanna, H.S., Paruchuri, V.D., and Yarema, K.J. (2009) Metabolic glycoengineering: sialic acid and beyond. *Glycobiology.* **19,** 1382-1401

15. Sarkar, A.K., Fritz, T.A., Taylor, W.H., and Esko, J.D. (1995) Disaccharide uptake and priming in animal cells: inhibition of sialyl Lewis X by acetylated Gal beta 1--> 4GlcNAc beta-O-naphthalenemethanol. **92,** 3323-3327

16. Jones, M.B., Teng, H., Rhee, J.K., Lahar, N., Baskaran, G., and Yarema, K.J. (2004) Characterization of the cellular uptake and metabolic conversion of acetylated N-acetylmannosamine (ManNAc) analogues to sialic acids. *Biotechnol.Bioeng.* **85,** 394-405

17. Kim, E.J., Sampathkumar, S.G., Jones, M.B., Rhee, J.K., Baskaran, G., Goon, S., and Yarema, K.J. (2004) Characterization of the metabolic flux and apoptotic effects of O-hydroxyl-and N-acyl-modified N-acetylmannosamine analogs in Jurkat cells. *J.Biol.Chem.* **279,** 18342-18352

18. Aich, U., Campbell, C.T., Elmouelhi, N., Weier, C.A., Sampathkumar, S.G., Choi, S.S., and Yarema, K.J. (2008) Regioisomeric SCFA attachment to hexosamines separates metabolic flux from cytotoxicity and MUC1 suppression. *ACS Chem Biol.* **3,** 230-240

19. Elmouelhi, N., Aich, U., Paruchuri, V.D.P., Meledeo, M.A., Campbell, C.T., Wang, J.J., Srinivas, R., Khanna, H.S., and Yarema, K.J. (2009) Hexosamine template. A platform for modulating gene expression and for sugar-based drug discovery. *J.Med.Chem.* **52,** 2515-2530

20. Wang, Z., Du, J., Che, P., Meledeo, M.A., and Yarema, K.J. (2009) Hexosamine analogs: from metabolic glycoengineering to drug discovery. *Curr.Opin.Chem.Biol.* **13,** 565-572

21. Campbell, C.T., Aich, U., Weier, C.A., Wang, J.J., Choi, S.S., Wen, M.M., Maisel, K., Sampathkumar, S.G., and Yarema, K.J. (2008) Targeting pro-invasive oncogenes with short chain fatty acid-hexosamine analogues inhibits the mobility of metastatic MDA-MB-231 breast cancer cells. *J.Med.Chem.* **51,** 8135-8147

22. Almaraz, R.T., Tian, Y., Bhattarcharya, R., Tan, E., Chen, S., Dallas, M.R., Chen, L., Zhang, Z., Zhang, H., Konstantopoulos, K., and Yarema, K.J. (2012) Metabolic flux increases glycoprotein sialylation: Implications for cell adhesion and cancer metastasis. *Molecular & Cellular Proteomics.* **11,** M112-017558.

23. Jourdian, G.W., Dean, L., and Roseman, S. (1971) The sialic acids. *J.Biol.Chem.* **246,** 430-435

24. Malicdan, M.C., Noguchi, S., Tokutomi, T., Goto, Y., Nonaka, I., Hayashi, Y.K., and Nishino, I. (2012) Peracetylated N-acetylmannosamine, a synthetic sugar molecule, efficiently rescues muscle phenotype and biochemical defects in mouse model of sialic acid-deficient myopathy. *J.Biol.Chem.* **287,** 2689-2705

25. Gagiannis, D., Gossrau, R., Reutter, W., Zimmermann-Kordmann, M., and Horstkorte, R. (2007) Engineering the sialic acid in organs of mice using N-propanoylmannosamine. *BBA-General Subjects.* **1770,** 297-306

26. Almaraz, R.T., Aich, U., Khanna, H.S., Tan, E., Bhattacharya, R., Shah, S., and Yarema, K.J. (2012) Metabolic oligosaccharide engineering with N-Acyl functionalized ManNAc analogs: Cytotoxicity, metabolic flux, and glycan-display considerations. *Biotechnol.Bioeng.* **109,** 992-1006

27. Sampathkumar, S.G., Campbell, C.T., Weier, C., and Yarema, K.J. (2006) Short-chain fatty acid-hexosamine cancer prodrugs: The sugar matters. *Drug Future.* **31,** 1099-1116

28. Sampathkumar, S., Jones, M.B., Meledeo, M.A., Campbell, C.T., Choi, S.S., Hida, K., Gomutputra, P., Sheh, A., Gilmartin, T., and Head, S.R. (2006) Targeting glycosylation pathways and the cell cycle: sugar-dependent activity of butyrate-carbohydrate cancer prodrugs. *Chem.Biol.* **13,** 1265-1275

29. Meutermans, W., Le, G.T., and Becker, B. (2006) Carbohydrates as scaffolds in drug discovery. *ChemMedChem.* **1,** 1164-1194

30. Antonczak, A.K., Simova, Z., and Tippmann, E.M. (2009) A critical examination of Escherichia coli esterase activity. *J.Biol.Chem.* **284,** 28795-28800

31. Kim, E.J., Jones, M.B., Rhee, J.K., Sampathkumar, S., and Yarema, K.J. (2004) Establishment of N-Acetylmannosamine (ManNAc) analogue-resistant cell lines as improved hosts for sialic acid engineering applications. *Biotechnol.Prog.* **20,** 1674-1682

32. Jacobs, C.L., Goon, S., Yarema, K.J., Hinderlich, S., Hang, H.C., Chai, D.H., and Bertozzi, C.R. (2001) Substrate specificity of the sialic acid biosynthetic pathway. *Biochemistry (N.Y.).* **40,** 12864-12874

33. Viswanathan, K., Lawrence, S., Hinderlich, S., Yarema, K.J., Lee, Y.C., and Betenbaugh, M.J. (2003) Engineering sialic acid synthetic ability into insect cells:

identifying metabolic bottlenecks and devising strategies to overcome them. *Biochemistry (N.Y.).* **42,** 15215-15225

34. Tan, E., Almaraz, R.T., Khanna, H.S., Du, J., and Yarema, K.J. (2010) Experimental design considerations for in vitro non-natural glycan display via metabolic oligosaccharide engineering. *Current protocols in chemical biology.* ***2,*** 171-194

35. Laederach, A., and Reilly, P.J. (2003) Specific empirical free energy function for automated docking of carbohydrates to proteins. *J. Comp. Chem.* **24,** 1748-1757

CHAPTER 4

PHARMACOLOGICAL MODULATION OF INTRACELLULAR ESTERASE ACTIVITY THROUGH METABOLIC GLYCOENGINEERING OF SIALIC ACID

ABSTRACT

This chapter describes the pharmacological manipulation of intracellular esterase activity in human colon cancer (LS174T) and Chinese hamster ovary (CHO) cells by using butanoylated ManNAc analogs. In the first part of this study *in silico* analysis of intracellular esterases, in particular the carboxylesterases (CES1 and CES2) implicated in drug processing and detoxification, supported the hypothesis that these enzymes are modified with sialylated *N*-glycans that stabilize their active trimeric forms. Experimental support for this premise was obtained by enhancing esterase activty by treating cells with ManNAc analogs that increase sialylation whereas hexosamine analogs not targeted to the sialic acid biosynthetic pathway (e.g., butanoylated GlcNAc or GalNAc) had minimal or negligible impact on esterase activity. Characterization of mRNA and protein levels provided additional evidence that esterase activity was controlled at the level of post-translational modification and not through transcription or translation. Azide-modified ManNAc analogs, which are now widely used in metabolic glycoengineering, also enhanced esterase activity and provided unambiguous evidence that exogenously-supplied ManNAc analogs are coverted to sialosides and installed into

the glycan structures attached to esterases such as CES2. These results establish that sialylation with both natural and non-natural metabolic precursors controls the activity of intracellular esterases in ways relevant for the treatment of disease and compatible with emerging efforts to employ recombinant forms of these enzymes in biomedicine.

4.1 INTRODUCTION

Esterases are a versatile group of enzymes that contribute to several human diseases and play a significant role in drug metabolism; for example, these enzymes often degrade pharmacological agents and decrease drug effectiveness. Therefore, as discussed in a recent review,(1) selective inhibitors of esterases in theory could beneficially modulate the metabolism, distribution, and toxicity of pharmacological agents processed by this class of enzymes. Accordingly, the development of inhibitors – in particular for the drug processing human carboxylesterases 1 and 2 (hCES1 and hCES2) is now recognized as an important research area and efforts to develop these compounds are underway (1).

At other times, however, there is a need to maximize esterase activity. For example, degradation of intoxicants such as cocaine by esterases such as carboxylesterases 1 and 2 (CES1 and CES2) provides a protective mechanism for the host(2,3). In other situations, prodrugs rely on esterase processing to be converted to their active form; examples of esterase-activated drugs include acetyl salicylic acid (aspirin) (4) and CPT-11, a semisynthetic derivative of camptothecin, which is activated to SN-38 by carboxylesterases (5,6). Yet another area where the ability to enhance esterase activity would be useful is in diseases characterized by insufficient esterase activity. A few

examples include congenital mutations that impact esterase activity (7), reduced esterase activity that hinders monocyte-mediated killing of tumor cells (,8) and down-regulation of esterases in certain types of cancers when undergoing treatment with esterase-activated prodrugs (9). Unlike the situation for esterase inhibitors, however, where several examples of inhibitors are known (1), the development of pharmacologically useful small molecule esterase activators is virtually non-existent (10-12).

Accordingly, it was an intriguing possibility that sugar analogs used in metabolic glycoengineering (MGE), which comprise an emerging class of drug candidates that exemplify the idea that monosaccharides are a versatile template for drug discovery (13-15), could be used to enhance the activity of intracellular esterases implicated in drug metabolism and disease progression. To briefly elaborate on MGE, which is also referred to as metabolic oligosaccharide engineering (MOE (16,17)), *in vivo* applications of this strategy were largely pioneered by Reutter's group (18) who showed that exogenously-supplied, non-natural sugars could be introduced into biosynthetic pathways to modulate glycosylation (17,19). Because these sugars often lack plasma membrane transporters, a common strategy to increase cellular uptake has been to add ester-linked short chain fatty acids (SCFA) such as acetate (20,21) and more recently *n*-butyrate (22,23) to the core sugar. The SCFAs increase the lipophilicity of the sugar and facilitate passive diffusion across the plasma membrane thereby bypassing the need for transporter-mediated intake. Once inside a cell, esterases remove the SCFAs over a period of hours (24), allowing the sugar to intercept the targeted glycosylation pathway and, by altering cellular glycosylation, have an impact on the activity of various down-stream targets such as

integrins and CD44 as we have shown in previous work (25) and in this work, the drug-processing esterases themselves.

The most highly glycosylated esterases (AChE and BChE, as mentioned above) have a minimal role in intracellular drug detoxification or processing (26) because they are secreted. Nevertheless AChE and BChE provide precedent that glycosylation can be an important modulator of esterase activity and we were curious whether this principle extended to intracellular esterases. In particular, reports that an *N*-linked oligosaccharide is located at the interface between CES monomers (27,28), as well as an *in silico* analysis we present in this report that revealed that virtually all cellular esterases are subject to glycosylation led us to propose that MGE analogs that manipulate glycosylation broadly modulate esterase activity. In this study, this hypothesis was evaluated by a series of experiments that verified that an increase in aggregate esterase activity occurs within ManNAc analog-treated cells consistent with a key role for sialylation of intracellular esterases, in particular carboxylesterases CES1 and CES2.

4.2 Materials and Methods

4.2.1 Prediction of *N*-glycan site occupancy using NetNGlyc 1.0.

FASTA formatted amino acid sequences were attained from the NCBI database (http://www.ncbi.nlm.nih.gov). Sequences were attained for Carboxylesterase 1 (Accession no. AAI10339), Carboxylesterase 2 (Accession no. AAH32095), Carboxylesterase 3 (Accession no. ACD11491), Carboxylesterase 7 (Accession no. AAH69548), Carboxylesterase 8 (Accession no. AAH64573), Acetylcholinesterase

(Accession no. AAA68151), Butyrylcholinesterase (Accession no. AAH18141), Carboxyl Ester Lipase (Accession no. AAA51973) and Esterase D (Accession no. AAC99788). These sequences were entered into the N-glycosylation prediction tool: NetNGlyc (http://www.cbs.dtu.dk/services/NetNGlyc/) and this online software tool then was used to predict the sites and probabilities of *N*-glycosylation.

4.2.2 Modeling of *N*-Glycosylation of CES1 with Discovery Studio.

The "Build Fragment" and molecule sketching capabilities of Accelrys Discovery Studio 3.5 Visualizer were used to generate models of insect and human glycans into the crystal structure from PDB ID 1YA8 after water and other small molecules were removed. Initial models were minimized with a Dreiding-like forcefield to optimize geometries.

4.2.3 Cell culture and incubation with sugar analogs.

LS174T (ATCC® CL-188) cells were grown in Minimal Essential Medium Eagle supplemented with heat-inactivated 10 % fetal bovine serum (FBS), 100 units/mL penicillin and 100 μg/mL streptomycin (pen/strep), 1x (100x dilution of 100x stock) non-essential amino acids, and 110 mg/mL sodium pyruvate (Invitrogen, Carlsbad, CA). Chinese hamster ovary (CHO) cells - wild-type (WT, gift from the Betenbaugh laboratory, JHU), K1 (ATCC® CCL-61), Pro-5 (ATCC® CRL-1781), and Lec2 (gift from the Betenbaugh laboratory, JHU) were cultured in Dulbecco's modified Eagle's medium (DMEM) supplemented with heat-inactivated 10% FBS, penicillin/streptomycin (Pen/Strep) solution, and 2.0 mM L-glutamine. SCFA hexosamine analogs were synthesized and characterized using published methods (Bu_4ManNAc (22), 1,3,4-*O*-Bu_3ManNAc and 3,4,6-*O*-Bu_3ManNAc (14,29), and 1,3,4-*O*-Bu_3ManNAz and 3,4,6-*O*-Bu_3ManNAz (30), For treatment of cells, analogs (from a 100 mM stock solution in

ethanol (EtOH)) were added to 6-well tissue culture plates and the EtOH was allowed to evaporate. Cells were suspended in 2.0 mL of culture media and then added to each well and incubated with the sugar analogs for time periods up to 48 h.

4.2.4 Intracellular esterase activity assay.

Analog-treated cells were detached using 1.0 mL of enzyme free cell dissociation buffer (Millipore) and washed with D-PBS (Mediatech). Cells (200,000 cells) were then incubated with 600 µL of 1.0 µM carboxy fluorescein diacetate (CFDA; Marker Gene Technologies) or 400 µM resorufin acetate (Marker Gene Technologies) in the dark at room temperature under gentle vibration for 40 min or 10 min respectively. An aliquot (150 µL) of each sample was then loaded into a black 96 well plate and the fluorescence level was read using the Synergy™ 2 Multi-Mode Microplate Reader (Biotek). For CFDA, the reader was set to excite 475 nm and read at 530 nm for CFDA whereas for resorufin acetate, the reader was set to excite at 540 nm and read at 590 nm.

4.2.5 Tunicamycin treatment.

LS174T cells were incubated with 0.125 µg/mL of tunicamycin (Sigma-Aldrich) for 24 h. The appropriate volume of sugar analog was then added to each well to give concentrations ranging from 0 to 100 µM and the cells were then further incubated for 48 h at which time intracellular esterase activity was measured as described above.

4.2.6 Reverse transcription-polymerase chain reaction (rt-PCR).

Total RNA was isolated using Trisol® reagents (Gibco BRL) and reversed transcribed using the high capacity RNA-to-cDNA kit (Applied Biosystems). PCR amplifications were performed using the following primer pairs: GAPDH, 5'-

AGGTCATCCCTGAGCTGAACGG-3' (sense) and 5'-CGCCTGCTTCACCACCTTCTTG-3' (antisense); Acetylcholinesterase (*ACHE*), 5'-TTCGCCCAGCGACTGATGCG-3' (sense) and 5'-GCCATTGTGGGGCCTTGGGG-3' (antisense); Butrylcholinesterase (*BCHE*), 5'-AGATCCATAGTGAAACGGTGGGCA-3' (sense) and 5'-TGAAGACAGGCCAGCTTGTGCT-3' (antisense); Carboxyl Ester Lipase (*CEL*), 5'-GTGGGTTCGTGGAAGGCGTCAA-3' (sense) and 5'-GGAACCCAAGGGGGCCGACA-3' (antisense); Carboxylesterase 1 (*CES1*), 5'-AGCGCAGGGCGGTAACTCTGG-3' (sense) and 5'-CGAGGACGGATGCCCTGCCCA-3'; Carboxylesterase 3 (*CES3*), 5'-GGGCGTGAAGGGCACAGACC-3' (sense) and 5'- CAGTGCTGGCATCCCGCACA-3' (antisense); Carboxylesterase 7 (*CES7*), 5'-GCTCGATATCACAGAGAAGGAGCCA-3' (sense) and 5'-CCGGTTCGAGCAAAGGTAGCCC-3' (antisense). qRT-PCR was performed using the Step-One Plus Real-Time PCR system (Applied Biosystems) with the thermocycling conditions of 50 ˚C for 30 min, 95 ˚C for 10 min followed by 40 cycles of 95 ˚C for 15 s and 60 ˚C for 1.0 min. PCR amplification for carboxyesterase 2 (CES2) was performed using TaqMan® Gene Expression Assay (cat. No. 4331182, Applied Biosystems).

4.2.7 Western blot analysis.

Proteins were immunodetected using the following commercial antibodies: anti-CES1 (AV41877, Sigma-Aldrich), anti-CES2 (514-621, Novus Bio.) and HRP-linked anti-rabbit antibody (Cell Signaling).

4.2.8 Intracellular immunofluorescence staining and flow cytometry.

Analog treated cells were detached using 1.0 mL of enzyme free cell dissociation buffer and washed with D-PBS. The cells were then washed once with permeation buffer (D-PBS, 2.0 % heat inactivated FBS, 0.2 % sodium azide, 0.5 % saponin), washed once with super-permeation buffer (3 parts permeation buffer to 1 part FBS) and fixed using 3.75 % formaldehyde in DPBS for 15 min. Cells were then washed twice with staining buffer (PBS, 2.0 % heat inactivated FBS, 0.2 % sodium azide) and incubated with human-specific anti-CES1 (Sigma-Aldrich) primary antibody in permeation buffer for 1.0 h at room temperature. Cells were then washed with permeation buffer, incubated with FITC-linked anti-rabbit antibody (Sigma-Aldrich) secondary antibody for 1.0 h and washed again with permeation buffer. The cells were then re-suspended in PBS and analyzed using the C6 Flow Cytometry system (Accuri Cytometers).

4.2.9 Determination of sialic acid levels in analog-treated cells.

Cells were incubated for 48 h and then lysed by subjecting them to three freeze-thaw cycles. Lysates were analyzed using an adaptation of the periodate-resorcinol assay (31) to a 96 well plate format (32) to quantify total sialic acid. For each experiment, test samples were compared to a standard curve created using known concentrations of *N*-acetylneuraminic acid (Invitrogen).

4.2.10 Click chemistry enrichment of azide-labeled proteins in ManNAz-analog treated cells.

Cells (5.0×10^7) were incubated for 48 h with 0 μM or 100 μM 1,3,4-*O*-Bu_3ManNAz after which the cells were collected using 3.0 mL enzyme free cell dissociation buffer and washed once with 3 mL D-PBS. Cells were then lysed in 1.0 mL lysis buffer (Click

Chemistry Tools from the Bioconjugate Technology Company). Lysates were pelleted by centrifugation at 10,000 *g* for 5.0 min and the supernatant was collected. Copper catalyst solution (1.0 mL of a 2x solution, Bioconjugate Technology Company) and 0.2 mL of washed alkyne agarose resin (Bioconjugate Technology Company) were added and mixed on an end-over-end rotary shaker for 48 h at 4 ^{0}C. The resin was then washed 10 times with agarose wash buffer (Click Chemistry Tools) using a spin column and centrifuging at 1,000 *g* for 1.0 min, the column then was washed 5 times with 8 M urea/100 mM Tris pH-8 and finally washed 5 times with 20% acetonitrile. The washed resin was then resuspended in 0.2 mL elution buffer (100 mM sodium phosphate with 2% (v/v) hydrazine) and incubated for 120 min at room temperature: during this step the hydrazine cleaves a Dde linker thus releasing the bound proteins from the agarose resin. The eluted solution was collected by centrifugation and analyzed by western blotting.

4.2.11 Statistical analysis.

Data was expressed as means ± standard error (SEM). Statistical significance was determined using one way ANOVA to compare means of different samples with control. The null hypothesis was rejected in cases where *p*-values were < 0.05.

4.3 Results and Discussion

4.3.1 In silico evidence for glycosylation of intracellular esterases.

The hypothesis that intracellular esterase activity can be modulated by MGE depends on the glycosylation of these enzymes. To gain insight into this issue, we used NetNGlyc 1.0 for *in silico* prediction of *N*-glycosylation of several human esterases to query

whether these enzymes are typically subject to this PTM. As a positive control, this approach correctly predicted several already-known sites of *N*-glycosylation for ACHE and BCHE (**Table 4.1**) (10-12). NetNGlyc analysis also showed that, with the exception of Esterase D (ESD), all esterases tested had at least one requisite consensus sequon for the biosynthetic installation of *N*-glycans and indeed, were predicted to be *N*-glycosylated based on the algorithm used by the NetNGlyc 1.0 software.

The premise that intracellular esterase activity could be influenced by MGE was supported by anreport that liver carboxylesterases were glycosylated (33) as well as structural information suggesting that an *N*-linked oligosaccharide was located at the interface between CES1 monomers (27,28). An apparent conundrum, however, is that carboxylesterases such as CES1 or CES2 are "intracellular" proteins, a class of molecules that generally are not N-glycosylated. A conceptual solution to this discrepancy lies in the subcellular localization of these enzymes; under normal conditions they only partially transit the secretory apparatus and remain in the endoplasmic reticulum (ER) while removal of their ER-localization amino acid sequence is sufficient to allow for their secretion (34). In essence, carboxylesterases exemplify extracellular proteins insofar as they are subject to *N*-glycosylation and are routed towards secretion; the secretion process, however, is thwarted by the ER-localization sequence that ultimately results in the retention of these esterases inside of a cell.

4.3.2 In silico analyses of hCES glycosylation.

N-glycosylation of human carboxylesterases has already been reported (27,28) but several uncertainties remain. For example, only one (and in some cases two) GlcNAc residues of the N-glycan that are located proximal to the peptide chain and an undefined

sialic acid have been observed in crystal structures of hCES1 produced in *Spodoptera frugiperda* insect cells. We assumed that the sialic acid was a legitimate part of an N-glycan chain attached to hCES1 because the free monosaccharide form of this sugar is only present in very low concentrations in biological milieu and unlikely to have co-crystallized with the protein. Based on this assumption, we first ruled out that the positioning of sialic acid was due to crystal packing effects that do not represent the active form of this enzyme under normal cellular conditions. As shown in **Figure 4.2A**, the distance between a proximal GlcNAc and the closet sialic acid moieties on an adjacent crystal unit is ~45 Å while the longest *S. frugiperda N*-glycan (as well as the majority of human N-glycans (35)) are < 25 Å when fully extended. Based on this information, the sialic acid moieties observed in the published crystal structure can only plausibly be appended to N-glycan chains that are located within each trimeric assembly of CES1 that constitutes the active form of this enzyme in cells and are not a result of crosslinking due to crystal packing.

Once we were confident that the sialic acid observed in the published structures was not simply an artifact of the crystallization process, we explored addition details of the trimeric form of CES1 as depicted in **Figure 4.2B**. This figure shows location of the proximal GlcNAc on ASN97 at the interface of two CES1 peptide chains along with the closely-spaced but undefined sialic acid observed in the crystal structures, as explicitly illustrated in **Figure 4.2B(i)**. In another *in silico* approach, we modeled a typical *N*-glycan structure at the interface between the two CES1 subunits (**Figure 4.2B(ii)**), which indicates that the glycan is not large enough that its terminal sialic acids could "reach" to a distal site on the trimeric form of the proteins where a sialic acid was observed (e.g., to

the position shown in **Figure 4.2B(i)** nor is the glycan large enough to directly interfere with substrate binding (**Figure 4.2B(iii)**). Therefore, the impact that the glycan has on catalysis – as described subsequently in this report – must occur via allosteric effects including quaternary-level stabilization of the trimeric form of the enzyme.

Based on the evidence presented in **Figure 4.2A** and **B**, the sialic acid observed in the crystal structure of hCES1 could only plausibly be part of an N-glycan attached to nearby ASN97; the GlcNAc of this glycan proximal to this amino acid and the undefined sialic acid are shown at higher resolution in **Figure 4.2C**. Because the connecting portion of the N-glycan between the proximal GlcNAc and terminal sialic acid was not observed in the crystal form of hCES1, we modeled representative N-glycans to determine if the proximal GlcNAc reasonably could be connected to the sialic acid, which was "pinned" to the close-by ASN97 site of attachment to the protein. Although *S. frugiperda* cells (the source of crystallized CES1 in published studies) typically produce high mannose *N*-glycans that lack sialic acid, *Drosophila* sialylate a small fraction of glycan structures (< 10%), and can process ManNAc analogs into sialosides (36), These results suggest that insects do have a limited capacity for sialylation. with a single sialylation site on the α3 antennary branch of N-glycans. Therefore, we appended a sialylated arthropod *N*-glycan (37) to ASN79 and modeled this structure in an attempt to fill in the missing density between the non-reducing end of GlcNAc and the sialic acid. The entire glycan was minimized to correct for deviations in idealized geometries, and there were no geometric or steric difficulties in closing such a loop from GlcNAc to the terminal sialic acid, presumably because of the ample "open space" available for a complex-type insect

glycan to adopt the necessary configuration to locate the sialic acid in the position for a typical insect glycan, as indicated the published crystal structures (**Figure 4.2D**).

Next, the α6 antennary branch of the singly sialylated arthropod glycan was extended by a β-Gal-6α-Neu5Ac unit to model a typical complex biantennary mammalian *N*-glycan to increase the relevance of the modeling efforts to the experiments subsequently reported in this paper that were conducted in human and CHO cells. These results show that the second sialylated arm of the *N*-glycan can easily extend away from the surface of the CES1 complex to facilitate the binding of the sialylated arm to the position where sialic acid was observed in the crystal structure (**Figure 4.2E**). Finally, a fully fucosylated, triantennary *N*-glycan was modeled; although this particular glycan structure is not abundant we used it to represent an extreme case to ask whether the extra steric bulk from the added branching introduced by the third arm and fucose residues could prevent correct positioning of the sialic acid observed in the crystal structures. The results of this simulation (as shown in **Figure 4.2F**), however, showed that the terminal sialic acid could still be properly positioned, illustrating how the hCES1 trimer can accommodate a broad range of N-glycans (including numerous examples not shown here) and still position the proximal GlcNAc and undefined sialic acid as observed in the published crystal structures.

These *in silico* results were significant from several perspectives. First, they confirmed that CES1 can be *N*-glycosylated in a manner consistent with previously reported crystal structures and furthermore, that the observed sialic acid is legitimately a part of an appended N-glycan and not a serendipitously co-crystallized soluble sialic acid monosaccharide. Second, to be observed in the crystal structure, the sialic acid is

necessarily confined in space, which is unlike the connecting monosaccharide residues that were not observed in the crystal structure presumably because of a combination of rapid unconfined motion and the heterogeneity of N-glycan structures that connect the proximal GlcNAc residue with the terminal sialic acid. Third, once the minimal requirement of having a sialylated α3 antennary branch is met (as evidenced by the arthropod glycan shown in **Figure 4.2D**), additional elaboration of the *N*-glycan structure that typically occurs in mammals is not detrimental for hCES1 subunit assembly because the "extra" oligosaccharide chains can be easily oriented away from the globular protein into open space. Finally, the fact that sialic acid was observed in the crystal structures implies that sialylated *N*-glycans were over-represented in crystallized CES1 compared to their overall production in insect cells, which according to literature reports is comparatively minor. Consequently, while only a relatively small fraction of the hCES1 produced by the insect cells used to generate the crystals under discussion was expected to be modified with sialylated *N*-glycans, the under-represented sialylated species preferentially gave rise to the multimeric assemblies required for crystallization.

All in all, the *in silico* modeling results led us to formulate a hypothesis wherein sialic acid plays a stabilizing role in CES1 trimer formation and provided impetus for the experimental efforts described in this report to increase esterase sialylation using a MGE approach. Importantly, we had at our disposal ManNAc analogs that were expected to selectively modify sialic acid in a way predicted to increase esterase activity if our hypothesis was valid while corresponding hexosamines (e.g., GalNAc analogs) that do not modulate sialic acid but instead impact other aspects of glycosylation (e.g., added N-

glycan branching) that our modeling suggested was not important for esterase activity would serve as negative controls.

4.3.3 Increased esterase activity was observed in ManNAc analog treated cells.

The evidence presented above suggesting that sialic acid-bearing species become enriched during crystal formation of CES1 was particularly intriguing because multimeric assembly this enzyme is required for catalytic activity (27,38). These results implied that esterase activity – which depends on multimeric assembly – benefits from increased sialylation; accordingly, I reasoned that a ManNAc analog-based MGE approach that increases flux through the sialic acid pathway (22,29) and in turn increases protein sialylation (25,30), should increase esterase activity. To test this prediction, indicator dye assays were used to evaluate the impact of "high flux" butanoylated ManNAc analogs that increase sialylation (25,29,30) on esterase activity. At the outset, I was concerned that these assays might not be definitive because two factors had the potential to diminish the predicted increase in esterase activity. First, if a substantial portion of intracellular esterase activity was occupied in activating the hexosamine analogs themselves (the esterase processing of SCFA-hexosamine analogs is discussed extensively in our previous publications (21,23,24,29)), signal derived from the indicator dyes might be suppressed. A high basal level of esterase activity therefore was desirable to ensure adequate signal for unambiguous results leading me to select the human colon adenocarcinoma LS174T line for these experiments because of their high esterase activity (6).

The fluorescent dyes used to measure esterase activity in our assays are widely employed in live/dead cell assays. Therefore a second possible pitfall was that, if the

cells under test experience reduced viability as a consequence of well-established SCFA-hexosamine cytotoxicity (22), the ensuing decrease in esterase activity could offset the predicted sialic acid-driven increase. To avoid this possibility, two steps were taken. First, the analogs were used at sub-growth inhibitory doses (i.e., < 150 μM for Bu_4ManNAc and 1,3,4-*O*-Bu_3ManNAc and < 25 μM for 3,4,6-*O*-Bu_3ManNAc). Then, to deconvolute any remaining impact from the cytotoxicity of the analogs, initial experiments were performed with Bu_4ManNAc, 1,3,4-*O*-Bu_3ManNAc, and 3,4,6-*O*-Bu_3ManNAc because these three analogs have varying cytotoxicities(29) that would allow correlations between toxic analogs (Bu_4ManNAc and 3,4,6-*O*-Bu_3ManNAc) and trends in esterase activity to be deconvoluted if they existed. These concerns, however, were rendered moot when independent assays using different indicator dyes (carboxy fluorescein diacetate, CFDA; **Figure 4.3A** or resorufin acetate; **Figure 4.3B**) both showed an increase in esterase-generated fluorescent signal. This ManNAc analog-driven increase in sialylation confirmed our prediction that increased sialylation would increase esterase activity, and furthermore, that the increased activity was sufficiently robust to outweigh any secondary effect by which these compounds could theoretically diminish esterase activity.

4.3.4 Increased esterase activity is not correlated with gene expression or protein levels.

As predicted from the *in silico* results shown in **Figure 4.2**, butanoylated ManNAc analogs that increase sialic acid also enhanced intracellular esterase activity (**Figure 4.3**). At the outset of the experiments, the most likely esterase responsible for the processing of butanoylated ManNAc analogs in the LS174T cell line was thought to be CES2 because,

although both CES1 and CES2 are implicated in drug detoxification and metabolism (26), robust CES1 expression is restricted to liver- and monocyte-derived cell lineages (39,40). However, because of conservation of important catalytic and structural residues (41), I reasoned that the impact of sialylation would be similar for both carboxylases and initially focused on testing CES2. I found that neither gene or protein expression could explain the increase in esterase activity engendered by Bu_4ManNAc, 1,3,4-*O*-Bu_3ManNAc, and 3,4,6-*O*-Bu_3ManNAc by evaluating CES2 transcription (by qRT-PCR, **Figure 4.4A**) and translation (by western blot assays, **Figure 4.4B**) and found that Bu_4ManNAc increased transcription roughly equivalent to the magnitude of increased esterase activity (e.g., to 150 to 200 % of controls, **Figure 4.3**). The two tributanoylated analogs 1,3,4-*O*-Bu_3ManNAc, and 3,4,6-*O*-Bu_3ManNAc, however, did not increase transcription or translation of CES2 despite increasing esterase activity with approximately the same efficiency as Bu_4ManNAc (see **Figure 4.3)**. Therefore I concluded that the Bu_4ManNAc-driven increase in CES2 mRNA levels was either unrelated, unnecessary, or at most only a partial explanation for the increased esterase activity observed cells treated with butanoylated ManNAc analogs.

An alternate explanation for the discrepancy between the inconsistent changes in transcription and translation of CES2 and the consistent overall increase in cellular esterase activity was that esterases other than CES2 played an unexpectedly large role in LS174T cells. Accordingly, I expanded my analysis to additional esterases expressed in human cells and found that mRNA levels for several of these enzymes were either substantially down-regulated (e.g., for AChE, BChE, CEL, and CES3) or not affected (e.g., for CES1 and CES7) by Bu_4ManNAc (**Figure 4.4C**). Although the down-

regulation of several of these enzymes ran counter to the overall increase in esterase activity observed in ManNAc analog-treated cells, the specific esterases that experienced reduced mRNA levels have limited relevance to detoxification or drug metabolism. Therefore these esterases were not expected to process SCFA-hexosamine analogs or indicator dyes and thus were not expected to have a measurable effect in the fluorophore-based assays.

An important finding of the mRNA results was that CES1 was transcribed in the LS174T cell line, which was not expected *a priori* because, as mentioned above, CES1 is primarily associated with liver and monocyte-derived cell lineages rather than prostate cells. However, reported epigenetic control of CES1 by methylation in cancer (42) provides a plausible explanation for the expression of this enzyme in LS174T cells in the current experiments. To further probe the significance of CES1 transcription in these cells, western blot (**Figure 4.4D**) and immunofluorescence (**Figure 4.4E**) assays confirmed expression at the protein level. Therefore, in addition to CES2, which started out as the most likely candidate for SCFA-hexosamine processing in LS174T cells, the remainder of this report considers CES1 as an esterase that both processes (as indicated in **Figure 4.1**), and is modulated by, SCFA hexosamine analogs. All in all, because the mRNA and protein levels of CES1 were not affected by Bu_4ManNAc, 1,3,4-*O*-Bu_3ManNAc, or 3,4,6-*O*-Bu_3ManNAc, the mechanism of increased esterase activity in the analog-treated cells can best be explained by the glycosylation-based hypothesis presented in **Figure 4.2**.

4.3.5 Increased esterase activity was experimentally confirmed to be linked to glycosylation.

Having discounted transcription or translation as the primary mechanism controlling esterase activity in ManNAc analog-treated cells, I next conducted experiments to confirm that the glycosylation of these enzymes contributed to the observed increased activity in cells. In the first of these experiments cells were treated with tunicamycin, which is a compound that blocks *N*-glycosylation and inhibits liver carboxylesterase activity (33); as shown in **Figure 4.5A** tunicamycin prevented ManNAc analog-driven increases in esterase activity. Furthermore, treatment of the cells with an expanded panel of hexosamine analogs, revealed manipulation of *N*-glycans with analogs that did not alter sialylation did not have an impact on esterase activity. Specifically, butanoylated GalNAc and GlcNAc (i.e., Bu_4GalNAc and Bu_4GlcNAc, **Figure 4.5B**) had negligible and minimal effects on esterase activity compared to Bu_4ManNAc respectively, (**Figure 4.5C**) even though these analogs increase the production of UDP-GlcNAc, which is a critical building block for *N*-glycans and increase N-glycan branching (43). It is noteworthy that the minimal, but measurable, impact of butanolylated GlcNAc was commensurate with the small increase in sialic acid detected in cells treated with this analog (**Figure 4.5D**) (the increased sialic acid is likely a consequence of GlcNAc epimerization to ManNAc, the committed feedstock for sialic acid biosynthesis (44)). A final piece of evidence implicating sialic acid as the critical factor responsible for enhanced esterase activity was provided by supplementation with unmodified ManNAc (**Figure 4.5E**). Although high levels (e.g., tens of millimolar) of unmodified ManNAc were required to reproduce esterase activity-enhancing effects of the butanoylated

ManNAc analogs, the lower effectiveness of unmodified ManNAc was expected because it lacks the ability of butanoylated analogs to diffuse through the plasma membrane and efficiently enter cells (22). Because the exclusive metabolic role of ManNAc is to supply flux into the sialic acid pathway, however, (unlike the butanoylated compounds that can have epigenetic effects (14,23)), this experiment strongly implicated sialylation as a critical and necessary determinant of enhanced esterase activity.

4.3.6 Corroboration of the importance of sialylation in modulating esterase activity in CHO cells.

The impact of ManNAc analogs on esterase activity was tested next in Chinese hamster ovary (CHO) cells because I was interested in how robust analog-mediated enhancement of esterase activity was across cell lines and even species. I demonstrated that ManNAc-driven enhancement of esterase activity is broadly evident in mammalian cells by testing wild-type (WT) CHO cells and finding an approximately equivalent increase in activity (e.g., roughly two-fold, **Figure 4.6A**) as seen earlier in human cells at similar concentrations of butanoylated ManNAc analogs (**Figure 4.3**). Further, CHO mutant lines were available that allowed me to confirm qualitatively that the role of glycosylation (in general) and sialic acid (more specifically) was required for enhanced esterase activity. Specifically, a comparison of three mutant CHO lines (as summarized in Table 2) was consistent with the observations from the human cells. First, the K1 line that has mutations that ablate both *N*-glycan production and sialylation did not respond to butanoylated ManNAc analogs (**Figure 4.6B**). Second, the CHO5 line, which has a reduced (but measurable) capacity for sialylation of *N*-glycans, showed an attenuated but still measurably increased level of esterase activity upon ManNAc analog

supplementation. Finally, the Lec-2 line, which has defective Golgi transport of CMP-Neu5Ac that can be rescued by increased flux through the sialic acid pathway (e.g., *via* ManNAc analog supplementation in the current experiments), had a robust increase in esterase activity similar in magnitude to the WT cells. An interesting facet of the CHO cell experiments was that although all ManNAc analogs solicited qualitatively similar responses, the two analogs with "whole molecule" activity (e.g., Bu_4ManNAc and 3,4,6-*O*-Bu_3ManNAc as we discuss elsewhere (14,15,29)) increased esterase activity more than 1,3,4-*O*-Bu_3ManNAc. Therefore, it is noteworthy that while ManNAc – and by extension sialylation – is a critical component of esterase modulation in the CHO cells, other factors (beyond the scope of this report) may also contribute to this phenomenon.

4.3.7 Azido-modified sialic acids modulate esterase activity and are incorporated into CES2.

Moving beyond the use of ManNAc analogs to increase the production of natural sialic acid as has been reported so far in this paper, many examples of MGE technology employ sugar analogs modified with non-natural functionalities. One of the most common modifications involves the substitution of the natural *N*-acetyl group with an *N*-azido group (e.g., Bu_4ManNAz or 1,3,4-*O*-Bu_3ManNAz, **Figure 4.7A**) to install the corresponding azido-modified sialic acid into cell surface glycans. I was curious if ManNAz analogs would enhance esterase activity in a manner similar to the "natural" ManNAc analogs described earlier in this report. Accordingly, I tested Bu_4ManNAz and 1,3,4-*O*-Bu_3ManNAz and found that both compounds increased esterase activity; furthermore the magnitude increase (up to about 2-fold greater than untreated controls) was similar to increases observed with natural ManNAc (**Figure 4.7B**). Moreover, the

kinetics of the increase in esterase activity (e.g., over a ~ 2 day period) was consistent with the incorporation of various (e.g,. ketone (45) or azide-derivatized (30)) ManNAc analogs into glycoproteins. The ability of azido-modified ManNAc analogs to increase esterase activity was extremely significant from the viewpoint that MGE technologies, such as those used in this study to modulate esterase activity, broadly impact dozens (or even hundreds/thousands) of cellular sialoglycoconjugates and – when using the natural form of ManNAc to increase sialylation – it is difficult to verify that CES1, CES2, or another esterase, is directly impacted. The ability of azido-modified glycoconjugates to be used in click chemistry-based "pull-down" experiments (46) to identify glycoproteins that become labeled with the MGE sugar analog was exploited to resolve whether or not the sialylation status of CES was affected by ManNAc analog supplementation. In this experiment, after cell lysates were pulled down by a click chemistry approach, analog incorporation into CES2 was confirmed by the western blot results shown in **Figure 4.7C**), where signal was only detected in ManNAz analog-treated samples. This experiment unambiguously establishes that ManNAc analogs can be incorporated into the CES glycans and provides strong support for the *in silico* results presented above (e.g., in **Figure 4.2**).

4.4 CONCLUSIONS

This paper reports the discovery that monosaccharide analogs that increase sialic acid production elicit a concomitant increase in intracellular esterase activity consistent with the enhanced sialylation of the single *N*-glycan found on CES1 and CES2, the two enzymes most strongly tied to drug metabolism and detoxification in humans. This

demonstration that intracellular esterase activity can be modulated by MGE has several practical biomedical implications. One is the direct use of SCFA-hexosamines as drugs; conceptually this idea is supported by the treatment of HIBM (a muscle disorder characterized by reduced sialic acid production due to a genetic defect in GNE (47)), where Ac_4ManNAc has shown promise in a mouse model (48). Encouragingly, the HIBM study establishes that this class of compounds has acceptable pharmacological properties to be used *in vivo*. Moving forward, diseases characterized by insufficient esterase activity could be treated with ManNAc analogs to restore esterase activities. A few examples include congenital mutations that reduce esterase activity (7), reduced esterase activity that hinders monocyte-mediated killing of tumor cells (8), and down-regulation of esterases in certain types of cancers when undergoing treatment with esterase-activated prodrugs (9).

Another biomedical scenario where the correlation between sialic acid and esterase activity may prove important is provided by nascent efforts to produce recombinant versions of these enzymes (e.g., carboxylesterase CES2(34)), which could exploit ManNAc analog supplementation to maximize activity. Finally, the ability of butanoylated ManNAc analogs to *down-regulate* transcription of AChE, BChE, CEL, and CES3 (as shown in **Figure 4.4**) may be valuable in several disease contexts; one example is attenuation of increased BChE activity associated with Alzheimer's disease (49,50). Overall, this paper demonstrates that hexosamine analogs that manipulate glycosylation can be used as small molecule, pharmacologically relevant agents to fill the current void consisting of a lack of activators for intracellular drug processing and detoxification esterases.

4.5 ACKNOWLEDGMENTS

Funding for this project was provided by the National Institutes of Health (NCI R01CA112314, NIAMS R01AR054005, and NCI 1F32 CA189246-01). I would also like to acknowledge Dr. J. Gray and Dr. J. Labonte with whom I collaborated with on the *in silico* modeling of esterase glycan orientations.

4.6 FIGURES

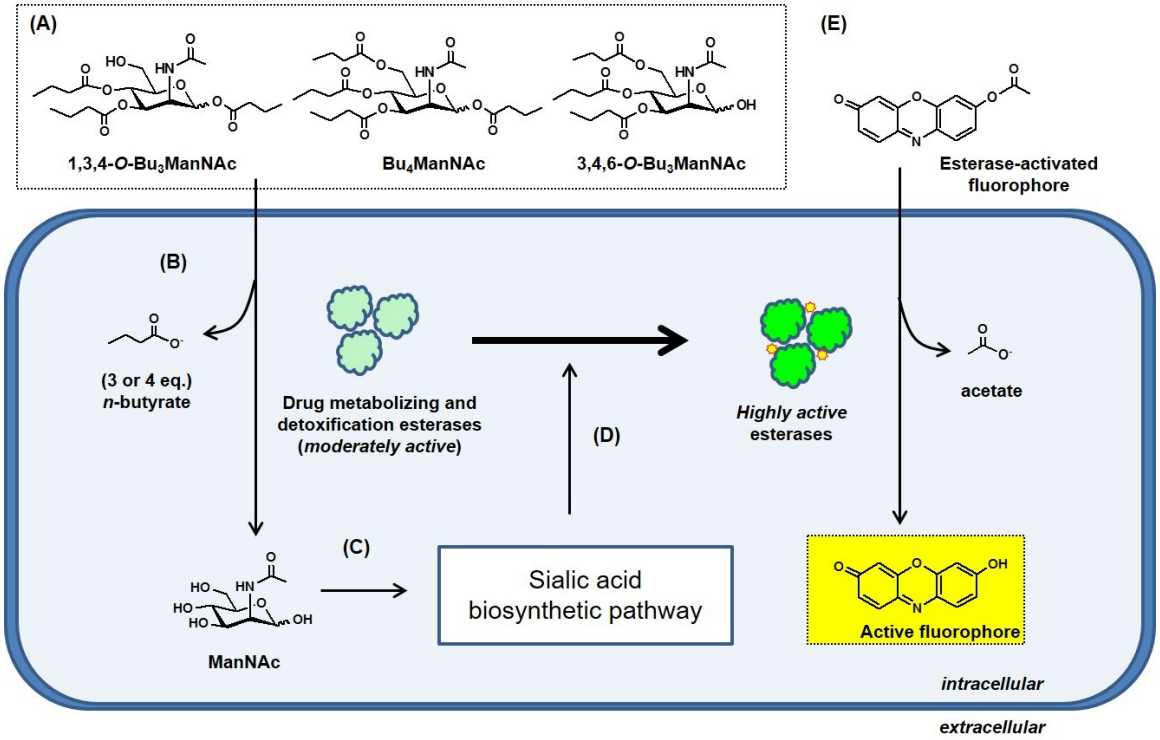

Figure 4.1. Overview of esterase processing of SCFA-derivatized ManNAc analogs and the subsequent impact on esterase activity. *(**A**) Structures of butanoylated ManNAc analogs that readily enter cells through membrane diffusion where (**B**) drug metabolizing esterases remove their ester-linked n-butyrate groups to generate unmodified ManNAc, which (**C**) acts as a feedstock that increased metabolic flux through the sialic acid biosynthetic pathway. (**D**) Increased sialylation is proposed to increase the activity of intracellular esterases as measured by (**E**) resorufin acetate (shown) or carboxy fluorescein diacetate (CFDA) assays; experimental results for both of these ester-activated fluorophores are shown in Figure 3.*

Figure 4.2. In silico evaluation of CES glycosylation. ***(A)*** *The hCES1 trimer and its closest crystal partner in the periodic image along the a axis. The a unit cell vector length is 55.78 Å. Glycan residues are shown as space-filling models and colored by element. The distance from a GlcNAc residue to the closest sialic acid residue is ~45 Å.* ***(B)*** *The hCES1 trimer with each monomer shown in a different shade of gray. Non-peptide residues and molecules are shown as space-filling models and colored by element. Carbon atoms for saccharide residues are shown in standard CFG colors. Carbon atoms for the substrate analogs are shown in yellow.* ***(C)*** *Protein subunits A and B of hCES1 are shown using dark gray and light gray ribbons, respectively, from the published crystal structure(27), with Asn79 (labeled) along with the proximal GlcNAc and undefined sialic acid shown in the position observed in the published crystal structure.* ***(D–F)*** *Protein subunits A and B of hCES1 are shown along with appended glycans representative of* ***(D)*** *an low-abundance complex-type insect N-glycan w/ sialic acid,* ***(E)*** *a representative mammalian bis-sialylated complex N-glycan, and* ***(F)*** *a tri-antennary fully fucosylated mammalian N-glycan (All carbohydrate atoms in C–F are shown with sticks and colored by element with representations of glycans relevant to hCES activity determined using the CFG standard symbol notation generated using GlycoWorkbench.(51) Models in* ***A–F*** *were created with Accelrys Discovery Studio Visualizer 3.5.)*

(**A**) CES1 from PDB ID 1YA8

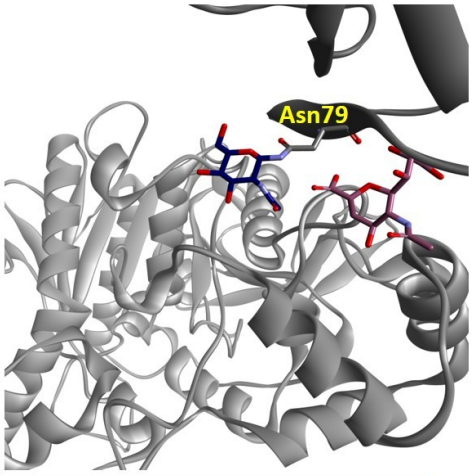

(**B**) Representative *N*-glycans

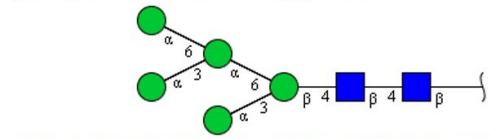

Typical insect high-mannose *N*-glycan w/o sialic acid

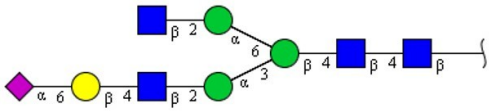

Low-abundance complex insect *N*-glycan w/ sialic acid

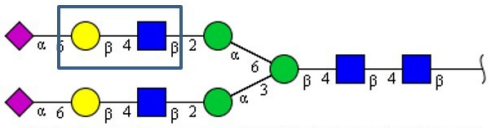

Typical complex mammalian *N*-glycan w/ sialic acid

(**C**) Modeled CES1 with low-abundance insect *N*-glycan

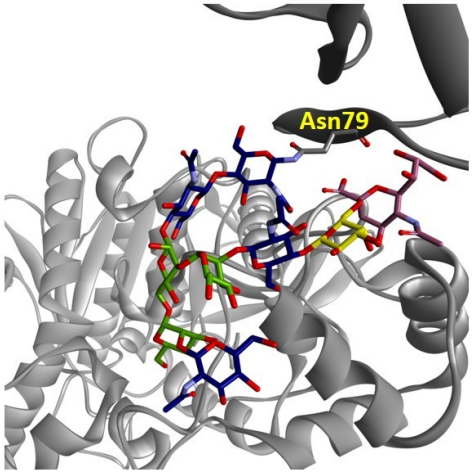

(**D**) Modeled CES1 with typical mammalian *N*-glycan

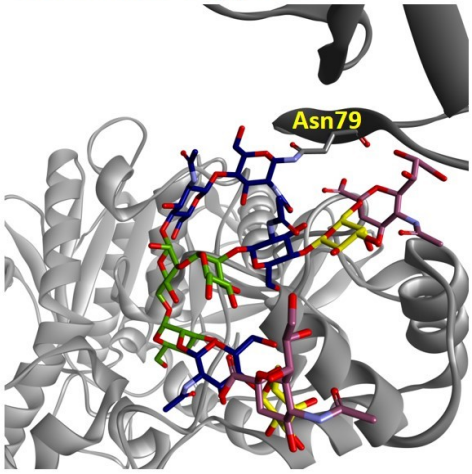

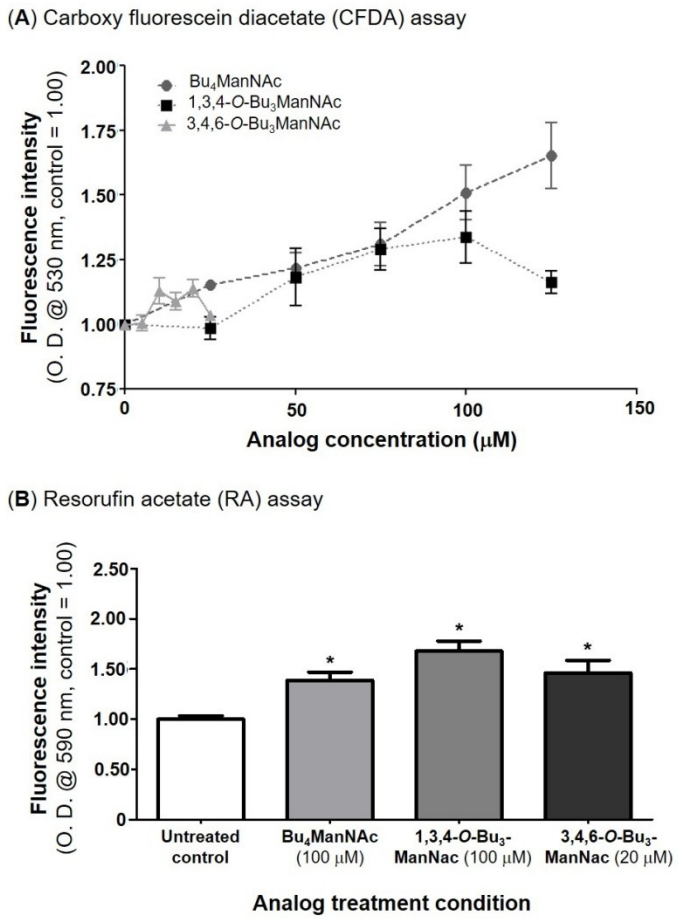

Figure 4.3. Intracellular esterase activity activities measured by activation of fluorescent dyes. *Fluorescence levels are shown for LS174T cells treated with Bu_4ManNAc, 1,3,4-O-Bu_3ManNAc, and 3,4,6-O-Bu_3ManNAc analyzed by two assays (**A**) carboxy fluorescein diacetate and (**B**) resorufin acetate. * - indicates a P value of < 0.05 in a two-tailed t test.*

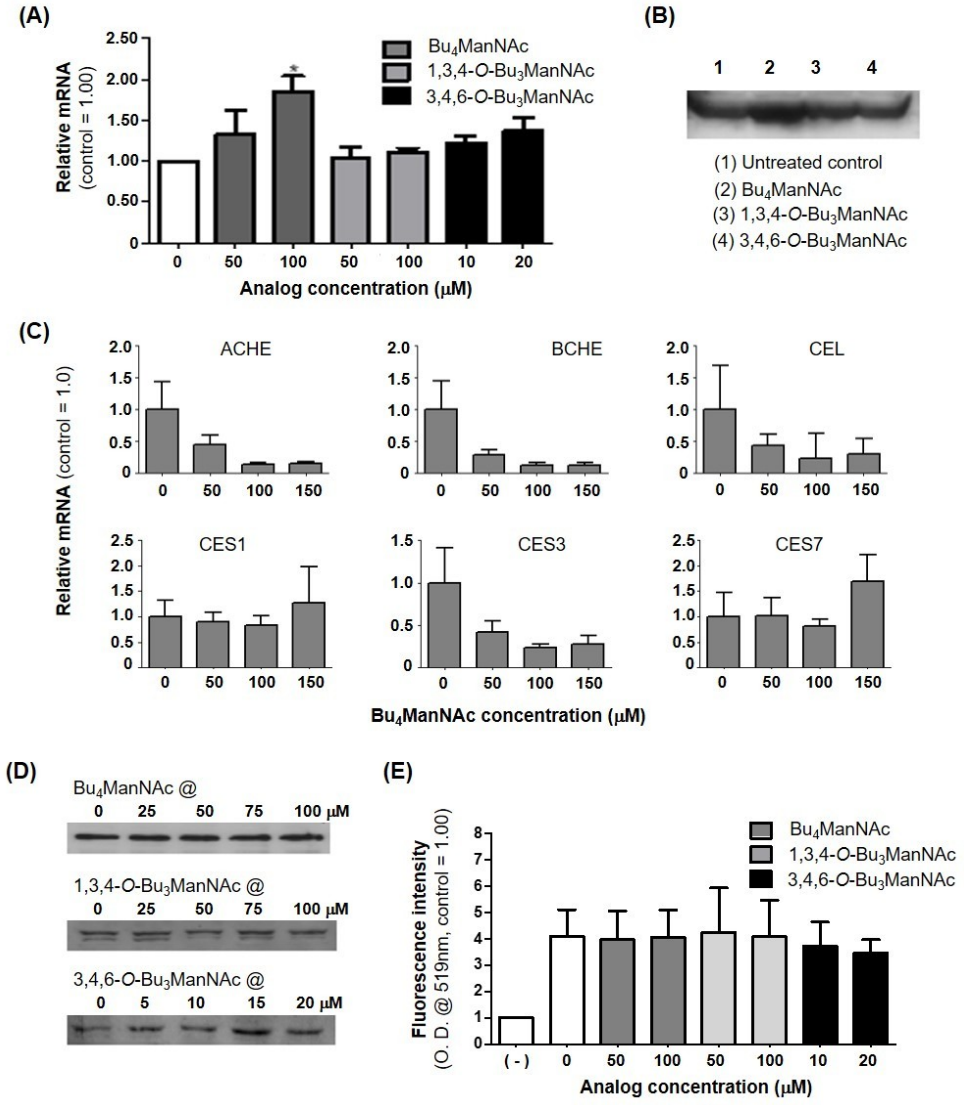

Figure 4.4. Transcriptional and translational control of esterases in LS174T cells. *Quantification of CES2 protein and RNA levels from LS174T cells via (**A**) qRT-PCR and (B) western blot respectively showed that overall levels of this esterase remained unchanged upon sugar analog treatment, with the exception of Bu_4ManNAc treatment where the signal increased. (**C**) qRT-PCR showed that mRNA levels for ACHE, BCHE, CEL, and CES3 in LS174T cells treated with Bu_4ManNAc were significantly down-regulated at higher concentrations while CES1 and CES7 were not affected. Quantification of CES1 from LS174T cells via (**D**) western blots and (**E**) immunofluorescence assays using flow cytometry showed that the overall levels of this esterase either remained the same upon sugar analog treatment. * - indicates a P value of < 0.05 in a two-tailed t test.*

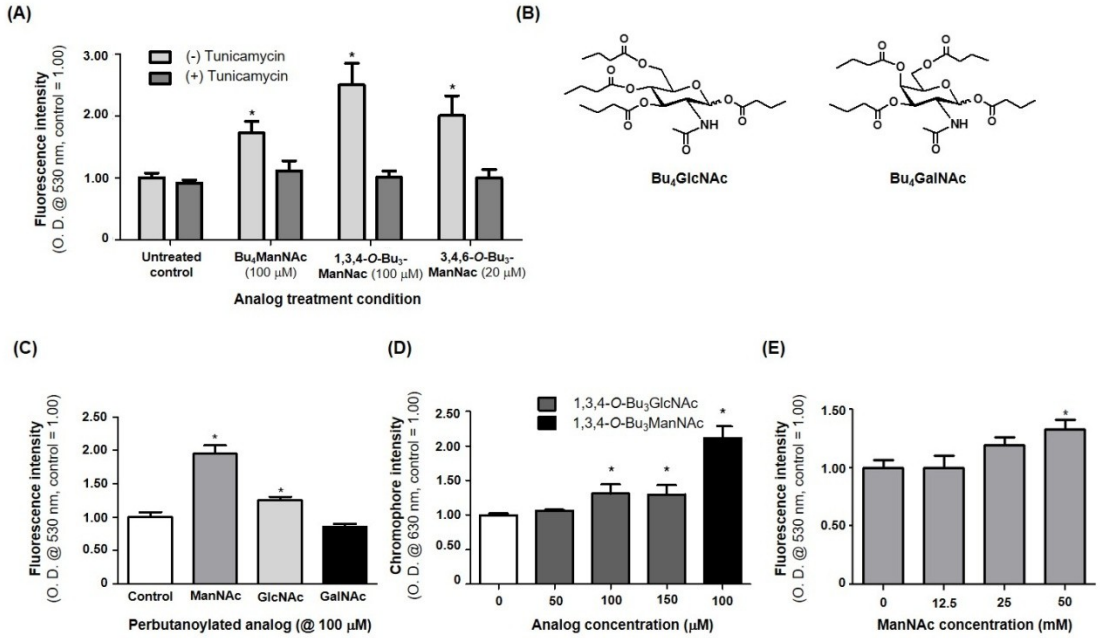

Figure 4.5. Expanded analysis of the effects of glycosylation on esterase activity*. (**A**) Tunicamycin treated LS174T cells that were also treated with ManNAc analogs did not experience an increase in esterase activity. (**B**) Structures of Bu_4GlcNAc and Bu_4GalNAc analogs, which (**C**) elicited a small or no increase in esterase activity (respectively) in LS174T cells (Bu_4ManNAc was included in this experiment as a positive control). (**D**) The periodate resorcinol assay was used to measure sialic acid content in 1,3,4-O-Bu_3GlcNAc-treated cells, with 1,3,4-O-Bu_3ManNAc again used as the positive control (no increase in sialic acid levels was observed for GalNAc analog treated cells, data not shown). (**E**) Intracellular esterase activity in cells treated with increasing concentrations of unmodified ManNAc. * - indicates a P value of < 0.05 in a two-tailed t test.*

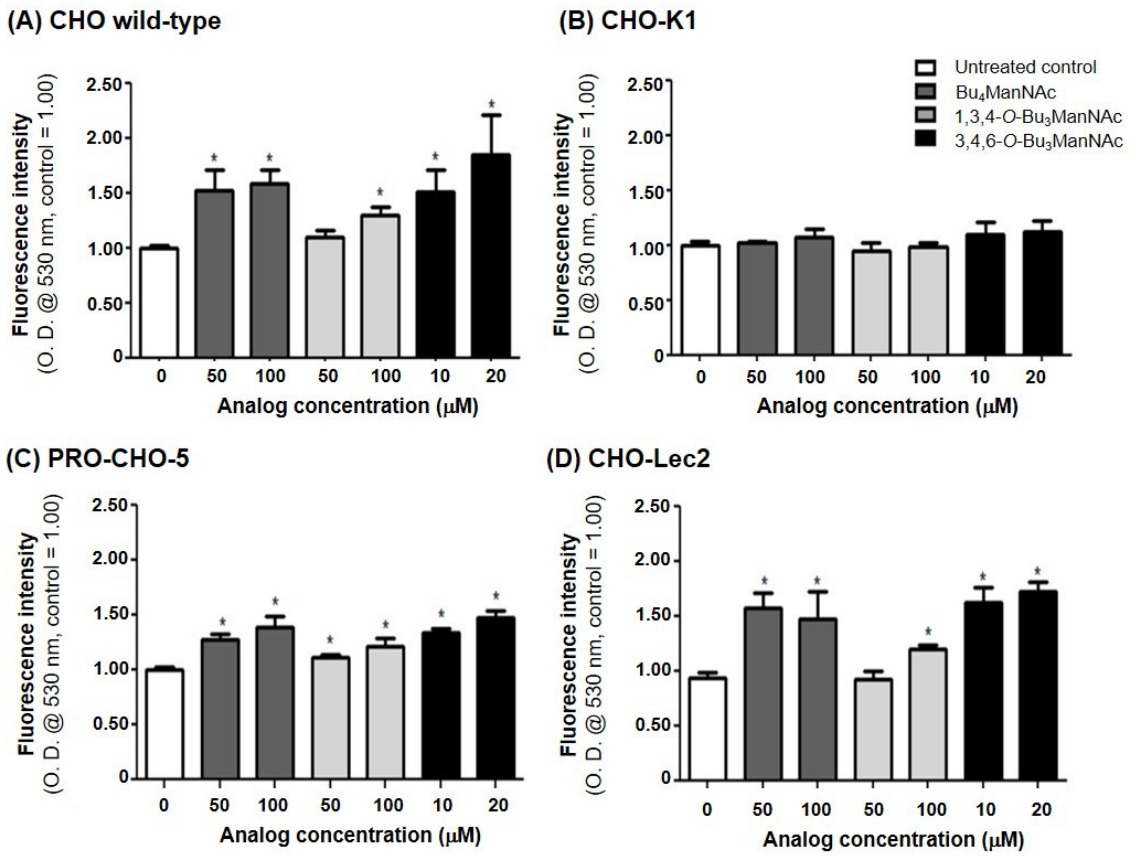

Figure 4.6. Analysis of esterase activity in various analog-treated CHO cell lines*. (**A**) Wild-type cells that treated with ManNAc analogs experienced an increase in esterase activity while (**B**) CHO-K1 cells did not experience a change in esterase activity under any condition; (**C**) Pro-CHO-5 cells demonstrated a less dramatic increase; and (**D**) CHO-Lec2 cells showed an increase in esterase activity comparable to the wild-type cells. * - indicates a P value of < 0.05 in a two-tailed t test.*

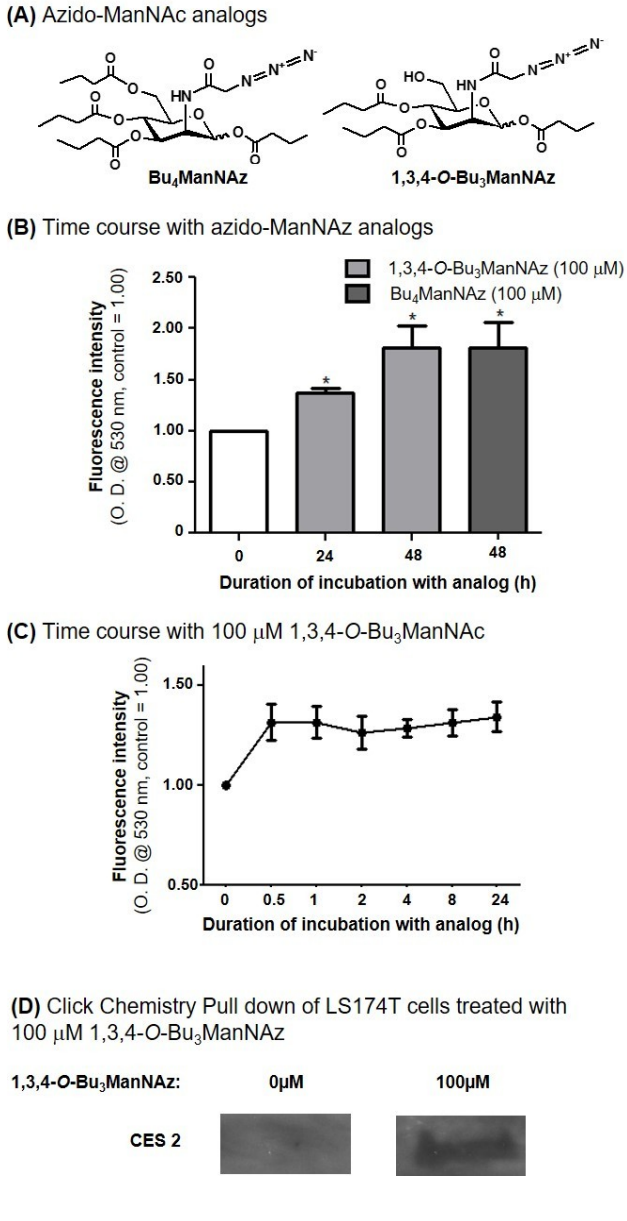

Figure 4.7. Time course of ManNAc analog induced changes and the effect of azido-labeled analogs on esterase activity. *(**A**) Structures of Bu_4ManNAz and 1,3,4-O-Bu_3ManAz, which (**B**) elicited an increase in esterase activity after 24 and 48 h of incubation of LS174T cells with the respective analogs. (**C**)Western blotting of proteins pulled down by click chemistry shows incorporation of SiaAz into CES2 in 1,3,4-O-Bu3ManNAz treated LS174T cells. * - indicates a P value of < 0.05 in a two-tailed t test.*

4.7 TABLES

Table 4.1. *In silico* prediction of esterase *N*-glycosylation

Name	Accession Number	No. of sites predicted	Sites	Jury Agreement	Probability of N-Glycosylation
ACHE	AAA68151	3	296	5/9	+
			381	7/9	+
			495	6/9	+
BCHE	AAH18141	9	45	9/9	++
			85	8/9	+
			134	8/9	+
			269	9/9	+++
			284	9/9	++
			369	5/9	+
			483	9/9	+++
			509	9/9	++
			514	4/9	+
CEL	AAA51973	1	210	9/9	++
ESD	AAC99788	NONE	N/A	N/A	N/A
CES1	AAI10339	1	79	7/9	+
CES2	AAH32095	1	175	9/9	++
CES3	ACD11491	1	105	6/9	+
CES7	AAH69548	3	363	6/9	+
			463	9/9	++
			474	6/9	+
CES8	AAH64573	3	95	9/9	+++
			157	9/9	++
			269	9/9	+++

Table 4.2. Synopsis of CHO cell line experiments

Cell line	Deficiency	Esterase activity	Possible explanation
K1	- Lack asparagine-linked glycosylation homolog ALG13 which heterodimerizes with ALG14 to catalyze the second step in N-linked glycosylation(52) - Lack ST6Gal sialyltransferase responsible for formation of α-2,6-linked sialic acid terminal bonds (53)	No increase	- Absence of ALG 13 could lead to *N*-glycosylation deficiencies in some of the esterases - Formation of α-2,6 sialic acid terminal bonds plays an important role in the changes in esterase acitivity
CHO-5	- Lack β4-Galactosyl transferase-6 essential for galactosylation of *N*-glycans(54) - This may reduce *N*-glycan terminal sialic acid as they are attached to galactose.	Small increase	- Reduced *N*-glycan capacity for addition of terminal sialic acid reduces the increase in esterase activity
Lec2	- Defective CMP-sialic acid transporters required to transport sialic acid into the Golgi complex(55)	Increase	- Increase in cytoplasm sialic acid concentration makes up for the defective transporter.

4.8 REFERENCES

1. Hatfield, M.J.; Potter, P.M. Carboxylesterase inhibitors. *Expert. Opin. Ther. Pat.* **2011**, *21*, 1159-1171.

2. Pindel, E.V.; Kedishvili, N.Y.; Abraham, T.L.; Brzezinski, M.R.; Zhang, J.; Dean, R.A.; Bosron, W.F. Purification and cloning of a broad substrate specificity human liver carboxylesterase that catalyzes the hydrolysis of cocaine and heroin. *J. Biol. Chem.* **1997**, *272*, 14769-14775.

3. Gao, D.; Narasimhan, D.L.; Macdonald, J.; Brim, R.; Ko, M.C.; Landry, D.W.; Woods, J.H.; Sunahara, R.K.; Zhan, C.G. Thermostable variants of cocaine esterase for long-time protection against cocaine toxicity. *Mol Pharmacol* **2009**, *75*, 318-323.

4. Lavis, L.D. Ester bonds in prodrugs. *ACS Chem. Biol.* **2008**, *3*, 203-206.

5. Tsuji, T.; Kaneda, N.; Kado, K.; Yokokura, T.; Yoshimoto, T.; Tsuru, D. CPT-11 converting enzyme from rat serum: purification and some properties. *J Pharmacobiodyn* **1991**, *14*, 341-349.

6. Jansen, W.J.; Zwart, B.; Hulscher, S.T.; Giaccone, G.; Pinedo, H.M.; Boven, E. CPT-11 in human colon-cancer cell lines and xenografts: characterization of cellular sensitivity determinants. *Int. J. Cancer* **1997**, *70*, 335-340.

7. Zhu, H.-J.; Patrick, K.S.; Yuan, H.-J.; Wang, J.-S.; Donovan, J.L.; DeVane, C.L.; Malcolm, R.; Johnson, J.A.; Youngblood, G.L.; Sweet, D.H.; Langaee, T.Y.; Markowitz, J.S. Two CES1 gene mutations lead to dysfunctional carboxylesterase 1 activity in man: Clinical significance and molecular basis. *Am. J. Hum. Genet.* **2008**, *82*, 1241-1248.

8. Oertel, J.; Hagner, G.; Kastner, M.; Huhn, D. The relevance of a-naphthyl acetate esterases to various monocyte functions. *Br J Heamatol* **1985**, *61*, 717-726.

9. Burkhart, D.J.; Barthel, B.L.; Post, G.C.; Kalet, B.T.; Nafie, J.W.; Shoemaker, R.K.; Koch, T.H. Design, synthesis, and preliminary evaluation of doxazolidine carbamates as prodrugs activated by carboxylesterases. *J. Med. Chem.* **2006**, *49*, 7002-7012.

10. Weikert, T.; Ebert, C.; Rasched, I.; Layer, P.G. Novel inactive and distinctively glycosylated forms of butyrylcholinesterase from chicken serum. *J. Neurochem.* **1994**, *63*, 318-325.

11. Saez-Valero, J.; Barquero, M.; Marcos, A.; McLean, C.A.; Small, D.H. Altered glycosylation of acetylcholinesterase in lumbar cerebrospinal fluid of patients with Alzheimer's disease. *J. Neurol. Neurosurg. Psych.* **2000**, *69*, 664-667.

12. Kolarich, D.; Weber, A.; Pabst, M.; Stadlmann, J.; Teschner, W.; Ehrlich, H.; Schwarz, H.P.; Altmann, F. Glycoproteomic characterization of butyrylcholinesterase from human plasma. *Proteomics* **2008**, *8*, 254-263.

13. Meutermans, W.; Le, G.T.; Becker, B. Carbohydrates as scaffolds in drug discovery. *ChemMedChem* **2006**, *1*, 1164-1194.

14. Elmouelhi, N.; Aich, U.; Paruchuri, V.D.P.; Meledeo, M.A.; Campbell, C.T.; Wang, J.J.; Srinivas, R.; Khanna, H.S.; Yarema, K.J. Hexosamine template. A platform for modulating gene expression and for sugar-based drug discovery. *J. Med. Chem.* **2009**, *52*, 2515–2530.

15. Wang, Z.; Du, J.; Che, P.-L.; Meledeo, M.A.; Yarema, K.J. Hexosamine analogs: from metabolic glycoengineering to drug discovery. *Curr. Opin. Chem. Biol.* **2009**, *13*, 565-572.

16. Dube, D.H.; Bertozzi, C.R. Metabolic oligosaccharide engineering as a tool for glycobiology. *Curr. Opin. Chem. Biol.* **2003**, *7*, 616-625.

17. Campbell, C.T.; Sampathkumar, S.-G.; Weier, C.; Yarema, K.J. Metabolic oligosaccharide engineering: perspectives, applications, and future directions. *Mol. Biosys.* **2007**, *3*, 187-194.

18. Kayser, H.; Zeitler, R.; Kannicht, C.; Grunow, D.; Nuck, R.; Reutter, W. Biosynthesis of a nonphysiological sialic acid in different rat organs, using *N*-propanoyl-D-hexosamines as precursors. *J. Biol. Chem.* **1992**, *267*, 16934-16938.

19. Du, J.; Meledeo, M.A.; Wang, Z.; Khanna, H.S.; Paruchuri, V.D.P.; Yarema, K.J. Metabolic glycoengineering: sialic acid and beyond. *Glycobiology* **2009**, *19*, 1382-1401.

20. Sarkar, A.K.; Fritz, T.A.; Taylor, W.H.; Esko, J.D. Disaccharide uptake and priming in animal cells: inhibition of sialyl Lewis X by acetylated Gal b1,4GalcNAc b-onaphthalenemethanol. *Proc. Natl. Acad. Sci. U. S. A.* **1995**, *92*, 3323-3327.

21. Jones, M.B.; Teng, H.; Rhee, J.K.; Baskaran, G.; Lahar, N.; Yarema, K.J. Characterization of the cellular uptake and metabolic conversion of acetylated *N*-acetylmannosamine (ManNAc) analogues to sialic acids. *Biotechnol. Bioeng.* **2004**, *85*, 394-405.

22. Kim, E.J.; Sampathkumar, S.-G.; Jones, M.B.; Rhee, J.K.; Baskaran, G.; Yarema, K.J. Characterization of the metabolic flux and apoptotic effects of *O*-hydroxyl- and *N*-acetylmannosamine (ManNAc) analogs in Jurkat (human T-lymphoma-derived) cells. *J. Biol. Chem.* **2004**, *279*, 18342-18352.

23. Sampathkumar, S.-G.; Jones, M.B.; Meledeo, M.A.; Campbell, C.T.; Choi, S.S.; Hida, K.; Gomutputra, P.; Sheh, A.; Gilmartin, T.; Head, S.R.; Yarema, K.J. Targeting glycosylation pathways and the cell cycle: sugar- dependent activity of butyrate-carbohydrate cancer prodrugs. *Chem. Biol.* **2006**, *13*, 1265-1275.

24. Mathew, M.P.; Tan, E.; Shah, S.; Bhattacharya, R.; Meledeo, M.A.; Huang, J.; Espinoza, F.A.; Yarema, K.J. Extracellular and intracellular esterase processing of SCFA-hexosamine analogs: implications for metabolic glycoengineering and drug delivery. *Bioorg. Med. Chem. Lett.* **2012**, *22*, 6929-6933.

25. Almaraz, R.T.; Tian, Y.; Bhattarcharya, R.; Tan, E.; Chen, S.-H.; Dallas, M.R.; Chen, L.; Zhang, Z.; Zhang, H.; Konstantopoulos, K.; Yarema, K.J. Metabolic flux increases glycoprotein sialylation: implications for cell adhesion and cancer metastasis. *Mol. Cell. Proteomics* **2012**, 10.1074/mcp.M1112.017558

26. Fukami, T.; Yokoi, T. The emerging role of human esterases. *Drug Metab. Pharmacokinet.* **2012**, *27*, 466-477.

27. Fleming, C.D.; Bencharit, S.; Edwards, C.C.; Hyatt, J.L.; Tsurkan, L.; Bai, F.; Fraga, C.; Morton, C.L.; Howard-Williams, E.L.; Potter, P.M.; Redinbo, M.R. Structural insights into drug processing by human carboxylesterase 1: Tamoxifen, mevastatin, and inhibition by benzil. *J. Mol. Biol.* **2005**, *352*, 165-177.

28. Bencharit, S.; Morton, C.L.; Xue, Y.; Potter, P.M.; Redinbo, M.R. Structural basis of heroin and cocaine metabolism by a promiscuous human drug-processing enzyme. *Nat. Struct. Biol.* **2003**, *10*, 349-356.

29. Aich, U.; Campbell, C.T.; Elmouelhi, N.; Weier, C.A.; Sampathkumar, S.G.; Choi, S.S.; Yarema, K.J. Regioisomeric SCFA attachment to hexosamines separates metabolic flux from cytotoxicity and MUC1 suppression. *ACS Chem. Biol.* **2008**, *3*, 230-240.

30. Almaraz, R.T.; Aich, U.; Khanna, H.S.; Tan, E.; Bhattacharya, R.; Shah, S.; Yarema, K.J. Metabolic oligosaccharide engineering with *N*-acyl functionalized ManNAc analogues: cytotoxicity, metabolic flux, and glycan-display considerations. *Biotechnol. Bioeng.* **2012**, *109*, 992-1006.

31. Jourdian, G.W.; Dean, L.; Roseman, S. The sialic acids. XI. A periodate-resorcinol method for the quantitative estimation of free sialic acids and their glycosides. *J. Biol. Chem.* **1971**, *246*, 430-435.

32. Yarema, K.J.; Goon, S.; Bertozzi, C.R. Metabolic selection of glycosylation defects in human cells. *Nat. Biotechnol.* **2001**, *19*, 553-558.

33. Kroetz, D.L.; McBride, O.W.; Gonzalez, F.J. Glycosylation-dependent activity of baculovirus-expressed human liver carboxylesterases: cDNA cloning and characterization of two highly similar enzyme forms. *Biochemistry* **1993**, *32*, 11606-11617.

34. Lamego, J.; Cunha, B.; Peixoto, C.; Sousa, M.F.; Alves, P.M.; Simplício, A.L.; Coroadinha, A.S. Carboxylesterase 2 production and characterization in human cells:

new insights into enzyme oligomerization and activity. *Appl. Microbiol. Biotechnol.* **2013**, *97*, 1161-1173.

35. Werz, D.B.; Ranzinger, R.; Herget, S.; Adibekian, A.; Von der Lieth, C.W.; Seeberger, P.H. Exploring the structural diversity of mammalian carbohydrates ("glycospace") by statistical databank analysis. *ACS Chem. Biol.* **2007**, *2*, 685-691.

36. Granell, A.E.; Palter, K.B.; Akan, I.; Aich, U.; Yarema, K.J.; Betenbaugh, M.J.; Thornhill, W.B.; Recio-Pinto, E. DmSAS is required for sialic acid biosynthesis in cultured Drosophila third instar larvae CNS neurons. *ACS Chem. Biol.* **2011**, *6*, 1287-1295.

37. Tiemeyer, M.; Selleck, S.B.; Esko, J.D. Chapter 24. Arthropoda. Cold Spring Harbor (NY): Cold Spring Harbor Laboratory Press; 2009.

38. Bencharit, S.; Morton, C.L.; Hyatt, J.L.; Kuhn, P.; Danks, M.K.; Potter, P.M.; Redinbo, M.R. Crystal structure of human carboxylesterase 1 complexed with the Alzheimer's drug tacrine. *Chem. Biol.* **2003**, *10*, 341-349.

39. Imai, T. Human carboxylesterase isozymes: catalytic properties and rational drug design. *Drug Metab. Pharmacokinet.* **2006**, *21*, 173-185.

40. Markey, G.M. Carboxylesterase 1 (Ces1): from monocyte marker to major player. *J. Clin. Pathol.* **2011**, *64*, 107-109.

41. Sanghani, S.P.; Sanghani, P.C.; Schiel, M.A.; Bosron, W.F. Human carboxylesterases: an update on CES1, CES2 and CES3. *Protein Pept Lett* **2009**, *16*, 1207-1214.

42. Hori, T.; Hosokawa, M. DNA methylation and its involvement in carboxylesterase 1A1 (CES1A1) gene expression. *Xenobiotica* **2010**, *40*, 119-128.

43. Dennis, J.W.; Nabi, I.R.; Demetriou, M. Metabolism, cell surface organization, and disease. *Cell* **2009**, *139*, 1229-1241.

44. Luchansky, S.J.; Yarema, K.J.; Takahashi, S.; Bertozzi, C.R. GlcNAc 2-epimerase can serve a catabolic role in sialic acid metabolism. *J. Biol. Chem.* **2003**, *278*, 8036-8042.

45. Yarema, K.J.; Mahal, L.K.; Bruehl, R.E.; Rodriguez, E.C.; Bertozzi, C.R. Metabolic delivery of ketone groups to sialic acid residues. Application to cell surface glycoform engineering. *J. Biol. Chem.* **1998**, *273*, 31168-31179.

46. Tian, Y.; Almaraz, R.T.; Choi, C.H.; Li, Q.K.; Saeui, C.; Li, D.; Shah, P.; Bhattacharya, R.; Yarema, K.J.; Zhang, H. Identification of sialylated glycoproteins from metabolically oligosaccharide engineered pancreatic cells. *Clin Proteomics* **2015**, *12*, doi: 10.1186/s12014-12015-19083-12018.

47. Eisenberg, I.; Avidan, N.; Potikha, T.; Hochner, H.; Chen, M.; Olender, T.; Barash, M.; Shemesh, M.; Sadeh, M.; Grabov-Nardin, G.; Shmilevich, I.; Friedmann, A.; Karpati, G.; Bradley, W.G.; Baumbach, L.; Lancet, D.; Ben Asher, E.; Beckmann, J.S.; Argov, Z.; Mitrani-Rosenbaum, S. The UDP-N-acetylglucosamine 2-epimerase/N-acetylmannosamine kinase gene is mutated in recessive hereditary inclusion body myopathy. *Nat. Genet.* **2001**, *29*, 83-87.

48. Malicdan, M.C.V.; Noguchi, S.; Tokutomi, T.; Goto, Y.-i.; Nonaka, I.; Hayashi, Y.K.; Nishino, I. Peracetylated N-acetylmannosamine, a synthetic sugar molecule,

efficiently rescues muscle phenotype and biochemical defects in mouse model of sialic acid-deficient myopathy. *J. Biol. Chem.* **2012**, *287*, 2689-2705.

49. Greig, N.H.; Lahiri, D.K.; Sambamurti, K. Butyrylcholinesterase: an important new target in Alzheimer's disease therapy. *Int Psychogeriatr* **2002**, *14 (Suppl 1)*, 77-91.

50. Nordberg, A.; Ballard, C.; Bullock, R.; Darreh-Shori, T.; Somogyi, M. A review of butyrylcholinesterase as a therapeutic target in the treatment of Alzheimer's disease. *Prim Care Companion CNS Disord* **2013**, *15*, pii: PCC.12r01412.

51. Ceroni, A.; Maass, K.; Geyer, H.; Geyer, R.; Dell, A.; Haslam, S.M. GlycoWorkbench: a tool for the computer-assisted annotation of mass spectra of glycans. *J. Proteome Res.* **2008**, *7*, 1650-1659.

52. Xu, X.; Nagarajan, H.; Lewis, N.E.; Pan, S.; Cai, Z.; Liu, X.; Chen, W.; Xie, M.; Wang, W.; Hammond, S. The genomic sequence of the chinese hamster ovary (CHO)-K1 cell line. *Nat. Biotechnol.* **2011**, *29*, 735-741.

53. Gao, X.D.; Tachikawa, H.; Sato, T.; Jigami, Y.; Dean, N.A. Alg14 recruits Alg13 to the cytoplasmic face of the endoplasmic reticulum to form a novel bipartite UDP-N-acetylglucosamine transferase required for the second step of N-linked glycosylation. *J. Biol. Chem.* **2005**, *280*, 36254-36362.

54. Lee, J.H.; Sundaram, S.; Shaper, N.L.; Raju, S.; Stanley, P. Chinese hamster ovary (CHO) cells may express six β4-Galactosyltransferases (β4GalTs). *J. Biol. Chem.* **2001**, *276*, 13924-13934.

55. Eckhardt, M.; Gotza, B.; Gerardy-Schahn, R. Mutants of the CMP-sialic acid transporter causing the Lec2 phenotype. *J. Biol. Chem.* **1998**, *274*, 20189-20195.

CHAPTER 5

METABOLIC GLYCOENGINEERING SENSITIZES DRUG-RESISTANT PANCREATIC CANCER CELLS TO TYROSINE KINASE INHIBITORS ERLOTINIB AND GEFITINIB

ABSTRACT

Metastatic human pancreatic cancer cells (the SW1990 line) that are resistant to the EGFR-targeting tyrosine kinase inhibitor drugs (TKI) erlotinib and gefitinib were treated with 1,3,4-*O*-Bu_3ManNAc, a "metabolic glycoengineering" drug candidate that increased sialylation by ~2-fold. Consistent with genetic methods previously used to increase EGFR sialylation, this small molecule reduced EGF binding, EGFR transphosporylation, and downstream STAT activation. Significantly, co-treatment with both the sugar pharmacophore and the existing TKI drugs resulted in strong synergy, in essence re-sensitizing the SW1990 cells to these drugs. Finally, 1,3,4-*O*-Bu_3ManNAz, which is the azido-modified counterpart to 1,3,4-*O*-Bu_3ManNAc, provided a similar benefit thereby establishing a broad-based foundation to extend a "metabolic glycoengineering" approach to clinical applications.

This chapter was originally published as **Mathew, M. P., Tan, E., Saeui, C. T., Bovonratwet, P., Liu, L., Bhattacharya, R., & Yarema, K. J. (2015). Metabolic glycoengineering sensitizes drug-resistant pancreatic cancer cells to tyrosine kinase inhibitors erlotinib and gefitinib.** ***Bioorganic & medicinal chemistry letters*****, *25*(6), 1223-1227.**

5.1 INTRODUCTION

Tumor-associated carbohydrate antigens (TACAs) have been associated with cancer for decades (1-4) and abnormal glycosylation is now accepted to be a universal feature of cancer (5). Despite the many roles glycosylation has been discovered to play in cancer progression and metastasis (6-9), progress in exploiting this knowledge in a clinical setting has been agonizingly slow (8, 10). The epidermal growth factor receptor (EGFR) exemplifies the "sweet and sour" (10) or "bittersweet" (8) nature of glycosylation in cancer. On one hand, several papers over the past ~15 years have reported that modulation of EGFR's glycosylation status – in particular changes to fucose and sialic acid – control this receptor's ability to drive cancer progression. For example, a recent report showed that increased sialylation or fucosylation of EGFR suppressed dimerization, inhibited subsequent phosphorylation, and dampened activation of downstream signaling in lung cancer cells (11). On the other hand, although these responses would be expected to slow cancer cell growth, the methods used to demonstrate these features in cell culture experiments, such as enzymatic removal of sugars or genetic over-expression of glycosyltransferases, are not easily translated to animal testing or to a human clinical setting thereby illustrating the general difficulties in developing carbohydrate-based cancer therapies.

In this chapter I overcome a hurdle towards clinical exploitation of the glycosylation status of EGFR by using small molecule "metabolic glycoengineering" sugar analogs to increase the sialylation of this receptor and reduce its activity in ways that were previously only accomplished genetically (11, 12). Metabolic glycoengineering (13) (also referred to as metabolic oligosaccharide engineering or MOE (14, 15)) is a

versatile technique used to change patterns of glycosylation by altering the availability or chemical composition of biosynthetic precursors of glycans (16, 17). For example, short chain fatty acid (SCFA)-modified ManNAc analogs can efficiently enhance metabolic flux through the sialic acid biosynthetic pathway (18, 19) and increase cell surface sialylation (20). The ester-linked SCFA moieties, which are usually acetate (21-23) or n-butyrate (19, 24), increase cellular uptake by three orders of magnitude or more and upon entering a cell, intracellular esterases rapidly remove the SCFA groups (25), regenerating the core sugar that enters the targeted biosynthetic pathway. This strategy positions SCFA-modified sugars as viable drug candidates, as evidenced by the recent use of Ac_4ManNAc to reverse the symptoms of hereditary inclusion body myopathy in an animal model of this disease (26).

One drawback of SCFA-conjugated monosaccharide drug candidates is cytotoxicity that, while not severe, can hinder metabolic incorporation into cell surface glycans (18, 19, 27). Our laboratory has addressed this problem by exploiting structure activity relationships (SARs) that attribute analog-mediated cytotoxicity to the presence of a SCFA group at the C6 position of a hexosamine (28, 29). This discovery enabled the development of tributanoylated sugars such as 1,3,4-*O*-Bu_3ManNAc (**Figure 5.1**) that achieve high flux into the sialic acid pathway at low analog concentrations compared to the widely used peracylated compounds (e.g., Ac_4ManNAc, also shown in **Figure 5.1**) (20). Of particular relevance to our efforts to develop glycosylation-based therapies for chemotherapy-resistant pancreatic cancer, we found that EGFR in SW1990 cells treated with 1,3,4-*O*-Bu_3ManNAc experienced an increase in sialylation of ~2.3 fold by using

mass spectrometry-based “glycosite” (30) and glycan analysis methods similar to those already reported (31, 32).

5.2 MATERIALS AND METHODS

5.2.1 Cell Culture and Incubation with Sugar Analogs

SW1990 (ATCC® CRL-2172) cells were grown in Dulbecco's Modified Eagle Medium (DMEM) supplemented 10 % with heat-inactivated fetal bovine serum (FBS) and 1.0 % of 100x pen/strep antibiotic solution (Invitrogen). Cells were maintained at 37 °C in a humidified atmosphere containing 5% CO_2. For treatment of cells, cells typically were plated in 6-well tissue culture plates in 2.0 mL of culture media at a density of 300,000 cells/well. Sugar analogs, either 1,3,4-*O*-Bu_3ManNAc or 1,3,4-*O*-Bu_3ManNAz were synthesized and characterized as previously described (20, 28) and stored lyophilized at -80 °C. Stock solutions (100 mM) were made in ethanol (EtOH) and the compounds were added to each well to achieve the desired analog concentrations; the identical volume of ETOH (always less than 10 □. Stock solutions (100 mM) were made in ethanol (EtOH) and the compounds were added to each well to achieve the desired analog concentrations; the st concentration of analog. Cells were typically incubated for 48 h with the sugar analogs; in many experiments (as indicated below) the first 24 h of incubation was carried out in complete media and the cells were serum starved for the final 24 h before analysis following published protocols for monitoring EGFR phosphorylation and activation (11).

5.2.2 EGF Saturation Binding Assays

Cells were incubated for 48 h with 1,3,4-*O*-Bu_3ManNAc with serum starvation over the last 24 h. The cells were washed with PBS, treated with enzyme free cell dissociation buffer (Life Technologies) until they detached from the culture plate, collected, and counted and cell numbers were normalized using the Beckman Z2 cell coulter counter. Cells were then washed twice in Live Cell Imaging Solution (Life Technologies) supplemented with 1.0% bovine serum albumin (BSA) and 20 mM glucose. Cells were then incubated at room temperature for 2 h with 2 μg/mL of Alexa Fluor 488-linked EGF (Life Technologies). Cells were washed three times in Live Cell Imaging Solution and analyzed using flowcytometry with an Accuri C6 Flow cytometer.

5.2.3 Immunofluorescence

Cells were analyzed by fluorescence microscopy after incubation with analogs for 48 h including serum-starvation over the last 24 h after which they washed with phosphate buffered saline (PBS) and then incubated with 10 ng/mL recombinant human EGF (Peprotech AF-100-15) in PBS for 2.0 min to activate EGFR signaling from basal levels (11). Cells were then fixed, permeabilized, blocked and incubated with human specific anti-phospho-EGFR (Cell Signaling) primary antibody for 1.0 h at room temperature. After incubation with the primary antibody, cells were washed and incubated with FITC-linked anti-rabbit (Sigma-Aldrich) secondary antibody for 1.0 h at room temperature. Cells were then washed and incubated with 4,6-diamidino-2-phenylindole (DAPI) for 10 min to stain the nuclei of the cells. After incubation, cells were washed and images were taken using an excitation wavelength of 495 nm and an emission wavelength of 519 nm with a Zeiss Observer A1 microscope.

5.2.4 Western Blot Analysis

Proteins obtained from SW1990 cells were analyzed by western blots after the cells were incubated with 1,3,4-*O*-Bu_3ManNAc for 48 h including, as described above, serum starvation for the last 24 h and exposure to 10 ng/mL recombinant human EGF (Peprotech AF-100-15) in PBS for 2.0 min. Proteins were collected and were immuno-detected using the following commercial antibodies: anti-phospho-EGFR (Cell Signaling), anti-EGFR (Cell Signaling), anti-phospho-STAT3 (Cell Signaling), anti-□ in PBS for 2.0 min. Proteins were collected and were imy (Cell Signaling). Protein bands were quantified using the ImageJ software.

5.2.5 Growth Inhibition Assays to Determine Drug Synergy

Cells were incubated with 1,3,4-*O*-Bu_3ManNAc or 1,3,4,-*O*-Bu_3ManNAz for 48 h, typically at low concentrations (e.g., 25 or 50 □anNAz for 48 h, typically at low concentrations (e.g., 25 or 50 Signaling). Protein bands were quantified using the ImageJ software.Cell Signaling), anti-EGFR (Cell Signaling), anti-phospho the wells. After an additional 72 h incubation period the cells were washed, trypsinized, and counted using a Beckman Z2 cell coulter counter.

5.2.6 Statistical Analysis

Data was expressed as means ± standard error (SEM). Statistical significance was determined using one way ANOVA with a dunnett's post-test to compare means of different samples with the control. The null hypothesis was rejected in cases where p-values were < 0.05.

5.3 RESULTS AND DISCUSSION

Based on the precedent from at least two groups who used genetic methods to increase EGFR sialylation (11, 12), I reasoned that 1,3,4-*O*-Bu_3ManNAc would likewise reduce EGFR activity. This hypothesis was experimentally confirmed by the experiments shown in **Figure 5.2** where I first measured saturation binding to fluorescently-labeled EGF and showed a measurable decrease in available cell surface receptors for EGF (**Figure 5.2A**). In turn, immunofluorescence assays showed that analog treatment led to a decrease in EGFR phosphorylation (**Figure 2B** with additional images provided in **Supplemental Figure S5.1**), which was confirmed by western blots that also showed a decrease in phospho-EGFR (p-EGFR) in cells treated with 1,3,4-*O*-Bu_3ManNAc while the total amount of EGFR was unchanged (**Figure 5.2C**).

Although the changes in EGFR phosphorylation were relatively modest in 1,3,4-*O*-Bu_3ManNAc treated cells, small differences in starting conditions for receptors that initiate phosphorylation cascades typically are amplified downstream. To test whether this characteristic response of signaling pathways applied to 1,3,4-*O*-Bu_3ManNAc-driven changes to p-EGFR, phospho-STAT3 (p-STAT3) which is a "hallmark" downstream element of EGFR-initiated signaling, was monitored by western blot analysis. This experiment confirmed that the predicted enhanced response did occur for STAT3, with a stronger dose-dependent decrease in p-STAT3 levels observed in 1,3,4-*O*-Bu_3ManNAc-treated SW1990 cells as shown by western blots (**Figure 5.3A**) and quantification by Image J software (**Figure 5.3B**). The series of experiments beginning with reduction of EGF binding, progressing to show decreased EGFR phosphorylation, and culminating with dampened STAT activation brought about through the treatment of cells with 1,3,4-

O-Bu_3ManNAc indicate that even modest changes in behavior of surface receptors due to altered glycosylation have potential therapeutic benefit. To gain a sense whether these biochemical markers of signaling pathway activation had an impact on actual cell behavior, we monitored cell proliferation and found that, given sufficiently high levels of 1,3,4-*O*-Bu_3ManNAc, SW1990 cell proliferation decreased (**Figure 5.3C**).

Despite the decreased cell proliferation observed in 1,3,4-O-Bu_3ManNAc treated cells, the high concentrations required to substantially inhibit growth (e.g., > 250 μM) may be difficult to achieve *in vivo*; therefore, the prospects for using 1,3,4-*O*-Bu_3ManNAc as a "stand alone" drug for inhibiting EGFR in TKI resistant cell lines are uncertain. The mechanism by which increased sialylation impacts EGFR, however – which is reported to be decreased dimerization and a concomitant reduction in transphosporylation (11) – is orthogonal to other mechanisms by which cancer cells become resistant to TKIs such as single point mutations that affect the binding of these drugs to EGFR (33) or the constitutive activation of ERK signaling that can circumvent EGFR inhibition (34). Therefore regardless of current uncertainties in the exact mechanism by which 1,3,4-*O*-Bu_3ManNAc modulates EGFR activation and signaling, we reasoned that co-administration of this drug candidate with TKIs such as erlotinib or gefitinib would have an synergistic effect and, in a best case scenario, re-sensitize drug-resistant cells such as the SW1990 pancreatic cancer line to current TKI-acting drugs.

To evaluate synergy between 1,3,4-*O*-Bu_3ManNAc and TKIs, SW1990 cells were incubated with 0, 25, and 50 μM of 1,3,4-*O*-Bu_3ManNAc and then co-treated with a range of concentrations of erlotinib or gefitinib. These levels of 1,3,4-*O*-Bu_3ManNAc are sufficient to increase sialylation (20) and diminish phosphorylation of STAT (**Figure 5.3B**) but result in virtually no growth inhibition when the sugar analog is used alone (**Figure 5.3C**). As shown in **Figure 5.4A** neither erlotinib or gefinitib alone were effective at slowing proliferation SW1990 cells at low nanomolar concentrations but when used in combination with 1,3,4-*O*-Bu_3ManNAc the sensitivity to these drugs dramatically increased. Indeed, reduction in cell growth of 40 to 50% (which are levels associated with clinically effective response) occurred in the tens of nanomolar range for both erlotinib and gefitinib when the cells were co-treated with 50 μM of 1,3,4-*O*-Bu_3ManNAc; this level of sensitivity to these TKIs are comparable to that observed in drug-responsive pancreatic cancer lines (35). In essence, the sugar analog reversed the drug resistance of this cell line.

The Combination Index (CI) (36) was used to more rigorously quantify synergy between ManNAc analogs and existing drugs based on the following relationship:

$$\boldsymbol{CI} = \frac{\boldsymbol{D_1}}{(\boldsymbol{D_x})_1} + \frac{\boldsymbol{D_2}}{(\boldsymbol{D_x})_2}$$

To calculate the CI, D_1 (e.g., 1,3,4-*O*-Bu_3ManNAc) and D_2 (e.g., erlotinib or gefitnib) represent the concentrations of each drug in combination with each other that required to inhibit cell growth by a given amount (x%) and $(D_x)_1$ and $(D_x)_2$ are the concentrations of each drug required to cause x% inhibition when the drugs are used individually. A CI = 1 indicates an additive effect, a CI > 1 indicates an antagonistic effect, and a CI < 1 indicates a synergistic effect (36). **Figure 5.4B** plots the CI measured for each analog-drug combination (using data from **Figure 5.4A** for the TKI drugs when used alone and **Figure 5.3C** for 1,3,4-O-Bu_3ManNAc alone). Strong synergy was observed between 1,3,4-*O*-Bu_3ManNAc and both erlotinib and gefitinib with combination indexes ranging from 0.7 to as low as 0.23. It is noteworthy that stronger synergy (e.g., lower CI values) was observed for 25 μM of 1,3,4-*O*-Bu_3ManNAc compared to 50 μM, indicating that the beneficial effects of this sugar analog "kick in" at low concentrations. Overall, these results position sugar analogs such as 1,3,4-*O*-Bu_3ManNAc as valuable agents for sensitizing drug-resistant pancreatic cancer to existing therapies that target EGFR.

A final set of experiments investigated whether the azide-modified ManNAc analog 1,3,4-*O*-Bu_3ManNAz (shown in **Figure 5.1**), which is incorporated into cell surface glycans as the non-natural "Sia5Az" form of sialic acid (37), also provides synergy with EGFR-targeting TKI drugs. The use of a sialic acid precursor with a non-natural acyl group was of interest for two reasons; one was based on a previous report that this class of compounds could sensitize cancer cells towards chemotherapy and radiation treatment (38). Secondly, azido-modified sugar analogs are capable of labeling cells through click chemistry (20, 37), thereby opening new possibilities of not only synergistically combining carbohydrate analogs with EGFR-acting drugs, but to also

provide a means to direct additional diagnostic or therapeutic agents to sialylated glycans overexpressed in cancer (39, 40). In the current experiments, azido-modified 1,3,4-*O*-Bu_3ManNAz was more cytotoxic on its own (**Figure 5.4C**) compared to 1,3,4-*O*-Bu_3ManNAc, therefore lower concentrations of 12.5 and 25 μM were used to evaluate synergy (**Figure 5.4D**). Even at these low levels of 1,3,4-*O*-Bu_3ManNAz, strong incorporation into cellular glycans occurs (20) and synergy with erlotinib was observed with CI values ranging from 0.68 to as low as 0.34 (**Figure 5.4E**).

In summary, this chapter describes two important findings, the first is that the manipulation of EGFR glycosylation in ways that reduce signaling and dampen endpoints related to cancer progression can now be done with pharmacologically-relevant small molecules rather than the genetic approaches previously reported. The second finding is that treatment of TKI-resistant pancreatic cancer cells with the sugar analogs can restore sensitivity to erlotinib and gefitinib. These results provide a scientific foundation for further investigation beyond the scope of this chapter; for example it is not known how widely the drug synergy will apply across cell lines and tissue types and a detailed accounting of the mechanism by which synergy is achieved remains to be described.

5.4 ACKNOWLEDGMENTS

Funding was obtained from the National Institutes of Health, NCI grant R01CA112314.

5.5 FIGURES

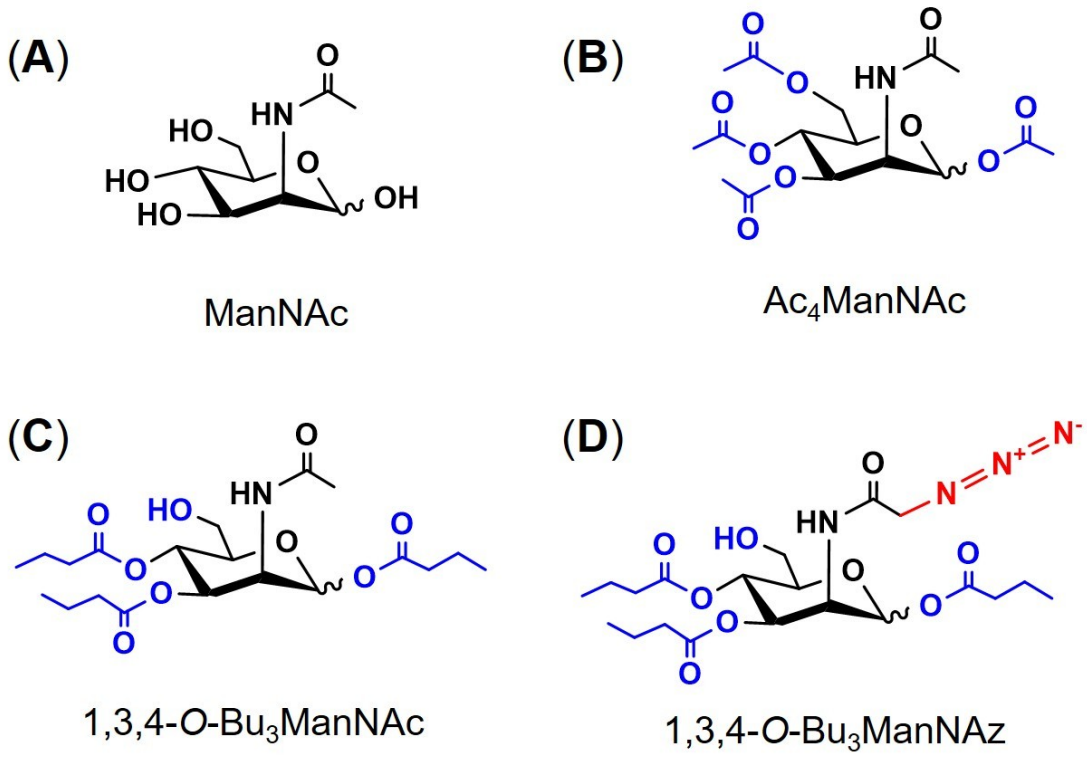

Figure 5.1. ManNAc and analogs used for metabolic glycoengineering pancreatic cancer cells for increased sensitivity to EGFR-targeting TKI drugs. *(**A**) Natural ManNAc. (**B**) Fully acetylated ManNAc, Ac_4ManNAc. (**C**) "High-flux" tributanoylated ManNAc, 1,3,4-O-Bu_3ManNAc. (D) Azide-modified high flux ManNAc, 1,3,4-O-Bu_3ManNAc*

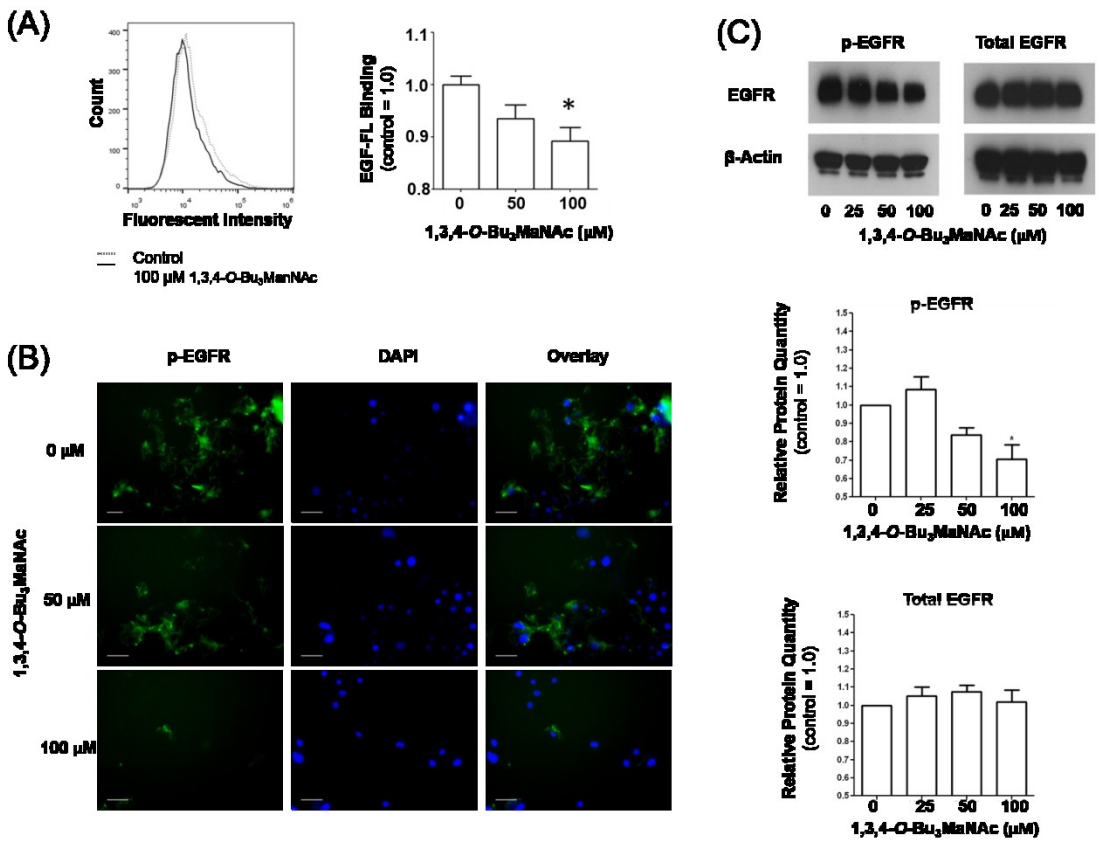

Figure 5.2. 1,3,4-O-Bu$_3$ManNAc decreases EGFR phosphorylation. *(**A**) Saturation binding where cells were incubated with Alexa Fluor® 488 labeled EGF for one hour at room temperature and then measured using flow cytometry shows a decrease in available surface bound EGFR. At least 3 biological replicates were carried out for each experiment with data expressed as mean ± standard error mean (SEM). (**B**) Representative images of immunofluorescence assays (additional images are provided in Supplemental **Figure S5.1**) where cells were incubated with EGF for 2.0 min, fixed and stained with anti-p-EGFR, FITC labeled anti-rabbit antibody, and stained with DAPI confirm that EGFR phosphorylation decreases with analog treatment. (**C**) Western blots of SW1990 pancreatic cancer cells treated with increasing levels of 1,3,4-O-Bu$_3$ManNAc showed a decrease in phosphorylated EGFR with no significant change in overall EGFR levels. * indicates a p value of < 0.05.*

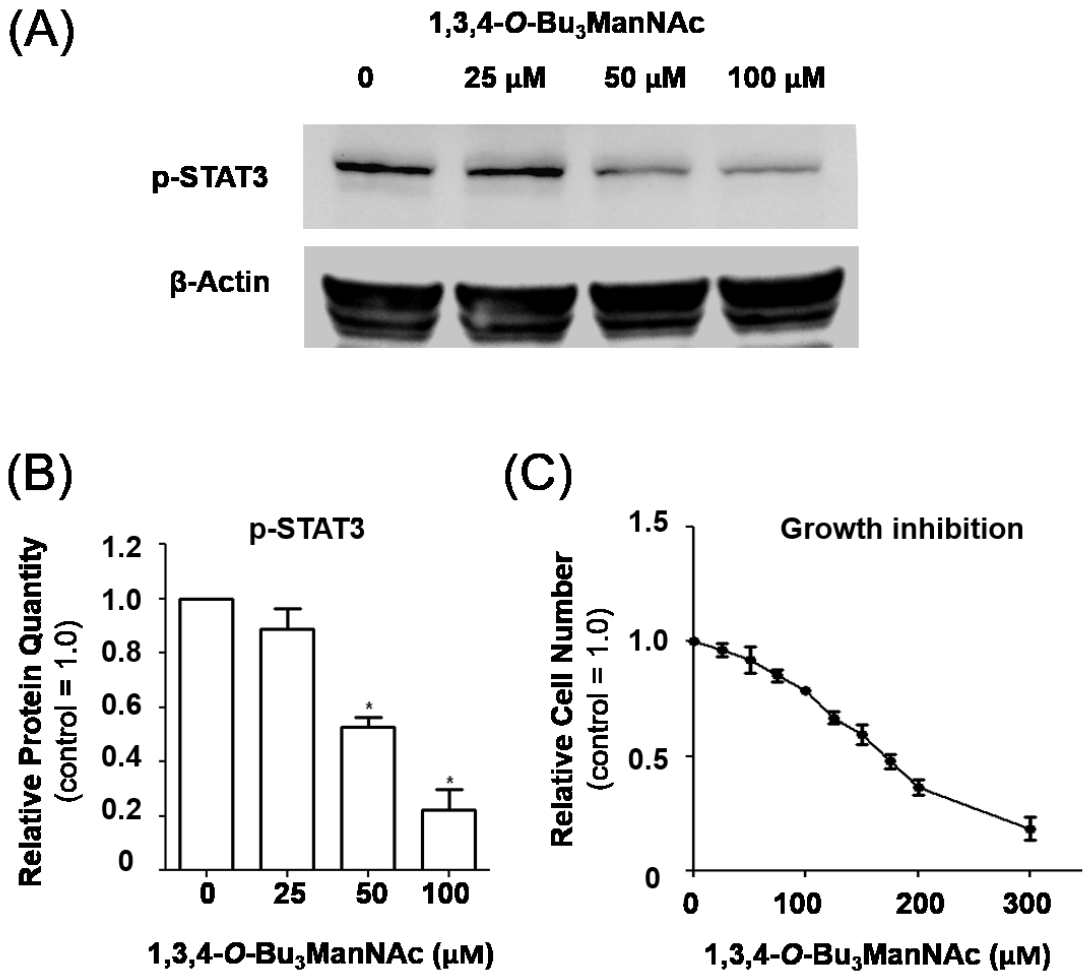

Figure 5.3. Downstream effects of 1,3,4-O-Bu$_3$ManNAc treatment of SW1990 cells and reduced EGFR phosphorylation. ***(A)*** *Representative images of western blots of SW1990 cells treated with different concentrations of 1,3,4-O-Bu$_3$ManNAc showed a significant decrease in phosphorylated STAT3 (as quantified by Image J analysis in Panel* ***B****). (****C****) Finally, 1,3,4-O-Bu$_3$ManNAc reduced cell proliferation albeit at higher concentrations than where effects on EGFR-mediated signaling endpoints were observed. At least 3 biological replicates were carried out for each experiment with data expressed as mean ± standard error mean (SEM). * indicates a p value of < 0.05.*

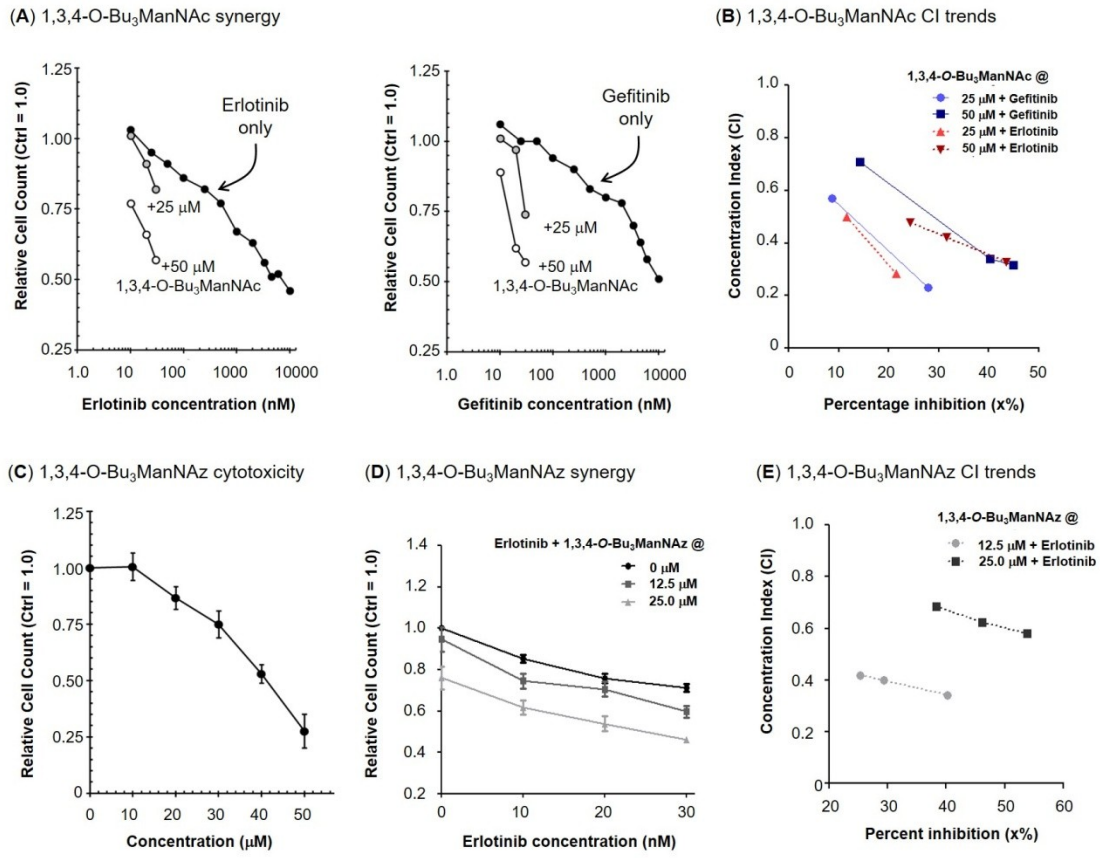

Figure 5.4. Determination of synergy between glycosylation and EGFR-acting drugs. ***(A)*** *Growth inhibition of SW1990 cells treated with gefitinib or erlotonib in combination with 1,3,4-O-Bu₃ManNAc. (**B**) The Combination Index (CI) for each analog-drug combination was determined and plotted against the percentage inhibition observed (x%), with both drugs showing strong synergy with the sugar analog. At least 3 biological replicates were carried out for each experiment with data expressed as mean ± standard error mean (SEM) as depicted in* ***Supplemental Figure S5.2****. **(C)** Growth inhibition of SW1990 cells treated with 1,3,4-O-Bu₃ManNAz. (**D**) Growth inhibition when erlotonib and 1,3,4-O-Bu₃ManNAz were used in combination with the combination index provided in Panel (**E**). At least 3 biological replicates were carried out for each experiment with data expressed as mean ± standard error mean (SEM).*

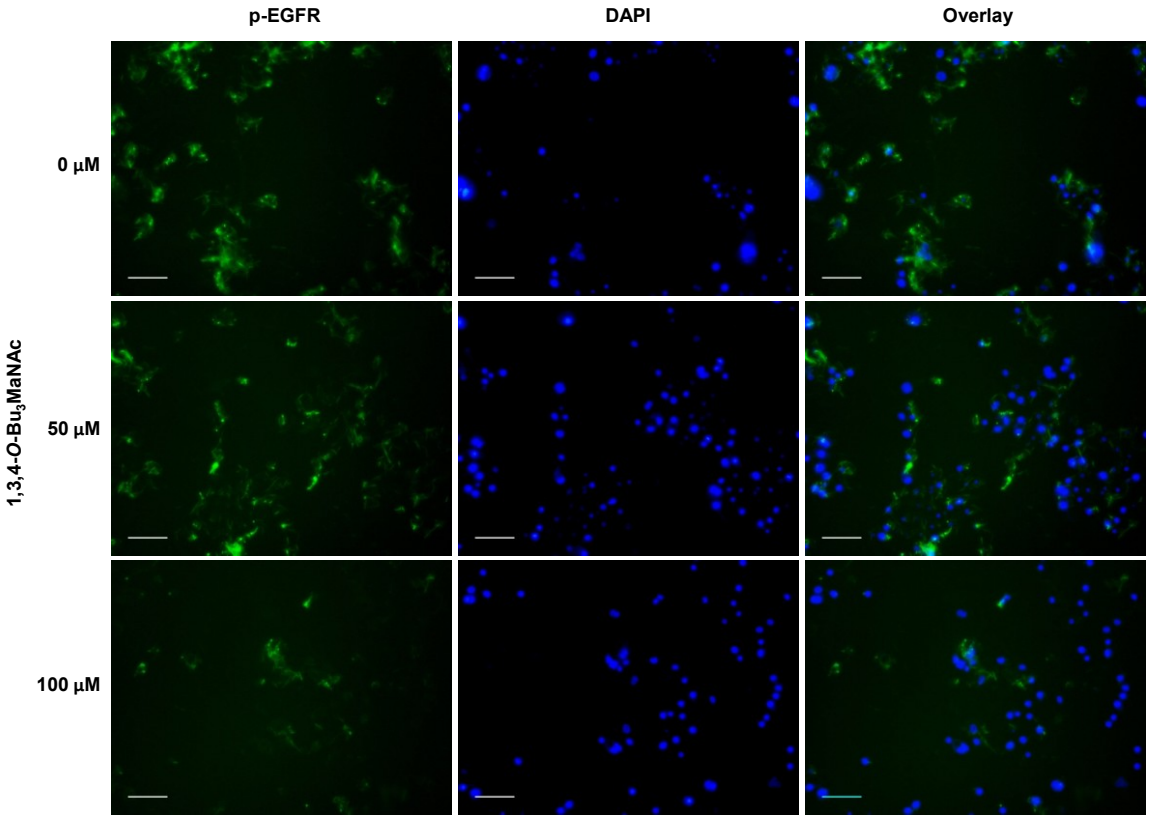

Supplemental Figure S5.1*: Representative images at 10 X magnification of immunofluorescence assays where cells were incubated with EGF for 2.0 min, fixed and stained with anti-p-EGFR, FITC labeled anti-rabbit antibody, and DAPI confirm that EGFR phosphorylation decreased with sugar analog treatment. The scale bar represents 100 □m. This figure shows additional "representative data" from immunofluorescence assays that demonstrate the ability of 1,3,4-O-Bu$_3$ManNAc to reduce p-EGFR levels in SW1990 cells. Similar data is provided in* ***Figure 5.2B****.*

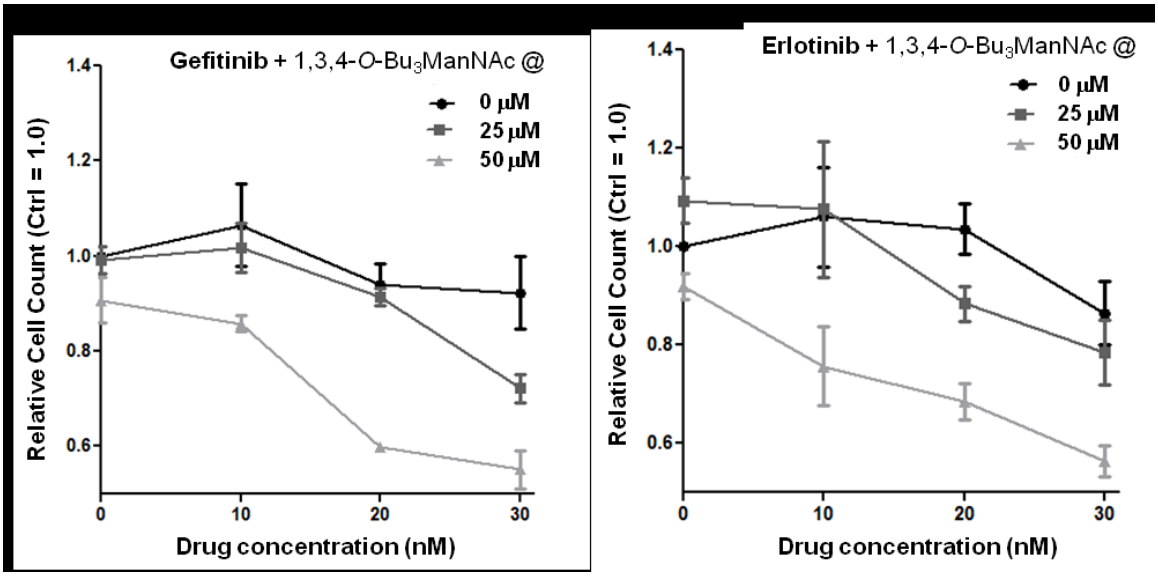

Supplemental Figure S5.2*: Details showing additional data obtained over low concentration ranges for the drug synergy experiments presented in* ***Figure 5.4A****. At least 3 biological replicates were carried out for each experiment with data expressed as mean ± standard error mean (SEM). This figure provides a more detailed depiction of low concentration ranges of the experiment used to determine drug synergy between 1,3,4-O-Bu$_3$ManNAc and erlotinib and gefitinib in* ***Figure 5.4A****.*

5.6 REFERENCES

1. Sell, S. (1990) Cancer-associated carbohydrates identified by monoclonal antibodies. *Hum.Pathol.* 21, 1003-1019

2. Hakomori, S. (2002) Glycosylation defining cancer malignancy: new wine in an old bottle. *Proc.Natl.Acad.Sci.* 99, 10231-10233

3. Hakomori, S. (1985) Aberrant glycosylation in cancer cell membranes as focused on glycolipids: overview and perspectives. *Cancer Res.* 45, 2405

4. Hakomori, S. (1984) Tumor-associated carbohydrate antigens. *Annu.Rev.Immunol.* 2, 103-126

5. Varki A, Kannagi R, Toole BP. Glycosylation Changes in Cancer. In: Varki A, Cummings RD, Esko JD, et al., editors. *Essentials of Glycobiology.* 2nd edition. Cold Spring Harbor (NY): Cold Spring Harbor Laboratory Press; 2009. Chapter 44. Available from: http://www.ncbi.nlm.nih.gov/books/NBK1963/

6. Hedlund, M., Ng, E., Varki, A., and Varki, N.M. (2008) alpha 2-6-Linked sialic acids on N-glycans modulate carcinoma differentiation in vivo. *Cancer Res.* 68, 388-394

7. Hakomori, S. (2002) Glycosylation defining cancer malignancy: new wine in an old bottle. *Proc.Natl.Acad.Sci.U.S.A.* 99, 10231-10233

8. Dove, A. (2001) The bittersweet promise of glycobiology. *Nat.Biotechnol.* 19, 913-917

9. Kim, Y.J., and Varki, A. (1997) Perspectives on the significance of altered glycosylation of glycoproteins in cancer. *Glycoconj.J.* 14, 569-576

10. Fuster, M.M., and Esko, J.D. (2005) The sweet and sour of cancer: glycans as novel therapeutic targets. *Nat.Rev.Cancer.* 5, 526-542

11. Liu, Y., Yen, H., Chen, C., Chen, C., Cheng, P., Juan, Y., Chen, C., Khoo, K., Yu, C., and Yang, P. (2011) Sialylation and fucosylation of epidermal growth factor receptor suppress its dimerization and activation in lung cancer cells. *Proc.Natl.Acad.Sci.* 108, 11332-11337

12. Park, J., Yi, J.Y., Jin, Y.B., Lee, Y., Lee, J., Lee, Y., Ko, Y., and Lee, M. (2012) Sialylation of epidermal growth factor receptor regulates receptor activity and chemosensitivity to gefitinib in colon cancer cells. *Biochem.Pharmacol.* 83, 849-857

13. Du, J., Meledeo, M.A., Wang, Z., Khanna, H.S., Paruchuri, V.D., and Yarema, K.J. (2009) Metabolic glycoengineering: sialic acid and beyond. *Glycobiology.* 19, 1382-1401

14. Dube, D.H., and Bertozzi, C.R. (2003) Metabolic oligosaccharide engineering as a tool for glycobiology. *Curr.Opin.Chem.Biol.* 7, 616-625

15. Campbell, C.T., Sampathkumar, S.G., and Yarema, K.J. (2007) Metabolic oligosaccharide engineering: perspectives, applications, and future directions. *Mol.BioSyst.* 3, 187-194

16. Kayser, H., Zeitler, R., Kannicht, C., Grunow, D., Nuck, R., and Reutter, W. (1992) Biosynthesis of a nonphysiological sialic acid in different rat organs, using N-propanoyl-D-hexosamines as precursors. *J.Biol.Chem.* 267, 16934

17. Keppler, O.T., Horstkorte, R., Pawlita, M., Schmidt, C., and Reutter, W. (2001) Biochemical engineering of the N-acyl side chain of sialic acid: biological implications. *Glycobiology.* 11, 11R-18R

18. Jones, M.B., Teng, H., Rhee, J.K., Lahar, N., Baskaran, G., and Yarema, K.J. (2004) Characterization of the cellular uptake and metabolic conversion of acetylated N-acetylmannosamine (ManNAc) analogues to sialic acids. *Biotechnol.Bioeng.* 85, 394-405

19. Kim, E.J., Sampathkumar, S.G., Jones, M.B., Rhee, J.K., Baskaran, G., Goon, S., and Yarema, K.J. (2004) Characterization of the metabolic flux and apoptotic effects of O-hydroxyl-and N-acyl-modified N-acetylmannosamine analogs in Jurkat cells. *J.Biol.Chem.* 279, 18342

20. Almaraz, R.T., Aich, U., Khanna, H.S., Tan, E., Bhattacharya, R., Shah, S., and Yarema, K.J. (2012) Metabolic oligosaccharide engineering with N-Acyl functionalized ManNAc analogs: Cytotoxicity, metabolic flux, and glycan-display considerations. *Biotechnol.Bioeng.* 109, 992-1006

21. Sarkar, A.K., Rostand, K.S., Jain, R.K., Matta, K.L., and Esko, J.D. (1997) Fucosylation of disaccharide precursors of sialyl LewisX inhibit selectin-mediated cell adhesion. *J.Biol.Chem.* 272, 25608-25616

22. Sarkar, A.K., Fritz, T.A., Taylor, W.H., and Esko, J.D. (1995) Disaccharide uptake and priming in animal cells: inhibition of sialyl Lewis X by acetylated Gal beta 1--> 4GlcNAc beta-O-naphthalenemethanol. *Proc.Natl.Acad.Sci.*. 92, 3323

23. Lemieux, G.A., Yarema, K.J., Jacobs, C.L., and Bertozzi, C.R. (1999) Exploiting differences in sialoside expression for selective targeting of MRI contrast reagents. *J.Am.Chem.Soc.* 121, 4278-4279

24. Sampathkumar, S., Jones, M.B., Meledeo, M.A., Campbell, C.T., Choi, S.S., Hida, K., Gomutputra, P., Sheh, A., Gilmartin, T., and Head, S.R. (2006) Targeting glycosylation pathways and the cell cycle: sugar-dependent activity of butyrate-carbohydrate cancer prodrugs. *Chem.Biol.* 13, 1265-1275

25. Mathew, M.P., Tan, E., Shah, S., Bhattacharya, R., Adam Meledeo, M., Huang, J., Espinoza, F.A., and Yarema, K.J. (2012) Extracellular and Intracellular Esterase Processing of SCFA-Hexosamine Analogs: Implications for Metabolic Glycongineering and Drug Delivery. *Bioorg.Med.Chem.Lett.* 22, 6929-6933.

26. Malicdan, M.C., Noguchi, S., Tokutomi, T., Goto, Y., Nonaka, I., Hayashi, Y.K., and Nishino, I. (2012) Peracetylated N-acetylmannosamine, a synthetic sugar molecule, efficiently rescues muscle phenotype and biochemical defects in mouse model of sialic acid-deficient myopathy. *J.Biol.Chem.* 287, 2689-2705

27. Kim, E.J., Jones, M.B., Rhee, J.K., Sampathkumar, S., and Yarema, K.J. (2004) Establishment of N-Acetylmannosamine (ManNAc) Analogue-Resistant Cell Lines as

Improved Hosts for Sialic Acid Engineering Applications. *Biotechnol.Prog.* 20, 1674-1682

28. Aich, U., Campbell, C.T., Elmouelhi, N., Weier, C.A., Sampathkumar, S.G., Choi, S.S., and Yarema, K.J. (2008) Regioisomeric SCFA attachment to hexosamines separates metabolic flux from cytotoxicity and MUC1 suppression. *ACS Chem Biol.* 3, 230-240

29. Wang, Z., Du, J., Che, P., Meledeo, M.A., and Yarema, K.J. (2009) Hexosamine analogs: from metabolic glycoengineering to drug discovery. *Curr.Opin.Chem.Biol.* 13, 565-572

30. Almaraz, R.T., Tian, Y., Bhattarcharya, R., Tan, E., Chen, S., Dallas, M.R., Chen, L., Zhang, Z., Zhang, H., Konstantopoulos, K., and Yarema, K.J. (2012) Metabolic Flux Increases Glycoprotein Sialylation: Implications for Cell Adhesion and Cancer Metastasis. *Molecular & Cellular Proteomics.* 11, M112-017558.

31. Shah, P.K., Yang, S., Sun, S., Aiyata, P., Yarema, K.J., and Zhang, H. (2013) Mass Spectrometric Analysis of Sialylated Glycans Using Solid Phase Labeling of Sialc Acids. *Anal.Chem.* 85(7), pp.3606-3613.

32. Zhang, H., Li, X., Martin, D.B., and Aebersold, R. (2003) Identification and quantification of N-linked glycoproteins using hydrazide chemistry, stable isotope labeling and mass spectrometry. *Nat.Biotechnol.* 21, 660-666

33. Yun, C.H., Mengwasser, K.E., Toms, A.V., Woo, M.S., Greulich, H., Wong, K.K., Meyerson, M., and Eck, M.J. (2008) The T790M mutation in EGFR kinase causes drug resistance by increasing the affinity for ATP. *Proc.Natl.Acad.Sci.U.S.A.* 105, 2070-2075

34. Patel, M.R., Jay-Dixon, J., Sadiq, A.A., Jacobson, B.A., and Kratzke, R.A. (2013) Resistance to EGFR-TKI can be mediated through multiple signaling pathways converging upon cap-dependent translation in EGFR-wild type NSCLC. *J.Thorac.Oncol.* 8, 1142

35. Buck, E., Eyzaguirre, A., Haley, J.D., Gibson, N.W., Cagnoni, P., and Iwata, K.K. (2006) Inactivation of Akt by the epidermal growth factor receptor inhibitor erlotinib is mediated by HER-3 in pancreatic and colorectal tumor cell lines and contributes to erlotinib sensitivity. *Mol.Cancer.Ther.* 5, 2051-2059

36. Chou, T. (2010) Drug combination studies and their synergy quantification using the Chou-Talalay method. *Cancer Res.* 70, 440-446

37. Saxon, E., and Bertozzi, C.R. (2000) Cell surface engineering by a modified Staudinger reaction. *Science.* 287, 2007-2010

38. Gnanapragassam, V.S., Bork, K., Galuska, C.E., Galuska, S.P., Glanz, D., Nagasundaram, M., Bache, M., Vordermark, D., Kohla, G., and Kannicht, C. (2014) Sialic acid metabolic engineering: a potential strategy for the neuroblastoma therapy *PLoS ONE*,*9*(8), e105403. http://doi.org/10.1371/journal.pone.0105403

39. Mahal, L.K., Yarema, K.J., and Bertozzi, C.R. (1997) Engineering chemical reactivity on cell surfaces through oligosaccharide biosynthesis. *Science.* 276, 1125-1128

40. Mahal, L. K.; Yarema, K. J.; Lemieux, G. A.; Bertozzi, C. R. (1999) Chemical approaches to glycobiology: Engineering cell surface sialic acids for tumor targeting, in *Sialobiology and Other Novel Forms of Glycosylation*, Inoue, Y.; Lee, Y. C.; Troy, F. A., III, eds. Gakushin Publishing Company: Osaka, 237-280.

CHAPTER 6

INSIGHTS INTO THE SENSITIZATION AND TARGETING OF THE EPIDERMAL GROWTH FACTOR RECEPTOR (EGFR) IN SW1990 PANCREATIC CANCER CELLS BY METABOLIC FLUX_DRIVEN SIALYLATION

ABSTRACT

We recently reported that advanced stage pancreatic cancer cells (the metastatic SW1990 line), which respond weakly to the EGFR-targeting tyrosine kinase inhibitors (TKIs) erlotinib and gefitinib can be resensitized to these drugs by treatment with 1,3,4-*O*-Bu_3ManNAc (*Bioorg. Med. Chem. Lett.* (2015) 25(6):1223-7). To gain insight into how increased sialylation experienced by many glycoproteins (including EGFR) in cells treated with this sugar inhibits this receptor and leads to synergy with TKI drugs, we took three approaches:

First, we verified that 1,3,4-*O*-Bu_3ManNAc treatment, a "high flux" ManNAc analog increases sialylation of EGFR, albeit to a lower extent than global sialylation, in human SW1990 pancreatic cancer cells. We then implemented a computational model that helped predict that this compound increased the internalization of EGFR consistent with weakening of the galectin lattice and a shift towards non-clathrin mediated (NCM) endocytosis.

Second, we experimentally verified these predictions by showing that EGFR was internalized at a faster rate in 1,3,4-*O*-Bu_3ManNAc-treated cells and that a shift away from clathrin coated internalization to NCM endocytosis did occur.

Third, we evaluated down-stream targets of EGFR signaling and linked drug synergy between 1,3,4-*O*-Bu_3ManNAc and existing TKI drugs to the bias away from clathrin-coated endocytosis, which allows EGFR signaling to continue after internalization, towards NCM endocytosis, which rapidly diminishes signaling.

This chapter is currently submitted and under review as **Mathew, M. P., Tan, E., Saeui, C. T., Bovonratwet, P., Skylar, S.,, Bhattacharya, R., & Yarema, K. J. (2015). Insights into the Sensitization and Targeting of the Epidermal Growth Factor Receptor (EGFR) in Pancreatic Cancer Cells by Metabolic Oligosaccharide Engineering. *Journal of Biological Chemistry*,**

6.1 INTRODUCTION

In mammals, glycosylation is a ubiquitous co/post-translational modification of cell surface proteins and lipids that modulates the activities of these molecules in a myriad of ways that – despite decades of study – often continue to be poorly understood and sometimes turn out to be downright surprising. An example of a such a result is the unexpected ability of 1,3,4-*O*-Bu_3ManNAc, a "high flux" *N*-acetylmannosamine (ManNAc) analog that increases sialylation (1-4), to sensitize drug-resistant pancreatic cancer cells to tyrosine kinase inhibitors (TKIs) (5).

To elaborate briefly, sialic acid has generally been regarded as a cancer-promoting sugar moiety, occurring in many tumor-associated carbohydrate antigens (TACAs) such as the sialylated Tn antigen (sTn), sialyl Lewis X (sLe^X) and ganglioside GM3 (6, 7); in addition, in many molecular contexts the bulk chemical properties of sialic acid are anti-adhesive and provide a pro-metastatic mechanism for cancer cells to detach from a primary tumor. Based on these factors, it is generally accepted that increased sialylation promotes cancer progression. Accordingly, increased sialylation is thought to be counter-productive in cancer therapy and this dogma has posed a conundrum for efforts to exploit metabolic oligosaccharide engineering (MOE (8, 9), also known as metabolic glycoengineering, MG or MGE (10), for which detailed background information is provided in the cited articles (11-14)) to treat cancer. To illustrate this point, MOE has potential to manipulate sialylated glycans in ways that have an anti-cancer impact by installing non-natural sialic acids in over-expressed TACAs for delivery of diagnostic (15, 16) or therapeutic agents (17) or even fluorinated sugars intended to have anti-metastatic properties (9, 18, 19). At the same time, however, these approaches have the

potential to promote cancer progression by increasing overall levels of sialylation and for this reason (and others beyond the scope of this discussion) MOE has made only paltry progress towards clinical adoption.

Based on the widely held assumption that sialylation is synonymous with increased carcinogenicity, several recently-reported results to the contrary are provocative. In particular, we recently reported that 1,3,4-*O*-Bu_3ManNAc – a ManNAc "pro-drug" that is rapidly activated by esterases in cells to generate ManNAc (20) that promotes high levels of flux through the sialic acid biosynthetic pathway (2) and substantially increases cell surface sialylation in human cancer cells (3) – had only a modest (in fact almost negligible) impact on endpoints related to metastasis such as *in vitro* cell motility (3). One explanation for this result could be that once increased sialylation has occurred, any additional increase is not capable of further exacerbating cancer progression. Indeed, although increased sialylation is associated with many aspects of oncogenesis (21, 22), too large of an increase in sialic acid may actually be detrimental to cancer progression. This idea is consistent with descriptions of only "slightly increased" levels of sialic acid in some types of cancer (23) and feedback mechanisms that carefully titer metabolic flux into the sialic acid biosynthetic pathway (24, 25).

The epidermal growth factor receptor (EGFR), an oncogene that has been linked to poor prognosis in pancreatic (and other) cancer (26-28), provides an example where over-sialylation deters cancer progression. The glycosylation status of EGFR has been linked to changes in receptor activity as well as to overall cell behavior (29, 30). For example, genetic deletion of the Asn-420 glycosylation site enabled ligand-free activation of EGFR

(31) and inhibition of N-glycosylation with tunicamycin sensitized human non-small lung cancer cells to erlotinib (32).

Focusing on sialic acid, increased levels of this sugar resulting from genetic manipulation (e.g., over-expression of sialytransferases) have been reported to inhibit EGFR activity in lung (29, 33) and colon (34) cancer cells. Building on these findings, our group recently showed that a pharmacologically relevant "small molecule" approach using 1,3,4-*O*-Bu_3ManNAc to increase sialylation could reproduce the biological effects of these genetic manipulations. In particular, this ManNAc analog sensitized drug-resistant cancer cell lines to the tyrosine kinase inhibitors (TKIs) erlotinib and gefitinib that are currently used as cancer therapeutics (5) but are only modestly effective because the rapid gain of drug resistance in patients (35). Based on the clinical potential of this finding, in this paper I sought to better understand the impact of 1,3,4-*O*-Bu_3ManNAc on EGFR signaling, gain insight into the underlying molecular mechanism, and further investigate the unusual synergy between TKIs and this sugar analog.

6.2 MATERIALS AND METHODS

6.2.1 Cell Culture and Incubation with Sugar Analogs.

SW1990 (ATCC® CRL-2172) cells were grown in Dulbecco's Modified Eagle Medium (DMEM) supplemented 10% with heat-inactivated fetal bovine serum (FBS) and 1.0% of 100x pen/strep antibiotic solution (Invitrogen). Cells were maintained at 37°C in a humidified, 5% CO_2-containing atmosphere. 1,3,4-*O*-Bu_3ManNAc was synthesized and characterized as previously described (1, 2) and stored lyophilized at -80°C. Stock

solutions (100 mM) were made in ethanol (EtOH). For analog treatment, cells typically were plated in 6-well tissue culture plates in 2.0 mL of culture media at a density of 300,000 cells/well and the appropriate volume of 1,3,4-*O*-Bu_3ManNAc was added to each well to achieve the desired analog concentrations; the identical volume of ETOH (always less than 10 μL/mL) was added to each well in each experiment to ensure that all cells were exposed to the same amount of solvent as those treated with the highest concentration of analog. Cells were typically incubated for 48 h with the sugar analogs; in certain experiments (as indicated below) the first 24 h of incubation was carried out in complete media and the cells were serum starved for the final 24 h before analysis following published protocols for monitoring EGFR phosphorylation and activation [29).

6.2.2 Western Blot Analysis.

Proteins obtained from SW1990 cells were analyzed by western blots after the cells were incubated with 1,3,4-*O*-Bu_3ManNAc, erlotinib or both for 48 h including, as described above, serum starvation for the last 24 h and exposure to 10 ng/mL recombinant human EGF (Peprotech AF-100-15) in PBS for 2.0 min, 30 min or 60 min. Proteins were collected and were immuno-detected using the following commercial antibodies: anti-phospho-EGFR (p-EGFR, Tyr1068 Cell Signaling #4267), anti-EGFR (D33B1, Cell Signaling, #4267), anti-STAT3 (STAT3, 79D7, Cell Signaling #4904), anti-phospho-STAT3 (p-STAT3, Tyr705, Cell Signaling #9131), anti-phospho-AKT (p-Akt, Ser473 (D9E) Cell Signaling #4060), anti-phospho-ERK1/2 (p-ERK1/2 Try202/204, Cell Signaling, #9101), anti-β-actin (Sigma-Aldrich) and HRP-linked anti-rabbit antibody (Cell Signaling). Protein bands were quantified using the ImageJ software. Where

necessary, blots were stripped with Gentle ReView Stripping Buffer (Amresco), reblocked and analyzed.

6.2.3 EGFR Immunopurification and Characterization of Sialylation.

Cells were incubated for 48 h with 100 μM 1,3,4-*O*-Bu_3ManNAc, rinsed in ice cold PBS, collected using cell scrapers, and resuspended in 0.5 mL of ice cold cell lysis buffer (Cell Signaling). Samples were sonicated on ice three times for 5 s each and then samples were centrifuged for 10 min at 4 ^{0}C at 14,000*g*. Protein from control and treated cells were collected from the supernatant, quantified using the Pierce 660 nm protein assay (Thermo Scientific); protein levels were then normalized to 1.0 mg/mL. EGFR from control and treated samples was then immunopurified using Sepharose bead conjugated EGFR mAb (Cell Signaling) following the manufacturer's protocol. After purification, the samples were divided in two with half of the samples boiled in loading buffer for 10 min and then analyzed for total EGFR protein levels by western blotting as described above. HRP-linked SNA-1 Lectin (EY Laboratories) was also used to stain western blots of immunopurified EGFR to determine the levels of α2-6 linked sialic acid. Band intensities were quantified using ImageJ software and normalized to EGFR levels.

6.2.4 Fluorescent Assisted Carbohydrate Electrophoresis (FACE).

The other half of the immunopurified EGFR samples were digested with sialidase (P0722L, New England BioLabs), wherein 10 μL of immunopurified EGFR on sepaharose beads was incubated with 200 units of sialidase in a 100 μL reaction volume for 48 h at 37^{0}C. After sialidase digestion, the samples were centrifuged at 14,000*g* and the amount of sialic acid released into the supernatants was determined by FACE following an established protocol (36, 37). Briefly, 50 mg graphitized carbon columns

were prepared and activated with 80% acetonitrile, 0.1% v/v trifluoroacetic acid (TFA) using three 1.0 mL washes and were then equilibrated with five 1.0 mL milli Q water washes under vacuum. The supernatants were then loaded onto the columns and the columns were washed five times with 1.0 mL of milliQ water under vaccum after which the released sialic acids were eluted under gravity using 1.0 mL of 25% acetonitrile, 0.1% v/v TFA. The samples were then lyophilized, resuspended in 150 μL of milli Q water, transferred into fresh 1.5 mL eppendorf tubes, and lyophilized again. These samples, along with sialic acid standards, were then labeled with 40 μL of a 6.25 mM 2-aminoacridone (Carbosynth) solution in DMSO overnight at 37 ^{0}C.

A gel solution was prepared with 500 mL of 40% acrylamide (BioRad), 100 mL tris-acetate (400 mM, pH 7.0), 370 mL milliQ water and 25 mL of glycerol. An aliquot of the gel solution (5 mL) was then mixed with 25 μL of 10% ammonium persulfate and 5 μL of TEMED (BioRad) and poured into preassembled casting plates with a 0.75 mm well comb. After 7.5 min the combs were removed and the gels were transferred into the gel apparatus (BioRad) and the apparatus was filled with 1X tris-borate EDTA (BioRad). The gel apparatus was then placed on ice for 2.0 h. An aliquot of each sample (2 μL) was then loaded onto the gel and the gel was run at 500 V for 40 min on ice. The gel was then transferred onto a visi-blue benchtop variable UV transilluminator and imaged. Band intensities were then quantified using ImageJ software and normalized to the EGFR levels measured in the western blots described above.

6.2.5 Confocal Microscopy for Cell Surface EGFR Measurement.

Cells were incubated for 48 h with 1,3,4-*O*-Bu_3ManNAc with serum starvation over the last 24 h. Cells were washed in 1.0 mL of PBS and then fixed in 3.7% formaldehyde for

10 min. Cells were then blocked with 5% bovine serum albumin (BSA) in PBS for 1.0 h. Cells were then incubated overnight at 4^0C with Alexa Fluor 488-conjugated EGFR mAb (Cell Signaling). Nuclei were stained with DAPI. After three washes in PBS, the cells were imaged on Zeiss AxioObserver with 780-Quasar confocal module & FCS**. Gross fluorescence was determined for** Alexa Fluor 488-conjugated EGFR mAb **and DAPI for each image using ImageJ software. The relative fluorescence of each** 1,3,4-*O*-Bu_3ManNAc-treated sample **was determined by normalizing** Alexa Fluor 488-conjugated EGFR mAb fluorescence to DAPI fluorescence and then normalizing to control samples not treated with analog.

6.2.6 Fluorescent Recovery After Photobleaching (FRAP) Assays.

Cells were incubated for 48 h with 1,3,4-*O*-Bu_3ManNAc with serum starvation over the last 24 h. The cells were washed in Live Cell Imaging Solution (Life Technologies) supplemented with 1.0% bovine serum albumin (BSA) and 20 mM glucose and then incubated at 37°C with 2.0 μg/mL of Alexa Fluor 488-conjugated EGF (Life Technologies). Cells were then analyzed by fluorescence recovery after photobleaching technique (FRAP) (38, 39) under two conditions. In the first approach, which was adapted from Sprague et al. who describe the use of FRAP for analysis of binding interactions (40); unbound Alexa Fluor 488-conjugated EGF was maintained in the bath, which allowed us to measure EGF on/off rate (as shown in **Figure 6.2C**). In the second set of experiments, unbound EGF was removed by washing before imaging, in which case membrane fluidity was measured (**Figure 6.5A**). Cells were incubated at 37 ˚C for the duration of the FRAP experiments. Then, using a Zeiss 780 FCS Confocal Microscope together with a 488 nm Argon ion laser for excitation of Alexa Fluor 488 we

monitored emissions at 525 nm. The laser intensity was adjusted to obtain a 75 % loss in fluorescence in a 3 μm by 1 μm rectangular photobleached region on the apical focal plane of the cell membrane; for rapid bleaching high laser intensities were used for a single bleaching scan (0.278s). Multiple regions were imaged pre- and post-photobleaching using low laser intensities and recovery fluorescence in the selected regions was tracked over time.

The fluorescent intensity measured at each time point (I(t)) was then converted to a normalized fluorescent intensity (NFI(t)) normalized using the following equation: Normalized Fluorescent Intensity= [{I(t)-I(post bleach)}/I(prebleach)]/I(post recovery) The NFI was then plotted against time and fit to a one phase exponential association curve using the GraphPad Prism 6 software (GraphPad Software, Inc.; La Jolla, CA). From the fit of the curves, time constants for half recovery were derived ($t_{0.5}$).

6.2.7 Mathematical Model of EGFR Trafficking.

The effect of parameter changes in the western blot and saturation binding experiments were analyzed by a macroscopic level model (41) that contained four components: synthesis, internalization, degradation, and recycling. The baseline parameters used in this study were based on those determined in human mammary epithelial cells by Hendricks *et al*., (41). We note that these parameters were derived from a different cell line and therefore were not necessarily quantitatively predictive in the currently-used SW1990 line. However because EGFR trafficking across cell types utilizes the four basic components synthesis, internalization, degradation, and recycling) described in this model, these modeling experiments were implemented to provide qualitative support for or against our postulated mechanism for 1,3,4-*O*-Bu_3ManNAc activity.

The model consisted of four differential equations with variables: free EGFR (Rs), internalized free EGFR (Ri), EGF-EGFR complex on surface (Cs), internalized EGF-EGFR complex (Ci). These equations account for the binding and release of EGF (L) from free EGFR (Rs), which are synthesized at rate S_r, at rates k_{on} and k_{off}, respectively. EGF-EGFR complexes on surface (Cs) are then internalized at rate k_{ec}, degraded at rate k_{xc}, and recycled at fraction f_{xc}. Free EGFR (Rs) is internalized at rate k_{er}, degraded at rate k_{xr}, and recycled at fraction f_{xr}. Internalization, k_e, is governed by rates k_{ec} and k_{er}. Degradation, k_x, is governed by rates k_{xc} and k_{xr}, while recycling, f_x, is governed by f_{xc} and f_{xr}.

The model was designed to simulate the conditions used in the western blots and EGF saturation binding experiments (5), which involved an overall incubation period of 48 h (with analog addition simulated through alterations in various rate constants) with serum starvation over the last 24 h, and finally 2 min exposure to 10 ng/mL of EGF. Rate constants then were varied incrementally to model the final values of total EGF-EGFR complexes (Cs+Ci), total available cell surface EGFR (Rs) and total EGFR (Rs+Ri+Cs+Ci). These values were then normalized against baseline values and then plotted against changes in rate constants normalized against baseline. The rate constants manipulated were k_{on}, k_{off}, and collectively, k_e, k_x.

6.2.8 Internalization Assays.

Cells were incubated for 48 h with 1,3,4-*O*-Bu_3ManNAc with serum starvation over the last 24 h. The cells then were washed with PBS, treated with enzyme free cell dissociation buffer (Life Technologies) until they detached from the culture plate, collected, and counted and cell numbers were normalized using the Beckman Z2 cell

coulter counter. Cells were then washed twice in Live Cell Imaging Solution (Life Technologies) supplemented with 1.0% bovine serum albumin (BSA) and 20 mM glucose and treated with 0.5 μg/mL of filipin (Sigma Aldrich) or 100 mM of lactose (Carbosynth) for 60 min. Cells were then incubated at 37°C for 30 min with 2.0 μg/mL of Alexa Fluor 488-conjugated EGF (Life Technologies). Cells were washed three times, followed by acid washing for 5.0 min with 0.2 M glycine (pH 2.5), washed thrice and finally analyzed using flowcytometry with an Accuri C6 Flowcytometer. The cell population of interest was gated appropriately and 10^4 cells falling within the gated area were measured and used to determine the mean fluorescence of the cell population; the histograms for these experiments are shown in Suppl. Figure S3.

6.2.9 Lectin Binding Assays.

Cells were incubated for 48 h with 1,3,4-*O*-Bu_3ManNAc. The cells were washed with PBS, treated with enzyme free cell dissociation buffer (Life Technologies) until they detached from the culture plate, collected, and counted and cell numbers were normalized using the Beckman Z2 cell coulter counter. Cells were then washed twice in PBS. Cells were then incubated at room temperature for 120 min with 5.0 μg/mL of Flourescein labeled RCA lectin (Vector Laboratories). Cells were washed three times in PBS and analyzed using flowcytometry with an Accuri C6 Flow cytometer. The cell population of interest was gated appropriately and 10^4 cells were used to determine mean fluorescence.

6.2.10 Confocal Microscopy for Endosome Sizing.

Cells were incubated for 48 h with 1,3,4-*O*-Bu_3ManNAc with serum starvation over the last 24 h. Cells were then washed in Live Cell Imaging Solution (Life Technologies) supplemented with 1.0% bovine serum albumin (BSA) and 20 mM glucose. Cells were

then incubated at 37°C for 10 min or 30 min with 2.0 µg/mL of Alexa Fluor 488-conjugated EGF (Life Technologies). Cells were then fixed, nuclei were stained with DAPI and then imaged on Zeiss AxioObserver with 780-Quasar confocal module & FCS**. Endosome size was determined using ImageJ software.**

6.2.11 Quantitative Reverse Transcription-Polymerase Chain Reaction (qRT-PCR).

Total RNA was isolated using Trisol® reagents (Gibco BRL) and reversed transcribed using the high capacity RNA-to-cDNA kit (Applied Biosystems). PCR amplifications were performed using the following **TaqMan® Gene Expression Assays from Applied Biosystems: *BCL3* (**Assay ID: Hs00180403_m1)**, MYC (**Assay ID: Hs00153408_m1)**, *VEGFA* (**Assay ID: **Hs00900055_m1), *MMP2* (**Assay ID: **Hs01548727_m1), *MMP7* (**Assay ID: **Hs01042796_m1) and *GAPDH* (**Assay ID: Hs03929097_g1)**. q**RT-PCR was performed using the Step-One Plus Real-Time PCR system (Applied Biosystems) with the thermocycling conditions of 50 ˚C for 2.0 min, 95 ˚C for 10 min followed by 40 cycles of 95 ˚C for 15 s and 60 ˚C for 1.0 min.

6.2.12 Statistical Analysis.

Data was expressed as means ± standard error (SEM). Statistical significance was determined using one way ANOVA with a Dunnett's post-test to compare means of different samples with the control or a Bonferroni post test to compare specific pairs of columns. The null hypothesis was rejected in cases where p-values were < 0.05.

6.3 RESULTS

6.3.1 Treatment with 1,3,4-O-Bu_3ManNAc Increased EGFR Sialylation.

In a previously-reported "glycosite" glycoproteomic analysis (3), we found with medium confidence that 1,3,4-*O*-Bu_3ManNAc increased sialylation by ~2.1 fold at least one N-glycan site on EGFR (ASN351 of EGFR isoform c, gi41327734)). To confirm that 1,3,4-*O*-Bu_3ManNAc legitimately increased EGFR sialylation, and to gain a sense of the overall change in the levels of the sugar (for context, the previous results only provided information on one of the 10-12 putative N-glycan sites found on EGFR) in the current experiments we used two additional methods to measure sialylation. In both cases I began by immunopurifying EGFR from control and analog-treated cells. Then, in one set of experiments, the purified EGFR was quantified by western blots (**Figure 6.1A**) and in tandem, stained for α2,6 sialic acid using HRP-linked SNA-1 lectin. In an independent method, the EGFR was digested with sialidase and the released sialic acid was determined by FACE analysis (**Figure 6.1B**). These experiments showed both an increase in overall sialylation level (as measured by FACE) as well as an increase in α2,6 sialylation (determined by SNA-1 staining).

6.3.2 Surface Localization of EGFR was Decreased by 1,3,4-O-Bu_3ManNAc Treatment.

EGF saturation binding assays from a previous study (5) suggested that surface display of EGFR was suppressed by 1,3,4-*O*-Bu_3ManNAc treatment. To gain further evidence for this observation, I directly labeled surface EGFR using Alexa Fluor-488-conjugated mAb followed by analysis using confocal microscopy (**Figure 6.2**). Quantification of image

fluorescence at two magnifications (20x, panel A and 43x, panel B) confirmed that analog treatment decreased surface localization of EGFR.

6.3.3 FRAP Assays Indicate Minimal Changes in Receptor-Ligand Binding Affinity. Based on reports by others that increased sialylation achieved through genetic manipulation diminishes EGFR signaling by inhibiting dimerization of this surface receptor (29, 33, 34), I initially expected that increased sialylation achieved through 1,3,4-*O*-Bu_3ManNAc treatment (e.g., as shown in **Figure 6.1**), would have a similar effect. Western blot assays (following the procedures described by Liu *et al*., (29), data not shown) however, were not able to reproduce the dimerization results in a statistically significant manner. Therefore I explored a second method to determine if the reduced surface presence of EGFR (**Figure 6.2**) was a consequence of reduced dimerization by using fluorescent recovery after photobleaching (FRAP) assays to evaluate receptor (EGFR)-ligand (EGF) binding kinetics, which several papers suggest could be influenced by receptor dimerization (42-44).

In these experiments, a portion of the cell membrane was photobleached while the cells were in a bath containing Alexa Fluor 488-conjugated EGF. The rate at which bleached EGF molecules were released and unbleached Alexa Fluor 488-conjugated EGF from solution bound to the vacated receptors was measured by monitoring the recovery of fluorescence. In this approach the $t_{0.5}$ value, which is inversely proportional to the rate at which bleached EGF molecules are released and unbleached Alexa Fluor 488-conjugated EGF from solution bind to the vacated receptors, provides an indirect measurement of receptor-ligand binding. The $t_{0.5}$ values determined for 1,3,4-*O*-Bu_3ManNAc-treated and control cells were statistically identical (7.497s and 8.368s,

respectively, **Figure 6.2C**) indicating that increased sialylation of EGFR did not directly affect EGF binding. Indications that ligand binding is linked to the dimerization status of EGFR (42-44) led to the expectation that EGF binding kinetics would have differed between 1,3,4-*O*-Bu_3ManNAc-treated and control cells if the dimerization status of EGFR had been perturbed by analog treatment. Because this expectation was not met, this experiment provided additional evidence that this compound did not primarily alter EGFR activity by changing its dimerization status.

6.3.4 Computational Modeling Supported the Galectin Lattice Mechanism and Predicted NCM-mediated Endocytosis.

The results reported above suggested that 1,3,4-*O*-Bu_3ManNAc-mediated changes to sialylation impact EGFR by a different mechanism compared to genetic methods that alter dimerization. Accordingly, I considered whether this compound affected EGFR trafficking *via* an alternative glycosylation-based mechanism, which is through changes to the galectin lattice (45), as illustrated in **Figure 6.3**. However before undertaking additional experiments to support this hypothesis, we implemented a MATLAB model of the surface dynamics and recycling kinetics of this receptor (**Figure 6.4A**) (41) to gain support for the galectin lattice mechanism and also to evaluate whether any competing, and perhaps more compelling, hypotheses existed. The modeling simulations were based on the equations shown in **Figure 6.4B**, which covered parameters relevant to experimental endpoints described in our previously published work that showed that 1,3,4-*O*-Bu_3ManNAc treatment led to decreased levels of p-EGFR (Cs+Ci) and no significant change in total amount of EGFR (Rs+Ri+Cs+Ci) for a short time period (i.e., for 2 min) after addition of EGF (5); in addition the model accounted for the lower levels

of surface-localized EGFR (Rs) present on the cells immediately before the addition of EGF (e.g., as shown in **Figure 6.2**).

The usefulness of the model for deciphering different ways by which 1,3,4-*O*-Bu_3ManNAc could affect EGFR is illustrated by scenarios illustrated in **Figure 6.4,** panels **C** through **F**. For example, altering k_{on} values predicted that this parameter was correlated with EGFR phosphorylation without affecting overall protein levels (**Figure 6.4C**), which was consistent with our previous data on the impact of 1,3,4-*O*-Bu_3ManNAc on EGFR (5). The k_{on} rate, however, did not have an impact on cell surface levels of EGFR, which was contrary to experimental data (e.g,. as shown in **Figure 6.2**). To address this discrepancy, k_{off} values were varied, leading to the prediction that an increase in k_{off} would decrease EGFR phosphorylation with no significant effect on overall protein levels (**Figure 6.4D**). However, in this case the amount of surface-displayed EGFR was not altered, which again was inconsistent with our experimental findings. Based on an iterative process of this type, we systematically evaluated changes to individual internalization rates, recycling rates, and recycling fractions along with changes to various combinations of these factors; **Supplementary Figure S6.2** shows a sampling of various "negative" results where the model predictions did not match one or another aspect of our experimental data.

The modeling results allowed us to discount alternative biochemical mechanisms and focus subsequent experimental verification on the galectin lattice, which our early results – combined with the modeling – indicated was a plausible biochemical endpoint to explain the effects of 1,3,4-*O*-Bu_3ManNAc. In particular, a key simulation that provided a match between the modeled and experimental results occurred by varying the simulated

internalization and recycling rates. In this case, the model predicted that an increase in the internalization rate (k_e) along with a decrease in the recycling rate ($1/k_x$) would result in decreased EGFR phosphorylation accompanied by a very slight increase in overall EGFR levels **(Figure 6.4E, upper panel**). Significantly, this set of variables also predicted the lower initial EGFR levels observed on the cell surface after treatment with 1,3,4-*O*-Bu_3ManNAc (i.e., as shown in **Figure 6.2**) seen before the simulated addition of EGF (**Figure 6.4E, lower panel**).

The simulation just mentioned (as shown in **Figure 6.4E)** indicated that 1,3,4-*O*-Bu_3ManNAc increased the rate of EGFR internalization, consistent with the galectin lattice mechanism outlined in **Figure 6.3**. In addition, the decreased recycling rate ($1/k_x$) predicted in **Figure 6.4E** was consistent with a shift towards non-clathrin mediated (NCM) endocytosis and away from clathrin mediated internalization. In particular, the shift away from clathrin mediated internalization was predicted by the simulation in **Figure 6.4F** that shows predicted EGFR behavior for clathin mediated internalization. Specifically, a simulated increase in both the internalization rate (k_e) and the recycling rate (k_x) – as occurs during clathrin mediated internalization – indicated that a rapid decrease in total EGFR levels (i.e., within the 2 min time frame covered in the simulation) should occur if this mode of EGFR recycling was taking place. This result, however, was not obtained experimentally as we previously showed (5) thereby leading us to consider alternative recycling mechanisms such as NCM endocytosis. Together, our early experimental results and the modeling supported a mechanism where 1,3,4-*O*-Bu_3ManNAc treatment shifted EGFR towards NCM endocytosis where, unlike clathrin-

coated internalization, internalized moieties are directed for degradation rather than recycling (46), leading us to next investigate NCM endocytosis in more detail.

6.3.5 FRAP Assays Indicate Increased Membrane Fluidity and Support Internalization via NCM Endocytosis.

To evaluate whether increased membrane fluidity contributed to increased internalization of EGFR predicted by the model, FRAP assays were conducted in the absence of unbound Alexa Fluor 488-conjugated EGF, in which case the rate that fluorescently-labeled EGF bound to receptors adjacent to the bleached region diffuses into the bleached areas can be monitored to provide a measure of membrane fluidity. The $t_{0.5}$ values determined in this experiment, which are inversely proportional to the rate of diffusion were noticeably different in the 1,3,4-*O*-Bu_3ManNAc treated cells that had faster diffusion rates compared to non-treated controls (control $t_{0.5}$= 17.77, treated $t_{0.5}$= 7.112, **Figure 6.5A**). This finding was consistent with the proposed disruption of the galectin lattice caused by an increase in sialylation (**Figure 6.3**).

As a caveat, in a typical FRAP assay, the curve fit R^2 values did not achieve a sufficient degree of statistical confidence to definitively prove that increased membrane diffusion occurred. The observed trends nevertheless were repeatable and offered tentative support for the premise that the impact of 1,3,4-*O*-Bu_3ManNAc on cell surface dynamics was real. Importantly, the increased fluidity and subsequent changes in internalization suggested by the FRAP assays was confirmed in an independent flow cytometry assay (**Figure 6.5B**). Furthermore, this increase was completely ablated by filipin (an NCM endocytosis inhibitor) pretreatment (**Figure 6.5C**), confirming that NCM endocytosis played a role in the increased EGFR internalization.

Next, to further implicate the galectin lattice mechanism, pre-treatment with lactose (a galectin binding inhibitor) resulted in an increase in the internalization rate of EGFR in untreated controls towards levels observed in analog-treated cells (**Figure 6.5D**) indicating that the inhibitory impact of increased sialylation could be mimicked by this small molecule as expected if the galectin lattice played a role. Finally, *Ricinus communus* agglutinin (RCA) binding, a lectin that recognizes terminal galactose residues (which also are the critical binding epitopes for galectins when present on highly-branched *N*-glycans) showed decreased binding in 1,3,4-*O*-Bu_3ManNAc-treated cells (**Figure 6.5E**). The affinity of RCA and galectins for terminal galactose residues is regulated in a yin-yang manner by sialylation because sialic acids mask binding sites for these lectins (47). The RCA results (both from this study (**Figure 6.1**) and from our previous investigation of this cell line, (3)), therefore, indicated that potential galectin binding sites were masked with increasing levels of sialyation; in particular α2,6-linked sialic acids strongly increase (i.e., approximately double based on SNA staining, **Figure 6.3C**) in 1,3,4-*O*-Bu_3ManNAc-treated SW1990 cells (3, 4).

6.3.6 Time Course Experiments support NCM Endocytosis.

The premise that NCM endocytosis played a role in the mechanism of 1,3,4-*O*-Bu_3ManNAc necessitated as series of experiments conducted at longer time points than the two minute evaluation in our previous work and modeling simulations. In particular, NCM endocytosis requires 30 to 90 min to direct cell surface elements for degradation (46). Accordingly, to confirm that 1,3,4-*O*-Bu_3ManNAc treatment resulted in increased NCM endocytosis, two experiments were conducted over longer periods of times than the 2 min interval covered in the modeling simulations. In these experiments, I reasoned that

in advance of degradation, there should be evidence of a shift from clathrin-coated internalization to NCM endocytosis. To assess these two modes of recycling at 10 and 30 min time points leading up to the onset of degradation, I measured endosome size based on evidence that clathrin-coated endosomes (~100-150 nm) (48-50) are larger than NCM endosomes (~50-80 nm) (51, 52) by directly visualizing endocytosis. In these experiments, 1,3,4-*O*-Bu_3ManNAc-treated and control cells were incubated with Alexa Fluor 488-conjugated EGF for 10 min (**Figure 6.6A**) or 30 min (**Figure 6.6B**) at 37^0C, fixed, and then imaged using confocal microscopy. Endosome sizing by Image J showed a significant shift in endosome population from larger endosomes toward smaller endosomes in the analog-treated cells compared to untreated controls. This shift toward smaller endosomes was consistent with increased NCM endocytosis at the expense of clathrin-coated endocytosis and provided additional support for the hypothesis that EGFR internalization became biased towards NCM endocytosis upon 1,3,4-*O*-Bu_3ManNAc treatment.

Finally, because NCM endosomes are primarily fated for degradation (46), I reasoned that EGFR would experience increased degradation at longer EGF exposure times (e.g,. at 30 min (**Figure 6.7A**) or 60 min (**Figure 6.7B**)) in 1,3,4-*O*-Bu_3ManNAc-treated cells compared to untreated controls. The progressive time-dependent increase in the degradation of EGFR provided in these data further supported the hypothesis that 1,3,4-*O*-Bu_3ManNAc increases internalization *via* NCM endocytosis.

6.3.7 ERK1/2- and AKT-driven Signaling do not Respond to 1,3,4-O-Bu_3ManNAc Treatment.

I next sought to gain additional insight into the consequences of increased internalization, and presumably, signaling activity, of EGFR. This receptor must be phosphorylated to initiate signaling and we previously showed that changes in p-EGFR levels in 1,3,4-*O*-Bu_3ManNAc treated SW1990 cells, while modest, were amplified downstream in stronger inhibition of STAT3 phosphorylation (p-STAT3) (5). Notably, this decrease, which was reproduced in the current experiments (**Figure 6.8A**) was not accompanied by a significant change in overall STAT3 levels (**Figure 6.8B**), suggesting that the decreased levels of p-STAT3 were a consequence of pathway activation and not changes in the overall levels of this protein.

Because p-ERK1/2 and p-AKT are activated by EGFR phosphorylation similar to p-STAT3, levels of these downstream effectors of EGFR signaling were expected to also be reduced concomitant with decreased p-EGFR in 1,3,4-*O*-Bu_3ManNAc-treated cells. Accordingly, to test this premise, EGFR-driven signaling via the ERK1/2 and AKT pathways was monitored by measuring phosphorylated ERK1/2 (p-ERK1/2) and phosphorylated AKT (p-AKT) levels using western blot analysis. These experiments, however, showed that no statistically significant change in SW1990 cells occurred (p-ERK1/2 results are shown in **Figure 6.8C** and p-AKT results in **Figure 6.8D**).

The lack of response for p-ERK1/2 and p-AKT in 1,3,4-*O*-Bu_3ManNAc-treated SW1990 cells can be explained by observations that ERK1/2 and AKT signaling can be activated via RAS (35, 53); indeed, mutations that constitutively activate RAS signaling have been reported in non-small cell lung cancer and metastatic colorectal cancer (54).

Relevant to this study, in pancreatic cancer the RAS pathway is constitutively activated in the SW1990 cell line (55) as well as in ≥ 81% of pancreatic cancer patients (56, 57). As a result, ERK1/2 and AKT signaling can be activated by these alternate pathways thereby rendering moot the influence of reduced p-EGFR levels in 1,3,4-*O*-Bu_3ManNAc-treated SW1990 cells on these two endpoints. Nevertheless, STAT3 activity, while linked to RAS signaling in a parallel and complementary manner (58), generally is not primarily driven by RAS (59, 60). Accordingly, it seemed reasonable that inhibition of STAT3 could provide therapeutic benefit even in the presence of constitutively active RAS; to test this premise I next evaluated the expression of selected STAT3-driven oncogenes in 1,3,4-*O*-Bu_3ManNAc-treated cells.

6.3.8 Downstream STAT3-driven Genes Respond to Analog-mediated p-EGFR Inhibition.

Although not all downstream effectors driven by p-EGFR are inhibited by 1,3,4-*O*-Bu_3ManNAc treatment in SW1990 cells (e.g., ERK1/2 and AKT signaling do not respond as just described), I found that several oncogenes activated by p-STAT3 were nonetheless successfully inhibited by treatment with this sugar analog. In particular, reduced p-STAT3 levels in 1,3,4-*O*-Bu_3ManNAc-treated cells (**Figure 6.8A**) was manifest in decreased expression of the STAT3-driven genes *BCL3, MMP2*, and *MMP7* (**Figure 6.9A**). This down-stream modulation of several genes that contribute to cancer progression demonstrates that even modest changes in the activity of surface receptors due to altered glycosylation has the potential to be therapeutically beneficial.

Conversely, offsetting events – including the lack of response of ERK1/2 and AKT to attenuated EGFR signaling (**Figure 6.8**) and the lack of inhibition of other EGFR-

responsive genes including MYC and VEGFA (61) (**Figure 6.9B**) – suggest that a compound such as 1,3,4-*O*-Bu_3ManNAc is unlikely to comprise a "stand alone" drug for advanced stage pancreatic cancers. Indeed, "glycosylation-only" EGFR-targeting therapies have recently been judged to be ineffective as cancer therapies (33). Instead, as we recently reported, synergy between otherwise marginally effective TKI drugs and our approach (5) holds potential for combination therapy. The mechanism behind the observed synergy was unclear, however, especially considering that very there are very few strategies where drug synergy is achieved by targeting the same biomolecular target (e.g., in this case EGFR). To address this issue, I sought to gain mechanistic insight into how two EGFR-targeting strategies that are only marginally effective in SW1990 cells when used alone work in concert to facilitate strong synergy.

6.3.9 Synergy Between 1,3,4-O-Bu_3ManNAc and Erlotinib.

To gain insight into the previously observed synergy between 1,3,4-*O*-Bu_3ManNAc and EGFR-targeting TKI drugs such as erlotinib (5), western blotting for various EGFR signaling components was performed for SW1990 cells treated with either 1,3,4-*O*-Bu_3ManNAc or the TKI drug, or both in combination. First, as expected from previous experiments, 1,3,4-*O*-Bu_3ManNAc alone did not significantly affect EGFR levels (**Figure 6.10A**). In this experiment, erlotinib treatment did decrease EGFR levels and cotreatment with both compounds led to a similar decrease in EGFR indicating a lack of synergy in this particular endpoint. Next, EGFR phosphorylation was tested and analog treatment (as expected from previous results) as well as erlotinib treatment led to decreased levels of p-EGFR but again cotreatment did not synergystically decrease p-EGFR levels (**Figure 6.10B**). Moreover, none of the treatment conditions significantly

altered either p-AKT or p-ERK1/2 levels (**Figure 6.10C** and **Figure 6.10D** respectively), again not providing insight into the synergy between 1,3,4-*O*-Bu_3ManNAc and erlotinib.

Instead, the observed synergy between 1,3,4-*O*-Bu_3ManNAc and erlotinib hinged on STAT3 where levels of p-STAT3, although not affected by erlotinib on its own, experienced an amplified decrease upon co-treatment with 1,3,4-*O*-Bu_3ManNAc compared to treatment with the sugar analog by itself (**Figure 6.10E**). Of the many conditions tested, the observation that co-treatment amplifies the inhibition of p-STAT3 provides at least a partial explanation for the synergy observed between 1,3,4-*O*-Bu_3ManNAc and TKI drugs; I emphasize that other factors such as control of STAT3 by cytokine, GPC, and toll-like receptors, which is beyond the scope of the current study, may also contribute to the synergy.

6.4 DISCUSSION

This report builds on previous studies where I characterized glycosylation in advanced stage pancreatic cancer SW1990 cells treated with 1,3,4-*O*-Bu_3ManNAc to understand how metabolic flux-driven increases in sialic acid contribute to cancer progression (3, 4). Our focus on pancreatic cancer was motivated by poor prognoses for this disease, which has a five year survival rate of only ~4% (62); I reasoned that gaining a better understanding of glycosylation could be valuable for devising new treatment strategies. In previous work, this premise was supported by our discovery that 1,3,4-*O*-Bu_3ManNAc synergistically sensitized TKI drug-resistant SW1990 cells to EGFR-targeting drugs (e.g., erlotinib and gefitinib) (5).

In this paper I first sought to provide a mechanistic understanding of how 1,3,4-*O*-Bu_3ManNAc – and by extension – increased sialylation, dampened EGFR signaling. Based on recent reports by others that increased sialylation achieved through genetic manipulation diminishes EGFR signaling by inhibiting dimerization of this surface receptor (29, 33, 34), I initially expected that increased sialylation brought about through 1,3,4-*O*-Bu_3ManNAc treatment (e.g., as shown in **Figure 6.1**) would have a similar effect. Experiments following the protocols described by Yen and coauthors (33), data not shown) showed a similar trend, but I were not able to unambiguously reproduce the dimerization results in a statistically significant manner. By contrast, I clearly showed a reduction in cell surface-localized EGFR in 1,3,4-*O*-Bu_3ManNAc-treated cells (**Figure 6.2A/B**). Together with data shown in **Figure 6.2C** where there was no difference in the on/off rate of EGF binding to treated or untreated cells, I concluded that the dimerization mechanism observed in other cell types (29, 33, 34) did not apply in the SW1990 cells, or at best, offered only a partial explanation for the impact of 1,3,4-*O*-Bu_3ManNAc on EGFR activity in this cell line. Either way, this disparity provided impetus for us to explore additional mechanisms by which sialylation could affect EGFR signaling.

Based on the data shown in **Figures 6.1** and **6.2** of this paper, plus our previous demonstration that 1,3,4-*O*-Bu_3ManNAc approximately doubles overall levels of α2,6-sialic acid in SW1990 cells (and the current evidence that α2,6-sialylation of EGFR is also increase, **Figure 6.1A**), an attractive alternative (but complementary) mechanism to the dimerization hypothesis is this compound had an impact on the galectin lattice (**Figure 6.3**). The basis for this idea is that α2,6-sialic acid inhibits galectin affinity (63) and the resulting negative regulation of the galectin lattice has the potential to direct

EGFR trafficking away from surface display towards internalization and thus reduce its signaling (45). In this case, contributions from both increased sialylation of EGFR itself (which can directly reduce affinity for lattice by reducing galectin crosslinking of this receptor with other surface moieties) and indirect effects due to bulk changes to cell surface properties (i.e., an increase in overall membrane fluidity) can help explain the reduced EGFR localization observed in **Figure 6.2** and the reduced downstream signaling previously reported (5).

Although the galectin lattice mechanism provides an attractive hypothesis to explain the effects of 1,3,4-*O*-Bu_3ManNAc on EGFR, the impact of glycosylation on a cell is manifold and before embarking on detailed experiments to address this mechanism we performed mathematical modeling to (i) confirm whether this hypothesis was plausible, (ii) gain evidence whether alternative mechanisms were involved, and (iii) gain deeper insight into either of these options. As shown in **Figure 6.4**, and described in detail in the Results section, the modeling results (i) were consistent with an increased internalization rate, which is a key feature of the galectin lattice mechanism outlined in **Figure 6.3** while (ii) no other biochemical mechanisms were implicated when cell surface and internalization parameters (i.e., k_{on}, k_{off}, k_{er}, and k_{ex}) were modeled. Furthermore, (iii) the modeling results provided important hints that EGFR internalization in 1,3,4-*O*-Bu_3ManNAc-treated SW1990 cells occurred by NCM endocytosis that directs EGFR for degradation and more quickly ablates signaling compared to clathrin-coated internalization.

Based on the hints from earlier experiments (e.g., our prior publications (3, 5) and **Figures 6.1** and **6.2** of this paper) and support from the modeling simulations (**Figure**

6.4), I conducted a series of experiments that supported increased internalization, and more over this internalized shifted to NCM endocytosis in the 1,3,4-*O*-Bu_3ManNAc treated cells (**Figure 6.5**). Next, I showed that EGFR-containing endosomes shifted to a smaller size profile in the analog-treated cells, again consistent with a shift away from clathrin-coated internalization to NCM endocytosis at shorter time points (e.g., 10 and 30 min) leading to the ultimate endpoint of degradation (**Figure 6.6**). Finally, I confirmed this final down-stream consequence of increased NCM endocytosis, which is enhanced degradation of EGFR over longer time periods of 30 to 60 min (**Figure 6.7**). Together, these sets of data provide an alternative and complementary mechanism based on the galectin lattice to describe how increased sialylation can alter EGFR trafficking and activity, which up to now has been focus more narrowly on EGFR:EGFR dimerization.

As the next major thrust of this work, I sought to gain additional insight into reasons why EGFR-targeting TKI drugs, despite the important role that this receptor plays in pancreatic cancer, have not been used to treat this type of malignancy successfully in the clinic (64). This lack of efficacy is evident from observations that many pancreatic cancer lines – including SW1990 cells, which were selected for use in this study in large part because they possess mutations such as constitutively-activated RAS and are resistant to TKI drugs in a way that reflects the majority of clinical cases of pancreatic cancer – require tens of micromolar concentrations of TKI drugs to observe a response (compared to corresponding nanomolar concentrations in sensitive cells) (65).

Finally, because 1,3,4-*O*-Bu_3ManNAc dramatically sensitized drug resistant SW1990 cells to the TKI drugs erlotinib and gefitinib (5) thereby enhancing the potential therapeutic value of this approach, I focused our attention on uncovering the mechanistic

underpinnings of this finding by focusing on known EGFR-responsive pathways. These efforts first provided some insight into why EGFR-targeting drugs are not particularly effective for treating pancreatic cancer insofar as an 1,3,4-*O*-Bu_3ManNAc-driven reduction in p-EGFR levels did not have an impact on ERK1/2 and AKT signaling in SW1990 cells, most likely because these pathways are upregulated by alternate mechanisms in pancreatic cancer. I nonetheless showed that the impact of 1,3,4-*O*-Bu_3ManNAc on STAT3, an important downstream effector pathway of EGFR, is sufficient to translate into potential anti-cancer activity through down-regulation of oncogenes such as *BCL3*, *MMP2* and *MMP7* (**Figure 6.9A**).

It is noteworthy that the synergy between 1,3,4-*O*-Bu_3ManNAc and the EGFR-directed TKI drugs erlotinib and gefitinib was achieved, at least in part, by targeting the same receptor. Because synergistic therapeutics typically are directed at completely different targets (although exceptions where the same receptor is targeted are known (66)), this was an unusual situation that our evidence suggests was facilitated by the ability of our approach to change the trafficking pattern of EGFR. To elaborate briefly, as far as drug synergy is concerned, erlotinib has no known way to impact the galectin lattice and EGFR is expected to be internalized normally via clathrin coated endocytois in cells treated with this drug. Therefore, even though this TKI reduces overall cellular levels of EGFR phosphorylation, signaling continues when this receptor is internalized. As a result, even though overall levels of EGFR decrease when SW1990 cells are treated with erlotinib (as shown in **Figure 6.10**) there is only a negligible impact on downstream signaling explaining why there have been reports that this TKI only has a minimal impact in this cell line (65).

Based on this explanation, the key contribution of 1,3,4-*O*-Bu_3ManNAc is to shunt EGFR internalization towards NCM endocytosis, which rapidly reduces signaling activity. As a result the reduced levels of EGFR brought about by erlotinib – although relatively minor – combine with the sugar analog's ability to shunt this molecule down a non-active internalization mechanism (i.e., NCM endocytosis) – and together result in a synergistic reduction in down-stream EGFR signaling that is much greater than that realized by either 1,3,4-*O*-Bu_3ManNAc or the TKI drugs on their own. Numerous studies have shown that EGFR signaling can continue from within endosomes (67, 68). In fact, even in the absence of surface signaling cues, clathrin-coated endosomal signaling can activate signaling pathways and be adequate to promote cell survival (69); moreover, clathrin-mediated endocytosis is essential for MAPK activation (70) and is responsible for the activation and cytoplasmic transport of STAT3 to the nucleus (71).

These observations offer an explanation for how erlotinib-treated SW1990 cells can maintain STAT3 activity despite lower overall levels of EGFR and p-EGFR. Instead, for the reduced levels of EGFR caused by erlotinib to be manifest at the whole cell level, co-treatment with 1,3,4-*O*-Bu_3ManNAc is needed to shift clathrin-mediated internalization towards NCM endocytosis. From a practical perspective, this synergy holds intriguing potential to combat drug-resistant pancreatic cancer, which remains virtually untreatable to date.

As concluding remarks, this paper provides evidence for a new way that flux-driven sialylation can impact EGFR signaling (e.g., through masking of galectin binding epitopes (72) rather than intervening in the production of these structures (73-75)) with considerable evidence presented that the galectin lattice is involved in directing EGFR

trafficking towards NCM endocytosis. However, due to the complexities of both glycosylation and cell signaling, I emphasize several caveats. First, while I did not obtain evidence to support a role of flux-driven sialylation in affecting the dimerization status of EGFR in SW1990 cells, my experiments also did not conclusively rule out this mechanism. Moreover, evidence exists that there is a third mechanism through which increased sialylation could suppress EGFR signaling by increasing cellular levels of ganglioside GM3 (76); this possibility was not addressed in the current study. In a second direction, another caveat is that by altering the galectin lattice and by extension the bulk fluidic properties of the plasma membrane, numerous additional pathways beyond EGFR signaling could be affected (74, 75, 77). Therefore, although I present strong evidence that 1,3,4-*O*-Bu_3ManNAc acts on EGFR through galectin lattice effects, the impact on cell-level behavior (e.g., synergy with TKI drugs) likely has additional inputs beyond the scope of this study. Finally, the complexities of cell signaling and glycosylation raise the cautionary note that the current results from SW1990 cells may not be widely applicable to any cell type, although I do note that the application of the computational EGFR trafficking model, which was previously optimized for human mammary epithelial cells (41), proved to provide valuable qualitative information that guided the study of this pancreatic cancer line.

6.5 ACKNOWLEDGEMENTS

Funding for this study was obtained from NIH grants R01CA112314, S10OD016374, and P01HL107147 and the Willowcroft Foundation. I would also like to acknowledge the valuable contributions of two undergraduates who worked with me on this project; Patawut Bovonratwet who helped implement the mathematical model and Samual Sklar who contributed towards a number of the western blotting experiments.

6.6 FIGURES

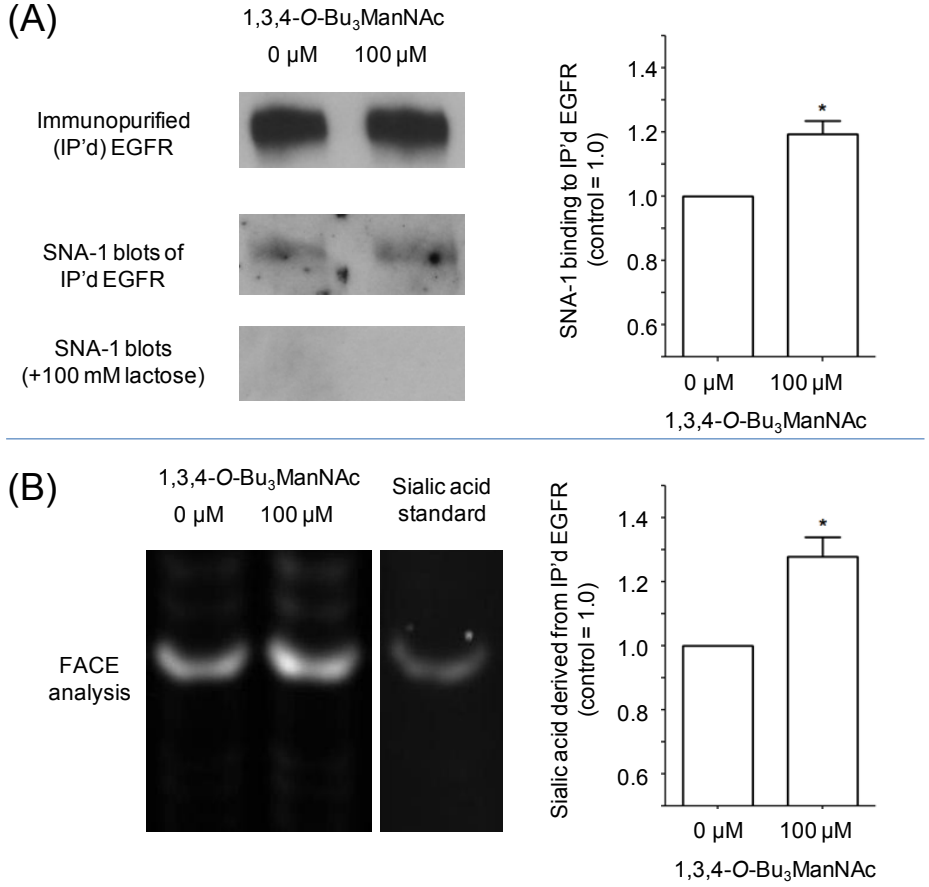

Figure 6.1: Sialylation of immunopurified (IP'd) EGFR from SW1990 cells. *The cells were treated with 100 μM (or 0 μM for controls) of 1,3,4-O-Bu$_3$ManNAc and EGFR was IP'd from each condition.* ***(A)*** *One aliquot of the IP'd EGFR was separated using PAGE and the resulting blots were probed with an EGFR-recognizing antibody or HRP-linked SNA-1 lectin; the SNA-1 staining was ablated by the binding competitor lactose. When the data from the western blot was quantified and normalized to EGFR levels, the bar graph verifies that there was an increase in α2,6 sialylation of EGFR in the 1,3,4-O-Bu$_3$ManNAc-treated cells.* ***(B)*** *A second aliquot of IP'd EGFR was digested with sialidase, which was analyzed by Fluorescent Assisted Carbohydrate Electrophoresis (FACE). Quantification of the FACE bands (normalized to EGFR levels determined from the western blots) provided independent verification that overall sialylation of EGFR increased with 1,3,4-O-Bu$_3$ManNAc treatment Each experiment includes at least three biological replicates and the bands were quantified using Image J with data expressed as mean ± standard error mean (SEM). * indicates a p value of < 0.05.*

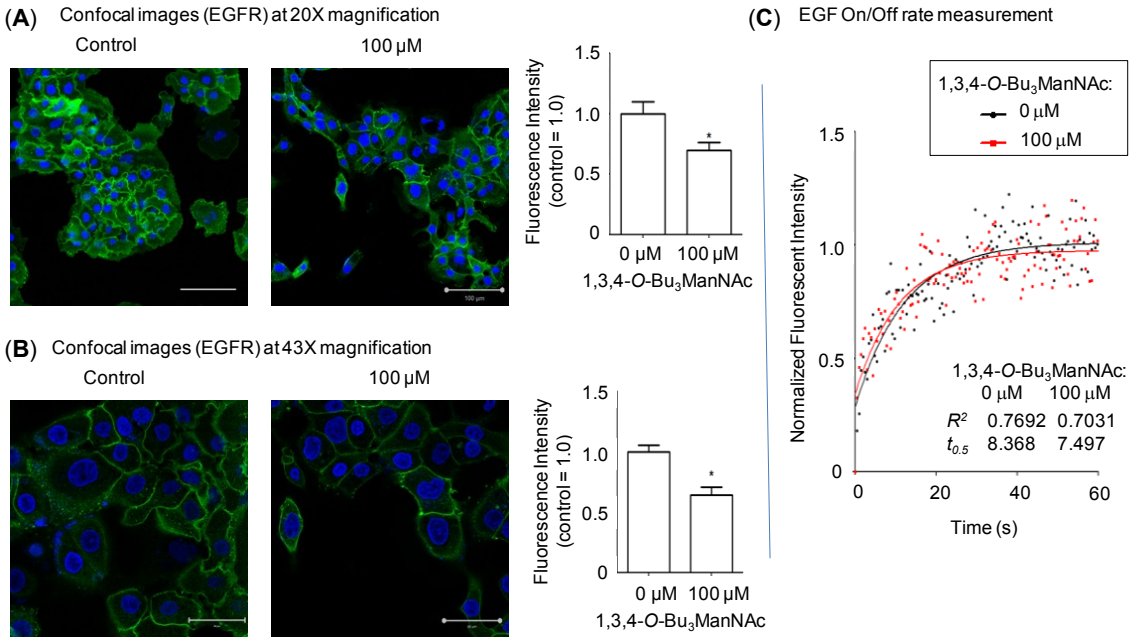

Figure 6.2: Confocal imaging of EGFR in SW1990 cells treated with 1,3,4-O-Bu$_3$ManNAc. *The treated cells, in comparison with untreated controls, were imaged at* ***(A)*** *20X and at* ***(B)*** *43X magnifications after being fixed and stained with Alexa Fluor-488 conjugated EGFR mAb (green) and DAPI (blue). Quantification of mAb staining, normalized to DAPI, showed a decrease in surface localized EGFR when SW1990 cells were treated with 100 µM of 1,3,4-O-Bu$_3$ManNAc as shown in the bar graphs. Each experiment includes at least three biological replicates and the fluorescent intensity of both Alexa Fluor-488 and DAPI were quantified using Image J with data expressed as mean ± standard error mean (SEM). * indicates a p value of < 0.05. Scale bars represent 100 µm and 50 µm respectively* ***(C)*** *A representative fluorescent recovery after photobleaching (FRAP) assay is shown, in which recovery rates are inversely proportional to $t_{0.5}$ when Alexafluor 488-conjugated EGF is present in the bath, indicated that receptor ligand affinities were not measurably different in the presence or absence of 1,3,4-O-Bu$_3$ManNAc.*

Figure 6.3: Proposed galectin lattice-mediated mechanism for modulation of EGFR signaling through 1,3,4-O-Bu$_3$ManNAc treatment*. The combined modeling and early experimental results were consistent with the depicted biochemical mechanism where destabilization of the galectin lattice occurs due to the masking of galectin-binding epitopes by analog-driven increased sialylation of N-linked glycans. (**A**) Cancer cells often have highly organized, less-mobile surface receptors (e.g., the green structure represents EGFR while the black structures represent any other cell surface glycoprotein) in part because of a highly formed galectin lattice. (**B**) One result of a strong galectin lattice is lengthened residence times for EGFR on the cell surface (45), resulting in enhanced phosphorylation that lead to increased downstream EGFR signaling, which contributes to cancer progression. (**C**) 1,3,4-O-Bu$_3$ManNAc treatment leads to an increase in sialylation of N-linked glycans bound to EGFR, based on lectin-staining data (specifically SNA binding as shown in the representative FACS plot depicts globally increased expression of α2,6-linked sialic upon 1,3,4-O-Bu$_3$ManNAc treatment, which is consistent with both the data shown in Figure 1 and our previous results (3)); glycans terminated with α2,6-linked sialic acids mask galactose residues and negatively regulate galectin binding (63). (**D**) In turn, reduced galectin binding decreases lattice strength, thereby increasing the surface mobility of EGFR and enhancing its removal from the cell surface (45). (**E**) Ultimately – over time periods longer (e.g., 30 to 90 min) than the 2 min time frame investigated in our previous work (5) – this increased rate of internalization predicts faster inactivation of EGFR, which is computationally and experimentally demonstrated subsequently in this report.*

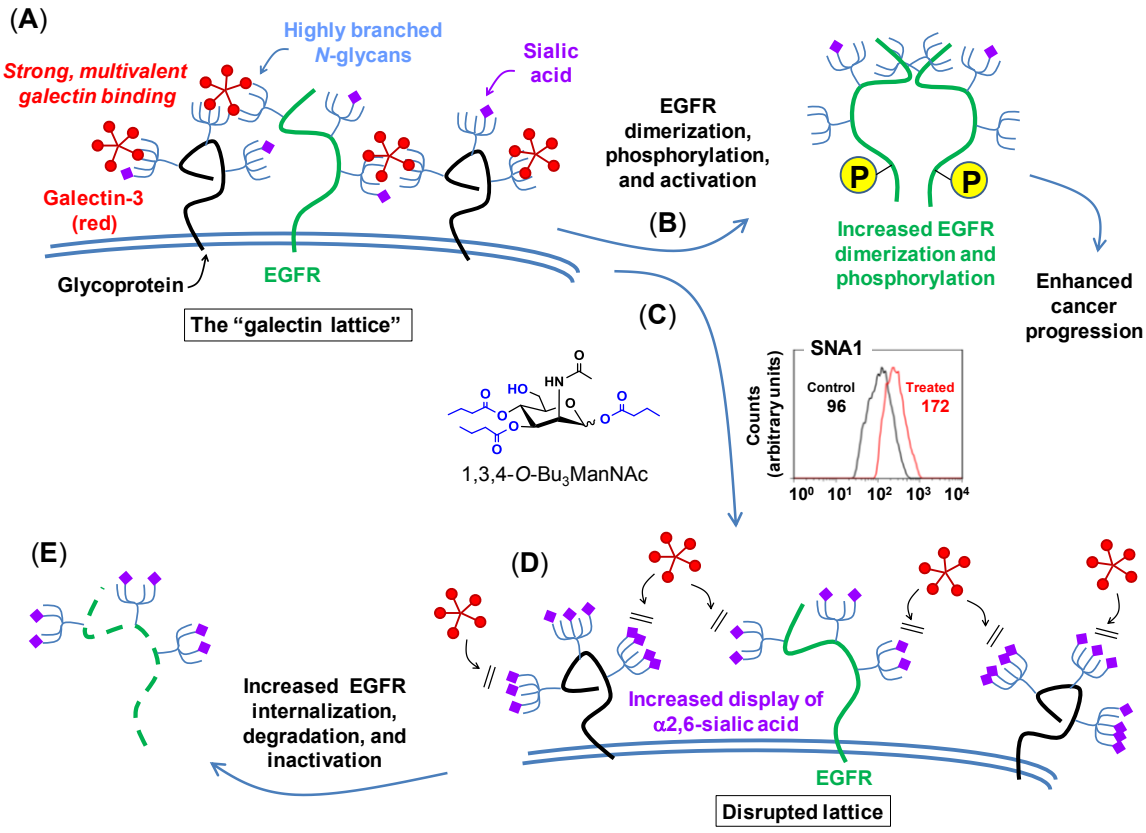
(A)
Highly branched
N-glycans
Sialic
acid
Strong, multivalent
galectin binding
Galectin-3
(red)
Glycoprotein
EGFR
The "galectin lattice"
EGFR
dimerization,
phosphorylation,
and activation
(B)
P
P
Increased EGFR
dimerization and
phosphorylation
Enhanced
cancer
progression
(C)
HO
HN
O
1,3,4-O-Bu3ManNAc
SNA1
Counts
(arbitrary units)
Control
96
Treated
172
10^0 10^1 10^2 10^3 10^4
(E)
(D)
Increased EGFR
internalization,
degradation, and
inactivation
Increased display of
α2,6-sialic acid
EGFR
Disrupted lattice

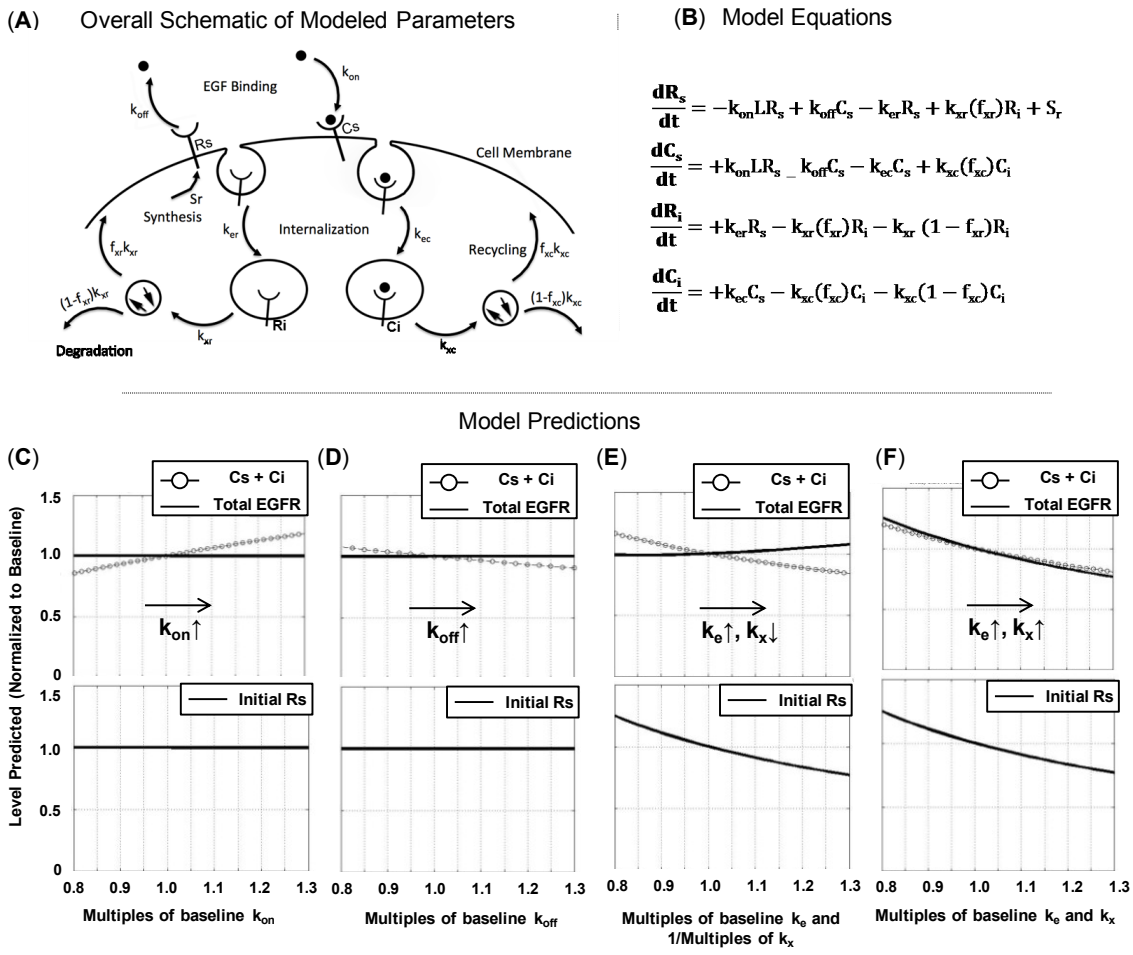

Figure 6.4: Mathematical model of EGFR trafficking. ***(A)*** *The general schematic (adapted from (41), with additional details provided in the main text) for modeling EGFR trafficking is shown, with the equations used for model output predictions given in* ***(B)****. In all cases, the simulated data shown represents predictions for 48 h of treatment with 1,3,4-O-Bu$_3$ManNAc at which time "initial" baseline levels of cell surface EGFR were given (as shown in each lower panel) followed by the simulated 2.0 min exposure to EGF (as shown in each upper panel). In each case, the predicted levels of total EGFR are shown in solid black and phosphorylated EGFR are shown in hollow circles in the upper graph, while predicted changes in surface expression of EGFR are depicted on the lower graph. Panels* ***(C)****,* ***(D)****,* ***(E)****, and* ***(F)*** *show simulated results for changes in k_{on}, k_{off} and a combination of k_e and k_x, respectively. In* ***(C)*** *and* ***(D)*** *k_{on} and k_{off} are respectively increased from left to right whereas in* ***(E)*** *k_e was increased, while k_x was decreased from left to right (which is indicated by "1/k_x" on the plots) and in* ***(F)****, both k_e and k_x were increased from left to right.*

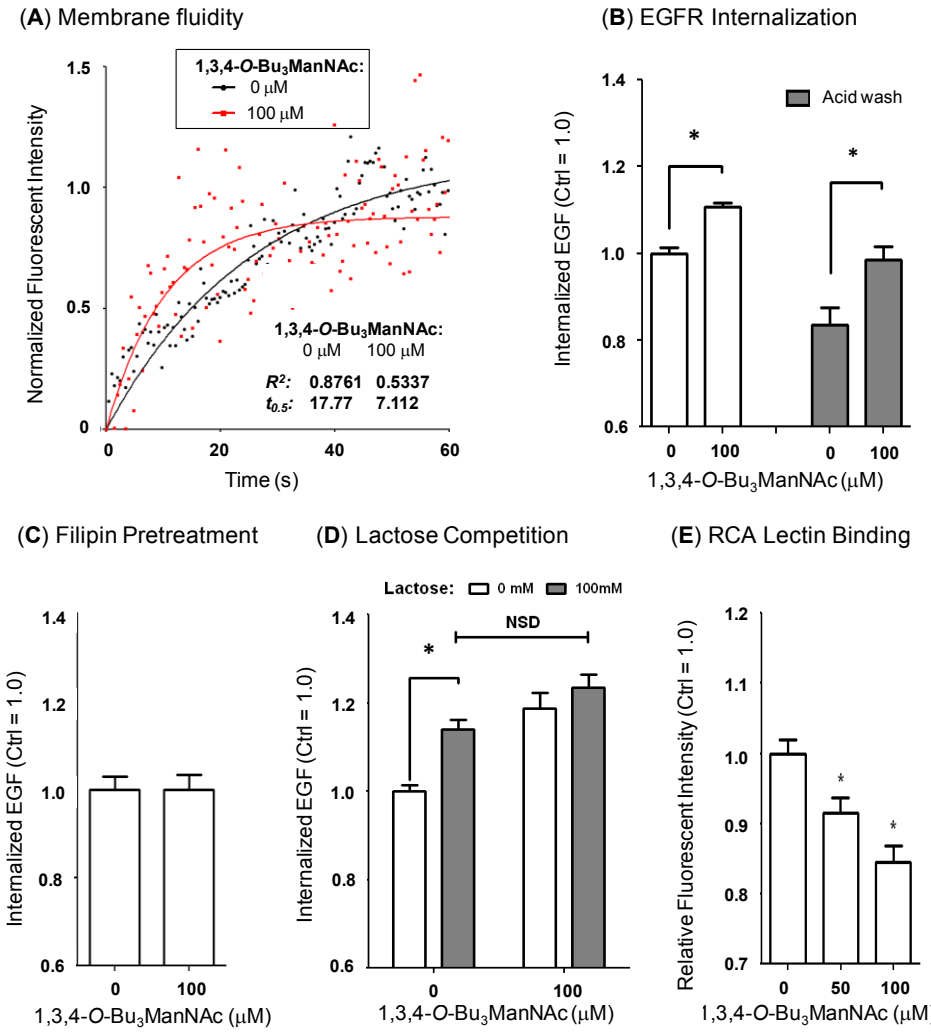

Figure 6.5: EGFR internalization assays. *(A) FRAP assays, conducted in the absence of excess fluorescently-labeled EGF, indicated that the recovery rate ($t_{0.5}$) was over twice as fast in cells treated with 1,3,4-O-Bu₃ManNAc indicated greater membrane fluidity consistent with decreased galectin lattice strength (as outlined in* ***Figure 6.3****).* ***(B)*** *Internalization assays conducted in the presence of fluorescently-labeled EGF for 30 min at 37 C showed that 1,3,4-O-Bu₃ManNAc treatment led to a significant increase in EGF, and by extension EGFR, internalization.* ***(C)*** *Internalization measured after filipin pretreatment, however, was not significantly different between the control and treated samples.* ***(D)*** *Lactose pretreatment, a competitive inhibitor of galectin binding, led to an increase in internalization in control cells comparable to the increase caused by 1,3,4-O-Bu₃ManNAc.* ***(E)*** *RCA lectin binding decreased significantly on treatment with 1,3,4-O-Bu₃ManNAc. At least three biological replicates were carried out for each experiment with data expressed as mean ± standard error mean (SEM) and * indicates $p < 0.05$.*

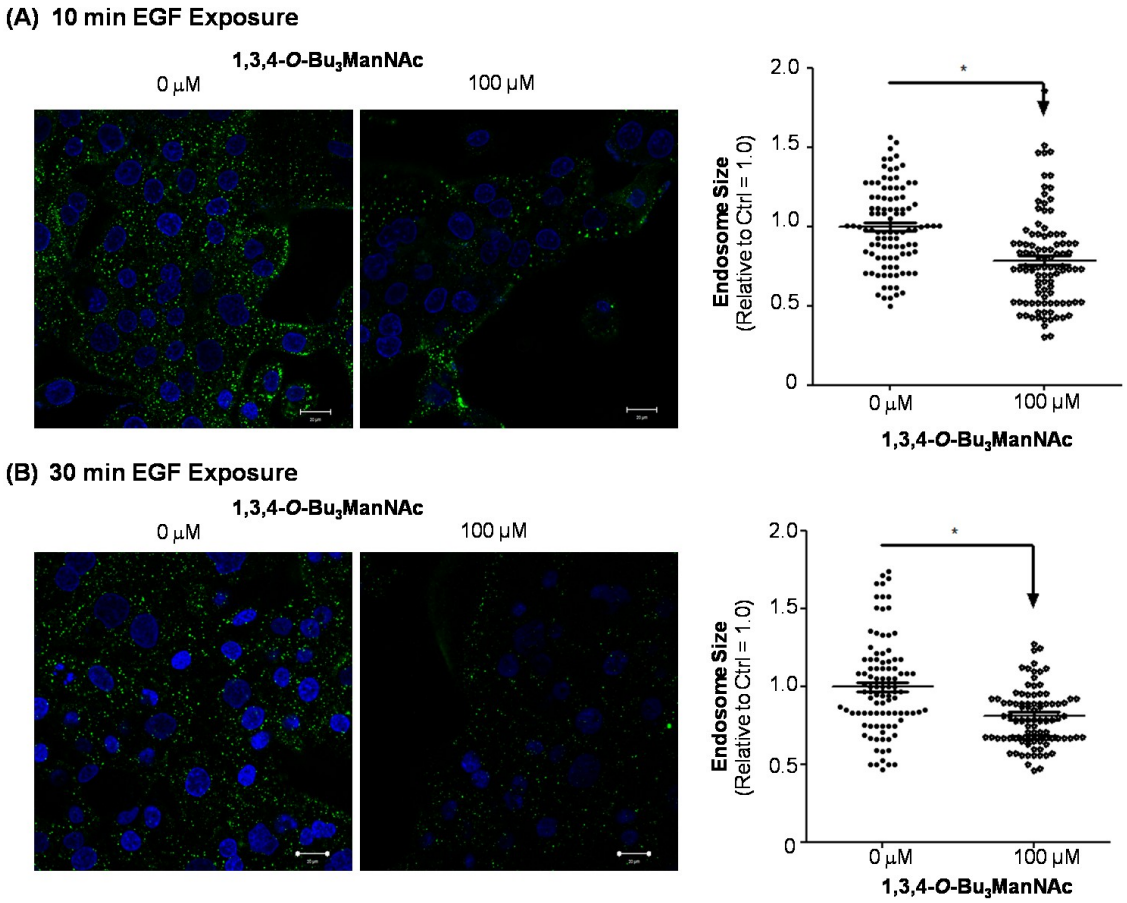

Figure 6.6: Confocal imaging of SW1990 cells *after* ***(A)*** *10 min and* ***(B)*** *30 min of exposure to 2 µg/ml Alexafluor 488-conjugated EGF at 37 ^{0}C showed a significantly greater density of larger endosomes in non-treated controls compared to cells treated with 1,3,4-O-Bu$_3$ManNAc. The endosomes were sized using ImageJ and * indicates a p value of < 0.05. Scale bars represent 20 µm.*

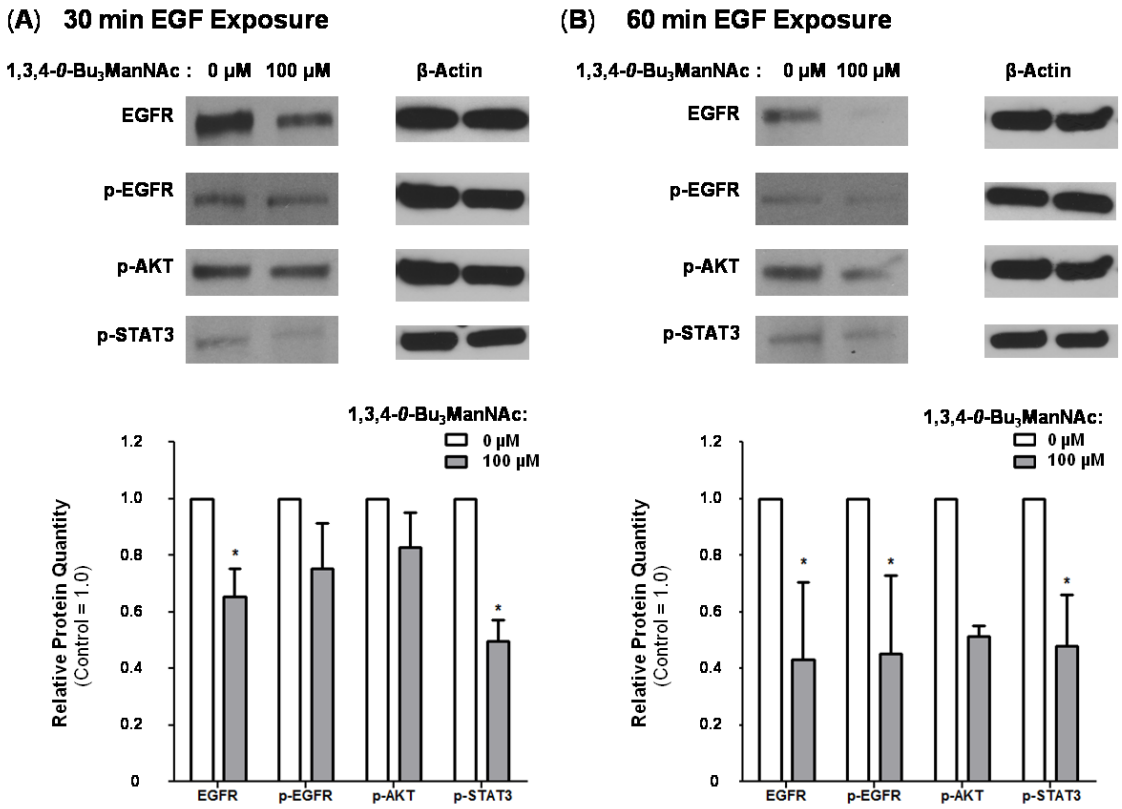

Figure 6.7: EGFR degradation is enhanced by 1,3,4-O-Bu$_3$ManNAc. *Western blot analysis of SW1990 cells exposed to 10 ng/ml of EGF for* ***(A)*** *30 min or* ***(B)*** *60 min after incubation with (or without) 1,3,4-O-Bu$_3$ManNAc revealed that longer exposures to EGF led to decreased EGFR levels for the treated cells. At least 3 biological replicates were carried out for each experiment with data expressed as mean ± standard error mean (SEM). * indicates a p value of < 0.05.*

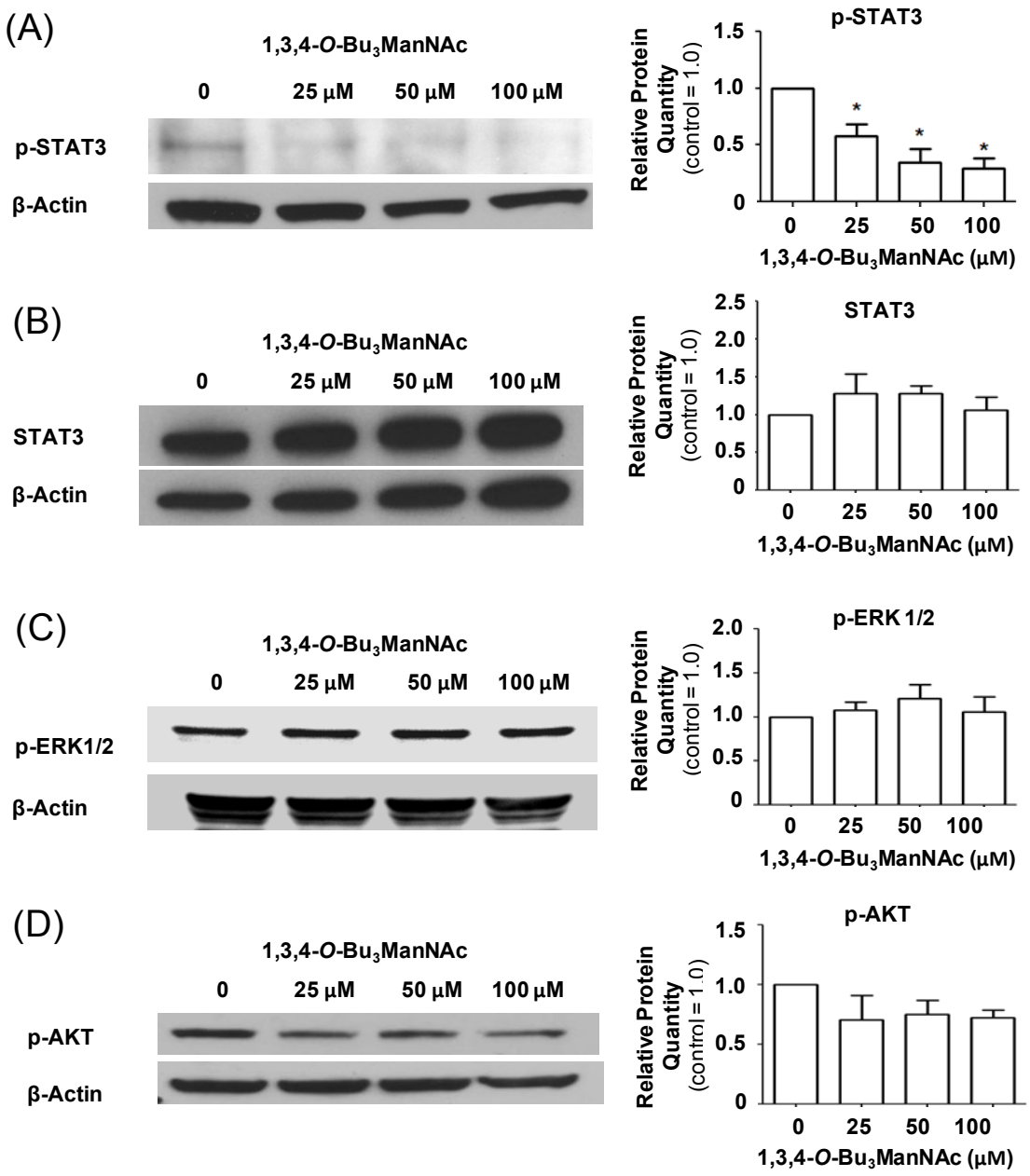

Figure 6.8: Downstrean signaling impact of 1,3,4-O-Bu$_3$ManNAc on STAT and ERK1/2. *Western blots of lysates from SW1990 cells treated with 1,3,4-O-Bu$_3$ManNAc. The treated (and control) cells were subsequently exposed to 10 ng/mL of EGF for 2.0 min and* ***(A)*** *the amount of phosphorylated STAT3 significantly decreased* ***(B)*** *without a corresponding decrease in STAT3 levels (****B****). At the same time, phosphorylation of ERK1/2* ***(C)*** *and AKT* ***(D)*** *were not affected. Each experiment includes at least three biological replicates and the blots were quantified using Image J with data expressed as mean ± standard error mean (SEM). * indicates a p value of < 0.05.*

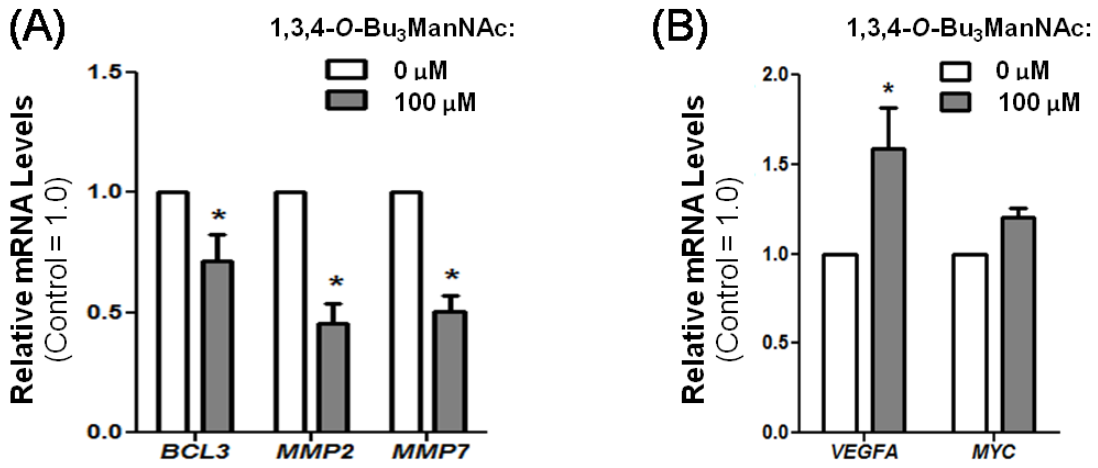

Figure 6.9: RT-PCR analysis of SW1990 cells *treated with and without 100 μM of 1,3,4-O-Bu$_3$ManNAc showed* ***(A)*** *a significant decrease in expression of STAT3 associated genes BCL3, MMP2 and MMP7 whereas* ***(B)*** *VEGFA and MYC, which can also be regulated by STAT3, showed increased expression (VEGFA) or was not affected (MYC). At least 3 biological replicates were carried out for each experiment with data expressed as mean ± standard error mean (SEM).* ******* *indicates a p value of < 0.05.*

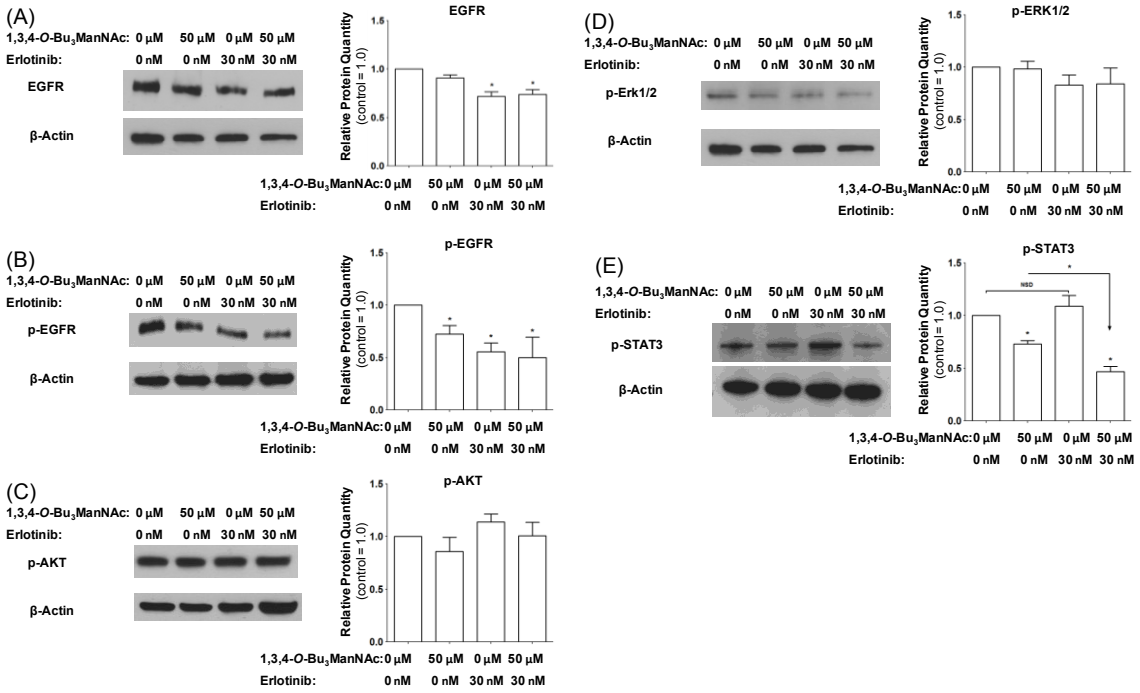

Figure 6.10: Western blot analysis of SW1990 cells *treated with 50 µM 1,3,4-O-Bu$_3$ManNAc, 30 nM of erlotinib, or both compounds in combination showed (**A**) EGFR levels that are not affected by the analog alone are decreased by erlotinib. (**B**) EGFR phosphorylation is inhibited by both compounds individually as well as in combination. (**C**) and (**D**) p-AKT and p-ERK1/2 levels, respectively, are not significantly affected by any of the treatment conditions. (**E**) p-STAT3 levels are inhibited by the analog but are not affected by erlotinib; however the combination of the two compounds leads to significantly lower p-STAT3 levels when compared to the analog alone. At least 3 biological replicates were carried out for each experiment with data expressed as mean ± standard error mean (SEM). * indicates a p value of < 0.05.*

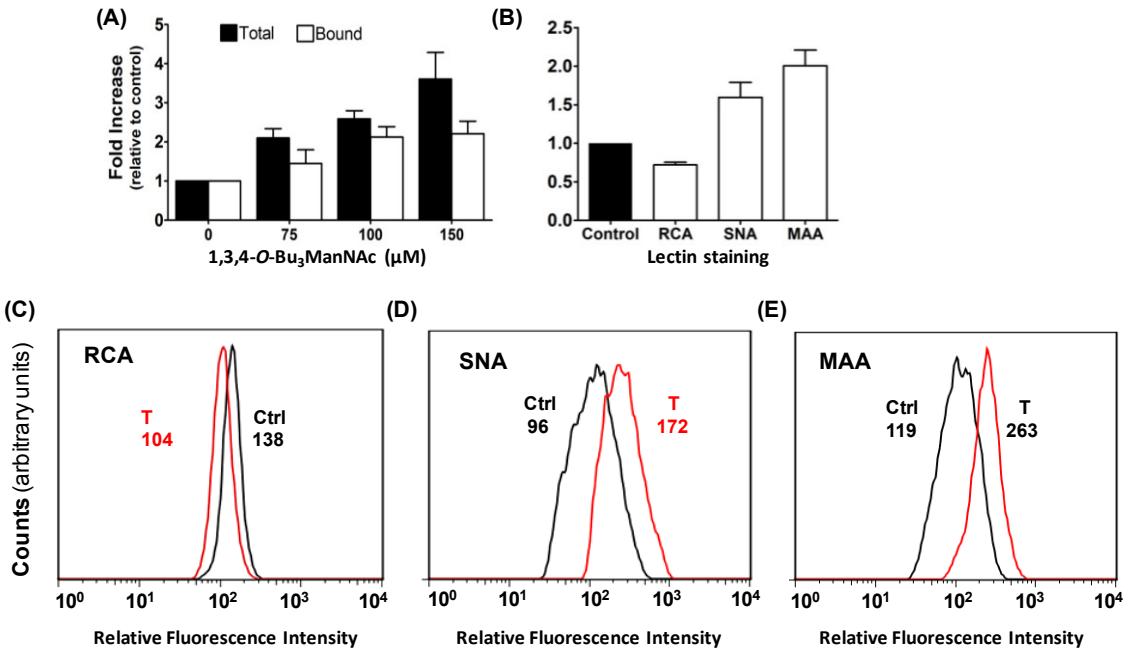

***Supplemental Figure S6.1**: **Changes in intracellular and surface sialic acid in 1,3,4-O-Bu$_3$ManNAc-treated SW1990 cells (adapted from Almaraz et al. (2)).** (**A**) Total (which includes all forms of sialic acid found within a cell, black bars) and "glycoconjugate-bound" (which also includes soluble CMP-sialic acid, white bars) sialic acid was measured by using the periodate resorcinol assay in cells incubated with the indicated concentrations of 1,3,4-O-Bu$_3$ManNAc for 2 days. Cells treated with 100 μM 1,3,4-O-Bu$_3$ManNAc for 2 days were analyzed by lectin binding with results summarized in (**B**) and representative flow cytometry data shown in (**C**) for ricin agglutinin (RCA), (**D**) Sambucus nigra agglutinin (SNA), and (**E**) Macckia amurensis agglutinin (MAA) flow cytometry. The error bars represent the S.D. of three different experiments.*

*This data supports the galectin lattice mechanism described in the main manuscript insofar as SNA binding represents levels of α2,6-linked sialic acids, which inhibit access to the underlying galactose/GalNAc residues bound by galectins and – as shown above – RCA. Of note, these global changes to sialylation are larger in magnitude than those observed for immunopurified EGFR, which was newly analyzed in the current study (with data provided in **Figure 6.**1 of the main manuscript).*

Supplemental Figure S6.2: *This figure shows an increased set of mathematical simulations (compared to those shown in Figure 3 of the parent publication) that were conducted to ascertain if there were additional plausible mechanisms to account for the decreased levels of surface EGFR and cellular p-EGFR observed in 1,3,4-O-Bu$_3$ManNAc-treated SW1990 cells.*

Model output predictions, for changes in (A) k_{er}, (B) k_{ec},(C) k_{xr}, (D) k_{xc}, (E) f_{xr}, (F) f_{xc}, (G) a combination of f_{xr} and, f_{xc}, and (H) a combination of k_e and k_x . In each case, predictions for changes in total EGFR are shown in solid black and phosphorylated EGFR are shown in hollow circles in the upper graph, while predicted changes in surface expression of EGFR are depicted in black on the lower graph. In each case the parameters increase from left to right.

(A) *Modeling of changes in internalization rate of available surface EGFR was not consistent with experimental data because while this endpoint did predict that an increase in internalization rate would lead to a decrease in EGFR phosphorylation and a decrease in surface bound EGFR, it also predicted that a similar decrease in overall EGFR levels would occur, which was not observed in the experimental data.*

(B) *Modeling of changes in internalization rate of EGF-EGFR complexes was not consistent with experimental data because it does not predict significant changes from the baseline conditions.*

(C) *Modeling of changes in recycling rate of unbound EGFR within endosomes was not consistent with experimental data because, while it did predict that an increase in recycling rate would lead to a decrease in available EGFR on the cell surface, it did not predict the decrease in EGFR phosphorylation that was previously observed.*

(D) *Modeling of changes in recycling rate of EGF-EGFR complexes within endosomes was not consistent with experimental data because it did not predict significant changes from the baseline conditions.*

(E) *Modeling of changes in recycling fraction of unbound EGFR within endosomes was not consistent with experimental data because while this endpoint did predict that a decrease in the recycling fraction would result in a decrease in EGFR phosphorylation and available surface bound EGFR (as observed) it also predicted a similar decrease in overall EGFR levels that was not observed experimentally.*

*(**F**) Modeling of changes in recycling fraction of EGF-EGFR complexes within endosomes was not consistent with experimental data because no significant changes from the baseline conditions were predicted.*

*(**G**) Modeling of changes in recycling fractions of both unbound EGFR and EGF-EGFR a complexes within endosomes was not consistent with experimental data because while it did predict that a decrease in the both recycling fractions would result in a decrease in EGFR phosphorylation and available surface bound EGFR, it also predicted a similar decrease in overall EGFR levels that was not observed experimentally.*

*(**H**) Modeling of changes in internalization and recycling rates of both available and bound EGFR was not consistent with experimental data because while it did predict that an increase in both the internalization and recycling rates would lead to an decrease in EGFR phosphorylation and a decrease in surface bound EGFR, it also predicted a similar decrease in overall EGFR levels that was not observed in the experimental data.*

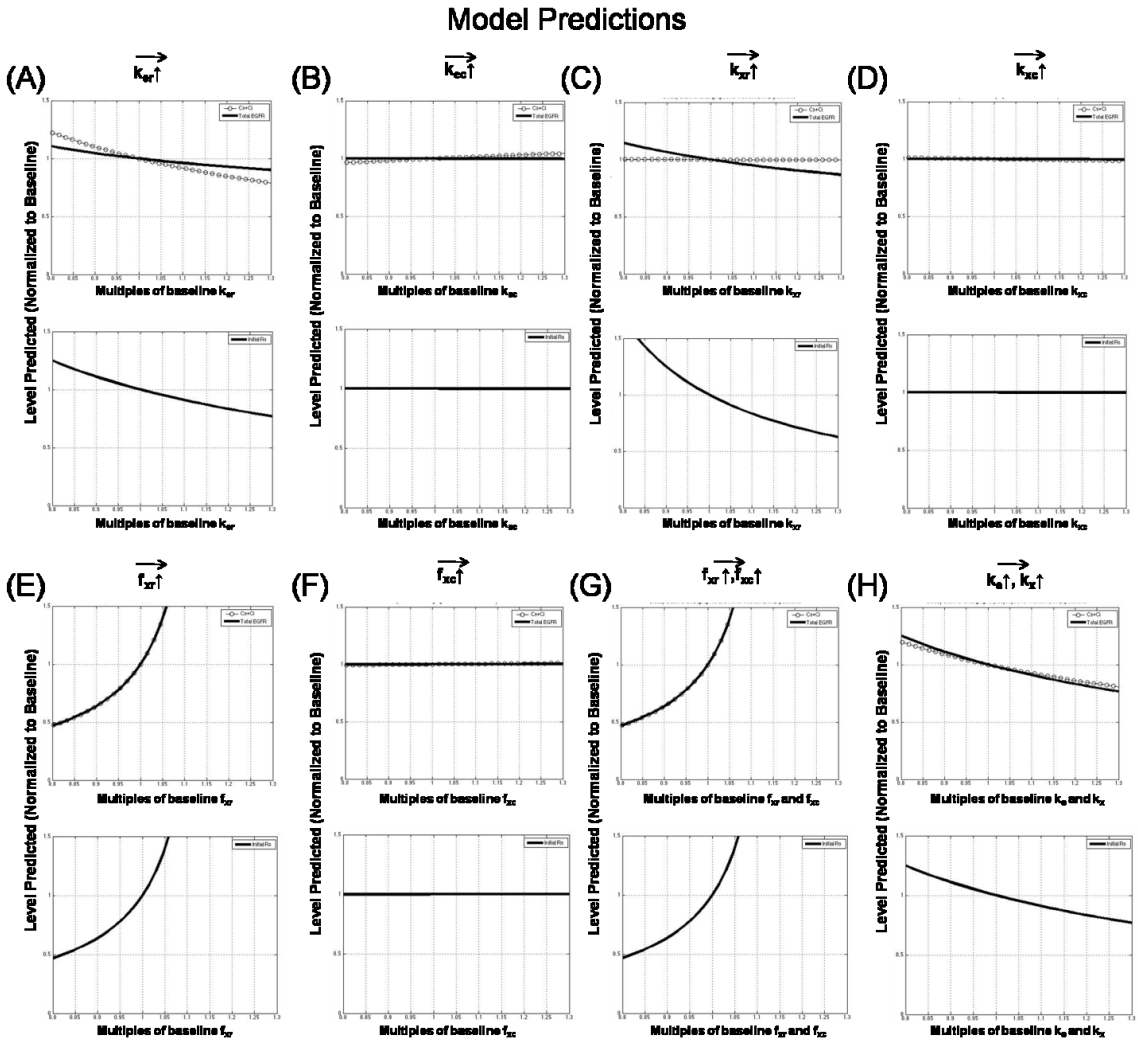
Model Predictions
(A)
(B)
(C)
(D)
(E)
(F)
(G)
(H)
Level Predicted (Normalized to Baseline)
Multiples of baseline

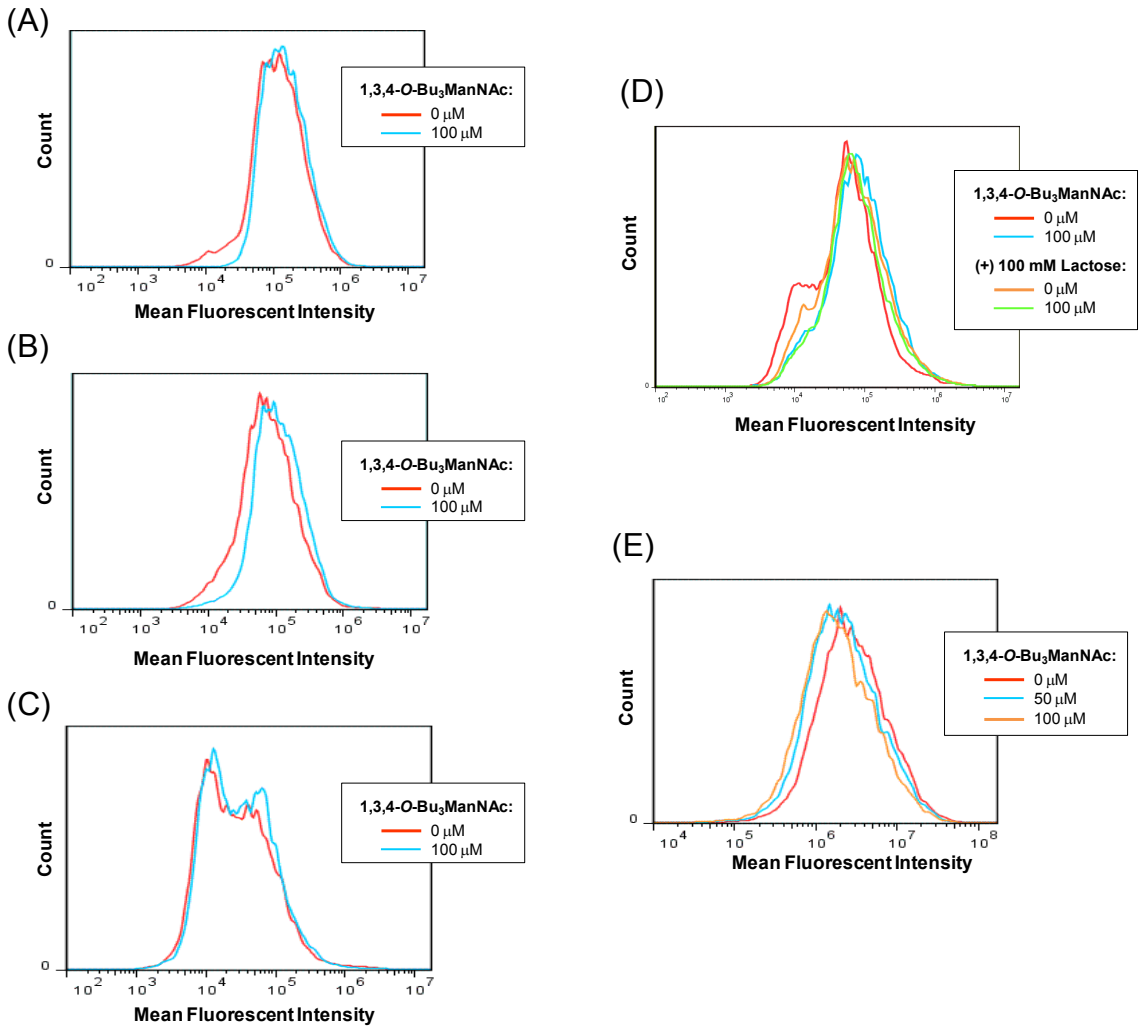

Supplemental Figure S6.3: EGFR internalization assays. *Internalization assays both* ***(A)*** *before and* ***(B)*** *after acid wash showed that 1,3,4-O-Bu$_3$ManNAc treatment (100 μM) leads to a significant increase in EGF internalization.* ***(C)*** *Internalization measured after filipin pretreatment, however, was not significantly different between the control and treated samples.* ***(D)*** *Lactose pretreatment led to an increase in internalization in control cells comparable to the increase caused by 1,3,4-O-Bu$_3$ManNAc.* ***(E)*** *RCA lectin binding decreased significantly on treatment with 1,3,4-O-Bu$_3$ManNAc. At least 3 biological replicates were carried out for each experiment with data expressed as mean ± standard error mean (SEM). * indicates a p value of < 0.05.*

6.7 REFERENCES

1. Aich, U.; Campbell, C.T.; Elmouelhi, N.; Weier, C.A.; Sampathkumar, S.G.; Choi, S.S.; Yarema, K.J. Regioisomeric SCFA attachment to hexosamines separates metabolic flux from cytotoxicity and MUC1 suppression. *ACS Chem. Biol.* **2008**, *3*, 230-240.

2. Almaraz, R.T.; Aich, U.; Khanna, H.S.; Tan, E.; Bhattacharya, R.; Shah, S.; Yarema, K.J. Metabolic oligosaccharide engineering with *N*-acyl functionalized ManNAc analogues: cytotoxicity, metabolic flux, and glycan-display considerations. *Biotechnol. Bioeng.* **2012**, *109*, 992-1006.

3. Almaraz, R.T.; Tian, Y.; Bhattarcharya, R.; Tan, E.; Chen, S.-H.; Dallas, M.R.; Chen, L.; Zhang, Z.; Zhang, H.; Konstantopoulos, K.; Yarema, K.J. Metabolic flux increases glycoprotein sialylation: implications for cell adhesion and cancer metastasis. *Mol. Cell. Proteomics* **2012**, 10.1074/mcp.M1112.017558

4. Shah, P.; Yang, S.; Sun, S.; Aiyetan, P.; Yarema, K.J.; Zhang, H. Mass spectrometric analysis of sialylated glycans with use of solid-phase labeling of sialic acids. *Anal. Chem.* **2013**, *85*, 3606-3613.

5. Mathew, M.P.; Tan, E.; Saeui, C.T.; Bovonratwet, P.; Liu , L.; Bhattacharya, R.; Yarema, K.J. Metabolic glycoengineering sensitizes drug-resistant pancreatic cancer cells to tyrosine kinase inhibitors erlotinib and gefitinib. *Bioorg. Med. Chem. Lett.* **2015**, *25*, 1223-1227.

6. Sell, S. Cancer-associated carbohydrates identified by monoclonal antibodies. *Hum. Pathol.* **1990**, *21*, 1003-1019.

7. Fukuda, M. Possible roles of tumor-associated carbohydrate antigens. *Cancer Res.* **1996**, *56*, 2237-2244.

8. Campbell, C.T.; Sampathkumar, S.-G.; Weier, C.; Yarema, K.J. Metabolic oligosaccharide engineering: perspectives, applications, and future directions. *Mol. Biosys.* **2007**, *3*, 187-194.

9. Almaraz, R.T.; Mathew, M.P.; Tan, E.; Yarema, K.J. Metabolic oligosaccharide engineering: Implications for selectin-mediated adhesion and leukocyte extravasation. *Ann. Biomed. Eng.* **2012**, *40*, 806-815.

10. Du, J.; Meledeo, M.A.; Wang, Z.; Khanna, H.S.; Paruchuri, V.D.P.; Yarema, K.J. Metabolic glycoengineering: sialic acid and beyond. *Glycobiology* **2009**, *19*, 1382-1401.

11. Kayser, H.; Zeitler, R.; Kannicht, C.; Grunow, D.; Nuck, R.; Reutter, W. Biosynthesis of a nonphysiological sialic acid in different rat organs, using *N*-propanoyl-D-hexosamines as precursors. *J. Biol. Chem.* **1992**, *267*, 16934-16938.

12. Keppler, O.T.; Horstkorte, R.; Pawlita, M.; Schmidt, C.; Reutter, W. Biochemical engineering of the *N*-acyl side chain of sialic acid: biological implications. *Glycobiology* **2001**, *11*, 11R-18R.

13. Goon, S.; Bertozzi, C.R. Metabolic substrate engineering as a tool for glycobiology. *J. Carbohydr. Chem.* **2002**, *21*, 943-977.

14. Prescher, J.A.; Dube, D.H.; Bertozzi, C.R. Chemical remodelling of cell surfaces in living animals. *Nature* **2004**, *430*, 873-877.

15. Mahal, L.K.; Yarema, K.J.; Bertozzi, C.R. Engineering chemical reactivity on cell surfaces through oligosaccharide biosynthesis. *Science* **1997**, *276*, 1125-1128.

16. Mahal, L.K.; Yarema, K.J.; Lemieux, G.A.; Bertozzi, C.R. Chemical approaches to glycobiology: Engineering cell surface sialic acids for tumor targeting. In: Inoue Y, Lee YC, Troy II FA, editors. Sialobiology and Other Novel Forms of Glycosylation. Osaka, Japan: Gakushin Publishing Company; 1999. p. 273-280.

17. Lemieux, G.A.; Yarema, K.J.; Jacobs, C.L.; Bertozzi, C.R. Exploiting differences in sialoside expression for selective targeting of MRI contrast reagents. *J. Am. Chem. Soc.* **1999**, *121*, 4278-4279.

18. Dafik, L.; d'Alarcao, M.; Kumar, K. Fluorination of mammalian cell surfaces via the sialic acid biosynthetic pathway *Bioorg. Med. Chem. Lett.* **2008**, *18*, 5945-5947.

19. Dafik, L.; d'Alarcao, M.; Kumar, K. Modulation of cellular adhesion by glycoengineering. *J. Med. Chem.* **2010**, *53*, 4277-4284.

20. Mathew, M.P.; Tan, E.; Shah, S.; Bhattacharya, R.; Meledeo, M.A.; Huang, J.; Espinoza, F.A.; Yarema, K.J. Extracellular and intracellular esterase processing of SCFA-hexosamine analogs: implications for metabolic glycoengineering and drug delivery. *Bioorg. Med. Chem. Lett.* **2012**, *22*, 6929-6933.

21. Varki, N.M.; Varki, A. Diversity in cell surface sialic acid presentations: implications for biology and disease. *Lab. Invest.* **2007**, *87*, 851-857.

22. Häuselmann, I.; Borsig, L. Altered tumor-cell glycosylation promotes metastasis. *Front. Oncol.* **2014**, *4*, 28. doi: 10.3389/fonc.2014.00028.

23. Sillanaukee, P.; Pönniö, M.; Jääskeläinen, I.P. Occurrence of sialic acids in healthy humans and different disorders. *Eur. J. Clin. Invest.* **1999**, *29*, 413-425.

24. Kornfeld, S.; Kornfeld, R.; Neufeld, E.F.; O'Brien, P.J. The feedback control of sugar nucleotide biosynthesis in liver. *Proc. Natl. Acad. Sci. U. S. A.* **1964**, *52*, 371-379.

25. Keppler, O.T.; Hinderlich, S.; Langner, J.; Schwartz-Albiez, R.; Reutter, W.; Pawlita, M. UDP-GlcNAc 2-epimerase: A regulator of cell surface sialylation. *Science* **1999**, *284*, 1372-1376.

26. Yamanaka, Y.; Friess, H.; Kobrin, M.S.; Buchler, M.; Beger, H.G.; Korc, M. Coexpression of epidermal growth factor receptor and ligands in human pancreatic cancer is associated with enhanced tumor aggressiveness. *Anticancer Res.* **1993**, *13*, 565-569.

27. Tobita, K.; Kijima, H.; Dowaki, S.; Kashiwagi, H.; Ohtani, Y.; Oida, Y.; Yamazaki, H.; Nakamura, M.; Ueyama, Y.; Tanaka, M. Epidermal growth factor receptor expression in human pancreatic cancer: Significance for liver metastasis. *Int. J. Mol. Med.* **2003**, *11*, 305-309.

28. Korc, M. Role of growth factors in pancreatic cancer. *Surgical Oncology Clinics of North America* **1998**, *7*, 25-41.

29. Liu, Y.C.; Yen, H.Y.; Chen, C.Y.; Chen, C.H.; Cheng, P.F.; Juan, Y.H.; Chen, C.H.; Khoo, K.H.; Yu, C.J.; Yang, P.C.; Hsu, T.L.; Wong, C.H. Sialylation and fucosylation of epidermal growth factor receptor suppress its dimerization and activation in lung cancer cells. *Proc. Natl. Acad. Sci. U. S. A.* **2011**, *108*, 11332-11337.

30. Wu, S.L.; Kim, J.; Bandle, R.W.; Liotta, L.; Petricoin, E.; Karger, B.L. Dynamic profiling of the post-translational modifications and interaction partners of epidermal growth factor receptor signaling after stimulation by epidermal growth factor using

Extended Range Proteomic Analysis (ERPA). *Mol. Cell. Proteomics* **2006**, *5*, 1610-1627.

31. Tsuda, T.; Ikeda, Y.; Taniguchi, N. The Asn-420-linked sugar chain in human epidermal growth factor receptor suppresses ligand-independent spontaneous oligomerization. Possible role of a specific sugar chain in controllable receptor activation. *J. Biol. Chem.* **2000**, *275*, 21988-21994.

32. Ling, Y.; Li, T.; Perez-Soler, R.; Haigentz Jr, M. Activation of ER stress and inhibition of EGFR N-glycosylation by tunicamycin enhances susceptibility of human non-small cell lung cancer cells to erlotinib. *Cancer Chemother. Pharmacol.* **2009**, *64*, 539-548.

33. Yen, H.Y.; Liu, Y.C.; Chen, N.Y.; Tsai, C.F.; Wang, Y.T.; Chen, Y.J.; Hsu, T.L.; Yang, P.C.; Wong, C.H. Effect of sialylation on EGFR phosphorylation and resistance to tyrosine kinase inhibition. *Proc. Natl. Acad. Sci. U. S. A.* **2015**, *112*, 6955-6960.

34. Park, J.-J.; Yi, J.Y.; Jin, Y.B.; Lee, Y.-J.; Lee, J.-S.; Lee, Y.-S.; Ko, Y.-G.; Lee, M. Sialylation of epidermal growth factor receptor regulates receptor activity and chemosensitivity to gefitinib in colon cancer cells. *Biochem. Pharmacol.* **2012**, *83*, 849-857.

35. Yun, C.-H.; Mengwasser, K.E.; Toms, A.V.; Woo, M.S.; Greulich, H.; Wong, K.-K.; Meyerson, M.; Eck, M.J. The T790M mutation in EGFR kinase causes drug resistance by increasing the affinity for ATP. *Proc. Natl. Acad. Sci. U. S. A.* **2008**, *105*, 2070–2075.

36. Jackson, P. Polyacrylamide gel electrophoresis of reducing saccharides labeled with the fluorophore 2-aminoacridone: subpicomolar detection using an imaging system based on a cooled charge-coupled device. *Anal. Biochem.* **1991**, *196*, 238-244.

37. Jackson, P. High-resolution polyacrylamide gel electrophoresis of fluorophore-labeled reducing saccharides. *Methods Enzymol.* **1994**, *230*, 250-265.

38. Axelrod, C.; Koppel, D.E.; Schlessinger, J.; Elson, E.; Webb, W.W. Mobility measurement by analysis of fluorescence photobleaching recovery kinetics. *Biophys. J.* **1976**, *16*, 1055-1069.

39. Day, C.A.; Kraft, L.J.; Kang, M.; Kenworthy, A.K. Analysis of protein and lipid dynamics using confocal fluorescence recovery after photobleaching (FRAP). *Curr Protoc Cytom* **2012**, *Chapter 2*, Unit 2.

40. Sprague, B.L.; Pego, R.L.; Stavreva, D.A.; McNally, J.G. Analysis of binding reactions by fluorescence recovery after photobleaching. *Biophys. J.* **2004**, *86*, 3473-3496.

41. Hendriks, B.S.; Opresko, L.K.; Wiley, H.S.; Lauffenburger, D. Epidermal Growth Factor Receptor 2 (HER2) levels and locations. Quantitative analysis of HER2 overexpression effects. *Cancer Res.* **2003**, *63*, 1130-1137.

42. Zhou, M.; Felder, S.; Rubinstein, M.; Hurwitz, D.R.; Ullrich, A.; Lax, I.; Schlessinger, J. Real-time measurements of kinetics of EGF binding to soluble EGF receptor monomers and dimers support the dimerization model for receptor activation. *Biochemistry* **1993**, *32*, 8193-8198.

43. Dawson, J.P.; Berger, M.B.; Lin, C.-C.; Schlessinger, J.; Lemmon, M.A.; Ferguson, K.M. Epidermal growth factor receptor dimerization and activation require ligand-induced conformational changes in the dimer interface. *Mol Cell Biol* **2005**, *25*, 7734-7742.

44. Macdonald-Obermann, J.L.; Pike, L.J. Different epidermal growth factor (EGF) receptor ligands show distinct kinetics and biased or partial agonism for homodimer and heterodimer formation. *J. Biol. Chem.* **2014**, *289*, 26178-26188.

45. Lajoie, P.; Partridge, E.A.; Guay, G.; Goetz, J.G.; Pawling, J.; Lagana, A.; Joshi, B.; Dennis, J.W.; Nabi, I.R. Plasma membrane domain organization regulates EGFR signaling in tumor cells. *J. Cell Biol.* **2007**, *179*, 341-356.

46. Sigismund, S.; Argenzio, E.; Tosoni, D.; Cavallaro, E.; Polo, S.; Di Fiore, P.P. Clathrin-mediated internalization is essential for sustained EGFR signaling but dispensable for degradation. *Dev. Cell* **2008**, *15*, 209-219.

47. Yarema, K.J.; Goon, S.; Bertozzi, C.R. Metabolic selection of glycosylation defects in human cells. *Nat. Biotechnol.* **2001**, *19*, 553-558.

48. Heuser, J. Three-dimensional visualization of coated vesicle formation in fibroblasts. *J. Cell Biol.* **1980**, *84*, 560-583.

49. Liu, S.-H.; Mallet, W.G.; Brodsky, F.M. Chapter 1. Clathrin-mediated endocytosis. In: Marsh M, editor. Frontiers in Molecular Biology: Endocytosis. New York: Oxford University Press; 2001.

50. Dautry-Varsat, A. Chapter 2. Cathrin-independent endocytosis. In: Marsh M, editor. Frontiers in Molecular Biology: Endocytosis. New York: Oxford University Press; 2001.

51. Rothberg, K.G.; Heuser, J.E.; Donzell, W.C.; Ying, Y.; Glenney, J.R.; Anderson, R.G. Caveolin, a protein component of caveolae membrane coats. *Cell* **1992**, *68*, 673-682

52. van Deurs, B.; Holm, P.K.; Sandvig, K.; Hansen, S.H. Are caveolae involved in clathrin-independent endocytosis? *Trends Cell Biol* **1993**, *3*, 249-251.

53. Castellano, E.; Downward, J. RAS interaction with PI3K more than just another effector pathway. *Genes Cancer* **2011**, *2*, 261-274.

54. Linardou, H.; Dahabreh, I.J.; Kanaloupiti, D.; Siannis, F.; Bafaloukos, D.; Kosmidis, P.; Papadimitriou, C.A.; Murray, S. Assessment of somatic k-RAS mutations as a mechanism associated with resistance to EGFR-targeted agents: a systematic review and meta-analysis of studies in advanced non-small-cell lung cancer and metastatic colorectal cancer. *Lancet Oncol.* **2008**, *9*, 962-972.

55. Halilovic, E.; She, Q.B.; Ye, Q.; Pagliarini, R.; Sellers, W.R.; Solit, D.B.; Rosen, N. PIK3CA mutation uncouples tumor growth and cyclin D1 regulation from MEK/ERK and mutant KRAS signaling. *Cancer Res.* **2010**, *70*, 6804-6814.

56. Mulcahy, H.E.; Lyautey, J.; Lederrey, C.; qi Chen, X.; Anker, P.; Alstead, E.M.; Ballinger, A.; Farthing, M.J.; Stroun, M. A prospective study of K-ras mutations in the plasma of pancreatic cancer patients. *Clin. Cancer Res.* **1998**, *4*, 271-275.

57. Benvenuti, S.; Sartore-Bianchi, A.; Di Nicolantonio, F.; Zanon, C.; Moroni, M.; Veronese, S.; Siena, S.; Bardelli, A. Oncogenic activation of the RAS/RAF signaling pathway impairs the response of metastatic colorectal cancers to anti-epidermal growth factor receptor antibody therapies. *Cancer Res.* **2007**, *67*, 2643-2648.

58. Fang, B. Genetic interactions of STAT3 and anticancer drug development. *Cancers (Basel)* **2014**, *6*, 494-525.

59. Siveen, K.S.; Sikka, S.; Surana, R.; Dai, X.; Zhang, J.; Kumar, A.P.; Tan, B.K.H.; Sethi, G.; Bishayee, A. Targeting the STAT3 signaling pathway in cancer: Role of synthetic and natural inhibitors. *Biochimica Biophys. Acta* **2014**, *1845*, 136-154.

60. Yu, H.; Lee, H.; Herrmann, A.; Buettner, R.; Jove, R. Revisiting STAT3 signalling in cancer: new and unexpected biological functions. *Nat. Rev. Cancer* **2014**, *14*, 736-746.

61. Pagès, G.; Pouysségur, J. Transcriptional regulation of the Vascular Endothelial Growth Factor gene–a concert of activating factors. *Cardiovasc. Res.* **2005**, *65*, 564-573.

62. Brenner, H. Long-term survival rates of cancer patients achieved by the end of the 20th century: a period analysis. *Lancet* **2002**, *360*, 1131-1135.

63. Zhuo, Y.; L, B.S. Emerging role of a2,6-sialic acid as a negative regulator of galectin binding and function. *J. Biol. Chem.* **2011**, *286*, 5935-5941.

64. Ioannou, N.; Dalgleish, A.G.; Seddon, A.M.; Mackintosh, D.; Guertler, U.; Solca, F.; Modjtahedi, H. Anti-tumour activity of afatinib, an irreversible ErbB family blocker, in human pancreatic tumour cells. *Br.J. Cancer* **2011**, *105*, 1554-1562.

65. Buck, E.; Eyzaguirre, A.; Haley, J.D.; Gibson, N.W.; Cagnoni, P.; Iwata, K.K. Inactivation of Akt by the epidermal growth factor receptor inhibitor erlotinib is mediated by HER-3 in pancreatic and colorectal tumor cell lines and contributes to erlotinib sensitivity. *Mol. Cancer Ther.* **2006**, *5*, 2051-2059.

66. Jia, J.; Zhu, F.; Ma, X.; Cao, Z.W.; Li, Y.X.; Chen, Y.Z. Mechanisms of drug combinations: interaction and network perspectives. *Nat. Rev. Drug. Discov.* **2009**, *8*, 111-128

67. Oksvold, M.P.; Skarpen, E.; Wierød, L.; Paulsen, R.E.; Huitfeldt, H.S. Re-localization of activated EGF receptor and its signal transducers to multivesicular compartments downstream of early endosomes in response to EGF. *Eur. J. Cell Biol.* **2001**, *80*, 285-294.

68. Le Roy, C.; Wrana, J.L. Clathrin-and non-clathrin-mediated endocytic regulation of cell signalling. *Nat. Rev. Mol. Cell Biol.* **2005**, *6*, 112-116.

69. Wang, Y.; Pennock, S.; Chen, X.; Wang, Z. Endosomal signaling of epidermal growth factor receptor stimulates signal transduction pathways leading to cell survival. *Mol. Cell. Biol.* **2002**, *22*, 7279-7290.

70. Kranenburg, O.; Verlaan, I.; Moolenaar, W.H. Dynamin is required for the activation of mitogen-activated protein (MAP) kinase by MAP kinase kinase. *J. Biol. Chem.* **1999**, *274*, 35301-35304.

71. Bild, A.H.; Turkson, J.; Jove, R. Cytoplasmic transport of Stat3 by receptor-mediated endocytosis. *EMBO J.* **2002**, *21*, 3255-3263.

72. de Oliveira, J.T.; de Matos, A.J.; Santos, A.L.; Pinto, R.; Gomes, J.; Hespanhol, V.; Chammas, R.; Manninen, A.; Bernardes, E.S.; Albuquerque Reis, C.; Rutteman, G.; Gärtner, F. Sialylation regulates galectin-3/ligand interplay during mammary tumour progression--a case of targeted uncloaking. *Int. J. Dev. Biol.* **2011**, *55*, 823-834.

73. Lagana, A.; Goetz, J.G.; Cheung, P.; Raz, A.; Dennis, J.W.; Nabi, I.R. Galectin binding to Mgat5-modified N-glycans regulates fibronectin matrix remodeling in tumor cells. *Mol. Cell. Biol.* **2006**, *26*, 3181-3193.

74. Lau, K.S.; Partridge, E.A.; Grigorian, A.; Silvescu, C.I.; Reinhold, V.N.; Demetriou, M.; Dennis, J.W. Complex N-glycan number and degree of branching cooperate to regulate cell proliferation and differentiation. *Cell* **2007**, *129*, 123-134.

75. Dennis, J.W.; Nabi, I.R.; Demetriou, M. Metabolism, cell surface organization, and disease. *Cell* **2009**, *139*, 1229-1241.

76. Huang, X.; Li, Y.; Zhang, J.; Xu, Y.; Tian, Y.; Ma, K. Ganglioside GM3 inhibits hepatoma cell motility via down-regulating activity of EGFR and PI3K/AKT signaling pathway. *J. Cell Biol.* **2013**, *114*, 1616-1624.

77. Boscher, C.; Dennis, J.W.; Nabi, I.R. Glycosylation, galectins and cellular signaling. *Curr. Opin. Cell Biol.* **2011**, *23*, 383-392.

BIBLIOGRAPHY

1. Mathew, M. P., Tan, E., Saeui, C. T., Bovonratwet, P., Skylar, S.,, Bhattacharya, R., & Yarema, K. J. (2015). Insights into the Sensitization and Targeting of the Epidermal Growth Factor Receptor (EGFR) in Pancreatic Cancer Cells by Metabolic Oligosaccharide Engineering. *Journal of Biological Chemistry*, (Submitted)

2. Mathew, M. P.[1], Tan, E.[1], Saeui, C. T., Bovonratwet, P., Liu, L., Bhattacharya, R., & Yarema, K. J. (2015). Metabolic glycoengineering sensitizes drug-resistant pancreatic cancer cells to tyrosine kinase inhibitors erlotinib and gefitinib. *Bioorganic & Medicinal Chemistry Letters*, 25(6), 1223-1227.

3. Badr, H. A., AlSadek, D. M., Mathew, M. P., Li, C. Z., Djansugurova, L. B., Yarema, K. J., & Ahmed, H. (2015). Nutrient-deprived cancer cells preferentially use sialic acid to maintain cell surface glycosylation. *Biomaterials*. 70, 23-36

4. Badr, H. A., AlSadek, D. M., Mathew, M. P., Li, C. Z., Djansugurova, L. B., Yarema, K. J., & Ahmed, H. (2015). Lectin staining and Western blot data showing differential sialylation of nutrient-deprived cancer cells to sialic acid supplementation. *Data in Brief*

5. Saeui, C. T., Urias, E., Liu, L., Mathew, M. P., & Yarema, K. J. (2015). Metabolic glycoengineering bacteria for therapeutic, recombinant protein, and metabolite production applications. *Glycoconjugate Journal*, 1-17.

6. Saeui, C. T., Mathew, M. P., Liu, L., Urias, E., & Yarema, K. J. (2015). Cell Surface and Membrane Engineering: Emerging Technologies and Applications. *Journal of functional biomaterials*, *6*(2), 454-485.

7. Meyer R. A.[1], Mathew M.P.[1], Sunshine J.C., Schmueli R.B., Ren Q., Yarema K.J., Green J.J., 'Anisotropic biodegradable supported lipid bilayers with spatially dynamic surface protein presentation' *Angewandte Chemie International Edition,* (Submitted)

8. Tan E.[1], Mathew M.P.[1], Shah S., Saeui C., Liu L., Bhattacharya R., & Yarema K.J., "Pharmacological modulation of intracellular esterase activity through Metabolic Glycoengineering of sialic acid." *(In Preparation)*

9. Mathew, M. P.[1], Tan, E.[1], Shah, S.[1], Bhattacharya, R., Meledeo, M. A., Huang, J. Espinoza F.A. & Yarema, K. J. (2012). Extracellular and intracellular esterase processing of SCFA–hexosamine analogs: Implications for metabolic glycoengineering and drug delivery. *Bioorganic & Medicinal Chemistry Letters*, 22(22), 6929-6933.

10. Almaraz, R. T., Mathew, M. P., Tan, E., & Yarema, K. J. (2012). Metabolic oligosaccharide engineering: implications for selectin-mediated adhesion and leukocyte extravasation. *Annals of Biomedical Engineering*, *40*(4), 806-815

CURRICULUM VITAE

MOHIT PHILIP MATHEW **03/22/2016**

Educational History

Ph.D. expected	March 2016	Biomedical Engineering	Johns Hopkins University, School of Medicine
		Mentor: Dr. Kevin Yarema Ph.D.	
M.S.E.	2012	Biomedical Engineering	Johns Hopkins University
B.E.	2010	Biotechnology	Manipal Institute of Technology

Other Professional Experience

Undergraduate Research Internship 2010-2010 Sangenomics Research Labs Pvt. Ltd., India,

- Undergraduate Research Internship 2009-2009 University of Lodz, Poland,

Honors and Achievements

Graduate Student Travel Award, EB conference, San Diego, 2014

BME Department PhD Council Co-president, July 2013-June 2014

Dean's Tuition Fellowship (JHU BME M.S.E Program)

Certificate of Excellence and Gold medal for 1st rank in the B.E. Biotechnology class of 2010, Manipal University, India

Certificate of Appreciation for outstanding academic performance 2008-2009, Dept. of Biotechnology, Manipal University, India

Served as the General Secretary of *Disha* (a social service club), August 2008 – June 2009

Ranked 74th all India in the National Science Olympiad 2005-2006

Peer Reviewed Publications

Mathew, M. P., Tan, E., Saeui, C. T., Bovonratwet, P., Skylar, S.,, Bhattacharya, R., & Yarema, K. J. (2015). Insights into the Sensitization and Targeting of the Epidermal Growth Factor Receptor (EGFR) in Pancreatic Cancer Cells by Metabolic Oligosaccharide Engineering. *Journal of Biological Chemistry*, (Submitted)

Mathew, M. P.[1], Tan, E.[1], Saeui, C. T., Bovonratwet, P., Liu, L., Bhattacharya, R., & Yarema, K. J. (2015). Metabolic glycoengineering sensitizes drug-resistant pancreatic cancer cells to tyrosine kinase inhibitors erlotinib and gefitinib. *Bioorganic & Medicinal Chemistry Letters*, 25(6), 1223-1227.

Badr, H. A., AlSadek, D. M**., Mathew, M. P.,** Li, C. Z., Djansugurova, L. B., Yarema, K. J., & Ahmed, H. (2015). Nutrient-deprived cancer cells preferentially use sialic acid to maintain cell surface glycosylation. *Biomaterials*. 70, 23-36

Badr, H. A., AlSadek, D. M., **Mathew, M. P**., Li, C. Z., Djansugurova, L. B., Yarema, K. J., & Ahmed, H. (2015). Lectin staining and Western blot data showing differential sialylation of nutrient-deprived cancer cells to sialic acid supplementation. *Data in Brief*

Meyer R. A.[1], **Mathew M.P.[1]**, Sunshine J.C., Schmueli R.B., Ren Q., Yarema K.J., Green J.J., 'Anisotropic biodegradable supported lipid bilayers with spatially dynamic surface protein presentation' *Angewandte Chemie International Edition,* (Submitted)

Tan E.[1], **Mathew M.P.[1]**, Shah S., Saeui C., Liu L., Bhattacharya R., & Yarema K.J., "Pharmacological modulation of intracellular esterase activity through Metabolic Glycoengineering of sialic acid." *(In Preparation)*

Saeui, C. T., Urias, E., Liu, L., **Mathew, M. P.,** & Yarema, K. J. (2015). Metabolic glycoengineering bacteria for therapeutic, recombinant protein, and metabolite production applications. *Glycoconjugate Journal*, 1-17.

Saeui, C. T., **Mathew, M. P.,** Liu, L., Urias, E., & Yarema, K. J. (2015). Cell Surface and Membrane Engineering: Emerging Technologies and Applications. *Journal of functional biomaterials*, *6*(2), 454-485.

Mathew, M. P.[1], Tan, E.[1], Shah, S.[1], Bhattacharya, R., Meledeo, M. A., Huang, J. Espinoza F.A. & Yarema, K. J. (2012). Extracellular and intracellular esterase processing of SCFA–hexosamine analogs: Implications for metabolic glycoengineering and drug delivery. *Bioorganic & Medicinal Chemistry Letters*, 22(22), 6929-6933.

Almaraz, R. T., **Mathew, M. P.,** Tan, E., & Yarema, K. J. (2012). Metabolic oligosaccharide engineering: implications for selectin-mediated adhesion and leukocyte extravasation. *Annals of Biomedical Engineering*, *40*(4), 806-815

Sykula-Zajac A., Turek M., **Mathew M.P.,** Patai F., Horvat M. & Jabalonska J., (2010) Determination of nickel in tea using the dimethylglyoxime method. *Zeszyty Naukowe. Chemia Spożywcza i Biotechnologia / Politechnika Łódzka*, Vol. 74, 5-11

Book Chapters

Jiang, X. S., **Mathew, M. P.,** & Du, J. (2014). Polyelectrolyte Hydrogels: Thermodynamics. In *Polyelectrolytes* (pp. 183-214). Springer International Publishing

Peer reviewd Abstracts and Poster Presentations

Mathew M.P.[1]**,** Tan E.[1], Saeui C., Bovonratwet P., Liu L., Bhattacharya R., Patel A. & Yarema K.J., "Increased non-clathrin mediated endocytosis plays a role in Erlotinib sensitization of pancreatic cancer cells by metabolic oligosaccharide engineering." *The NIH & FDA Glyco-Sciences Research Day,* Bethesda, MD, (2015)

Mathew M.P.[1]**,** Tan E.[1], Saeui C., Bovonratwet P., Liu L., Bhattacharya R., Yarema K.J., "Metabolic oligosaccharide engineering sensitizes pancreatic cancer cells to EGFR targeting drugs", *Experimental Biology Conference,* San Diego, CA, (2014)

Tan E., **Mathew M.P**., Saeui C., Shah S., Liu L., Bovonratawet P. Bhattacharya R. & Yarema K.J., "Cross-talk between SCFA-Hexosamine analog mediated metabolic flux and intracellular esterase activity." *Joint Meeting of the Society of Glycobiology and American Society for Matrix Biology (Abstract published in Glycobiology),* San Diego, CA, (2012)

Mathew M.P., Tan E., Shah S., Meledeo A., Bhattacharya R. & Yarema K.J., " Extracellular esterase and intracellular processing of SCFA-Hexosamine analogs: Implication for metabolic oligosaccharide engineering and drug delivery." *Joint Meeting of the Society of Glycobiology and American Society for Matrix Biology (Abstract published in Glycobiology),* San Diego, CA, (2012)

Du, J., Espinoza, F.A., Tan, E., Bhattacharya, R., Shah, S., **Mathew, M.P.,** & Yarema, K.J. "Regulation of cancer cell adhesion via 3D electrospun nanofibrous scaffolds and metabolic oligosaccharide engineering." *The Institute for NanoBiotechnology Spring Symposium-Cancer Nanotechnology*, Johns Hopkins University, Baltimore, MD, (2011)

Mathew M.P., Patai F., Horvat M., Sykula-Zajac A. & Turek M. "Determination of nickel in tea and comparison of methods of estimation." *Techtatva*, Manipal Institute of Technology, India (Won first prize)

Service and Leadership Experience

Co-president BME PhD Council	2013-2014	Johns Hopkins University, Baltimore,
Teaching Assistant,	2010-2016	Johns Hopkins University, Baltimore,
Volunteer Teacher	2006-2009	Disha, Manipal, India,